FLUME STUDIES ON THE KINEMATICS AND DYNAMICS OF LARGE-SCALE BED FORMS

by

KEVIN MICHAEL BOHACS

B. Sc., University of Connecticut
(1976)

SUBMITTED TO THE DEPARTMENT OF
EARTH AND PLANETARY SCIENCES
IN PARTIAL FULFILLMENT OF
THE REQUIREMENTS FOR THE
DEGREE OF

DOCTOR OF SCIENCE

at the

MASSACHUSETTS INSTITUTE OF TECHNOLOGY

June 1981

Signature of Author _____
Department of Earth and Planetary Sciences
May 22, 1981

Certified by _____
John B. Southard
Thesis Supervisor

Accepted by _____
Theodore R. Madden
Chairman, Departmental Committee
on Graduate Students

FLUME STUDIES ON THE KINEMATICS

AND DYNAMICS OF LARGE-SCALE BED FORMS

by

Kevin Michael Bohacs

Submitted to the Department of Earth and Planetary Sciences on May 1, 1981 in partial fulfillment of the requirements for the Degree of Doctor of Science

ABSTRACT

Two series of experimental runs (in medium and very coarse sands) in a large (60 x 2.1 x 1.5 m), hot-water flume investigated the kinematics and dynamics of large-scale bed forms. At constant flow depth (1.5 m) the bed configurations produced with increasing flow velocity are: ripples, two-dimensional dunes, three-dimensional dunes, and higher-velocity dunes (new provisional term). Higher-velocity dunes are large bed forms (height = 0.6 - 0.9 m; spacing = 4 - 10 m) whose development was restricted by the size of the flume; they may be the equivalent of some sand waves seen in natural environments.

The three types of dunes have similar dynamic behavior and seem to manifest one overall bed phase. There is a smooth progression of dependent flow variables and of bed-form size and migration rate with increasing flow velocity. There are, however, sufficient differences in the geometry and kinematics of the large-scale forms to warrant the subdivision of the dune phase.

The time required for these bed forms to reach equilibrium with the superjacent flow is a function of the magnitude and direction of the change in flow velocity. The adjustment proceeds fairly rapidly, on the order of the time required for a bed form to migrate one to two average spacings.

Thesis Supervisor: Dr. John B. Southard, Associate Professor of Geology

TABLE OF CONTENTS

LIST OF FIGURES

LIST OF TABLES

ACKNOWLEDGMENTS

An experimentally based thesis is a large and complex undertaking. I could not have completed it successfully without the support (scientific, technical, financial, and personal) of many people. Hence, I extend my thanks to:

-Professor John B. Southard, for this continued guidance and support; from lofty discussions of the mechanics of sediment transport to his hours of wielding power tools.

-Professors Ole S. Madsen and Jon C. Boothroyd, for their comments and criticism, both on this thesis and in the days of my general exams.

-William C. Corea and his family, for their constant support, engineering consultations, and endless resources.

-The denizens of the Center for Experimental Sedimentology: R. Kuhnle, C. Paola, P. Vrolijk, and J.D. Walker, for endless hours of discussions about the merits of the experimental approach.

-The Clones et al.: especially K. & J. Bartley, P. Bowen, C.S. Cameron, K. & L. Hodges, for keeping me honest geologically -- and for being my friends.

-J. A. Russell, C. B. Sutherland, and the other members of Midnight Enterprizes, for programming and other services.

-Mom and Dad, for all their patience and love -- and chocolate chip cookies.

This work was supported by the National Science Foundation under grant number 76-21979 ENG.

CHAPTER 1

INTRODUCTION

Geologists and engineers have long known that loose, cohesionless sediment subjected to turbulent shear flow organizes itself into a definite series of statistically similar shapes, known as bed forms or bed configurations. The usual sequence of these forms (no movement -- ripples -- dunes) in lower-flow-regime flows was recognized by G.K. Gilbert (1914) and explicitly defined and examined in the experiments of Simons and Richardson (1962, 1963).

More recent field studies have expanded this sequence, adding a third scale of bed form, sand waves (Neill, 1969; Klein, 1970; McCave, 1971). Also on the basis of field work, some investigators (Boothroyd and Hubbard, 1975; Hine, 1975; Dalrymple, Knight, and Lambiase, 1978) divide the dune phase into two subphases, variously named: Type 1 and Type 2 megaripples; linear and cuspate megaripples. The full bed-configuration sequence with increasing flow velocity, according to several authors, is presented in Table 1. Flume studies have recognized only the two types of dunes; sand waves have not been generated (Chabert and Chauvin, 1963; Costello and Southard, 1971, 1981; Pratt, 1971).

There is far from universal agreement on the existence of two orders of bed configuration larger than ripples. Even

TABLE 1

** Bed-configuration sequence in fine to medium sands **

No Movement -- Ripples -- 2D Dunes -- 3D Dunes -- Sand Waves

Two-Dimensional Dunes	Three-Dimensional Dunes
(Costello and Southard, 1981)	(Costello and Southard, 1981)
Linear Megaripples	Cuspate Megaripples
(Boothroyd and Hubbard, 1972)	(Boothroyd and Hubbard, 1972)
Type 1 Megaripples	Type 2 Megaripples
(Dalrymple et al., 1978)	(Dalrymple et al., 1978)
Bancs	Dunes
(Chabert and Chauvin, 1963)	(Simons et al., 1962,1963)
Ploskie Gryady (Flat Dunes)	Megaripples
(Znamenskaya, 1963)	(Coleman, 1969)
Intermediate Flattened Dunes	(Daboll, 1969)
(Pratt, 1971)	(Hartwell, 1970)
Bars	Lunate Megaripples
(Costello, 1974)	(Clifton et al., 1971)

Sand Waves (Costello and Southard, 1981)

Alternate Bars (Guy et al., 1966)

Dunes (Coleman, 1969)

Linguoid Bars (Collinson, 1970)

Higher-Velocity Dunes (This study)

granting their existence, there is still debate on the significance of dunes and sand waves: whether they are hydrodynamically distinct bed forms, and whether they can exist simultaneously in equilibrium.

The second chapter of this thesis details the data available from flume and field, discusses the problems with each type of study, and outlines the questions raised by these studies.

Two series of experimental runs were made to address these questions. Chapter 3 is a description of the experimental apparatus and procedures. Chapter 4 presents the results of these experiments: the geometry, kinematics, and dynamics of the bed forms generated. Chapter 5 contains a discussion of the experimental results, with respect to field studies and the conclusions of this study.

CHAPTER 2

PREVIOUS WORK

This chapter presents an overview of the properties and occurrence of large-scale bed configurations in field and flume. The data on this subject are sometimes conflicting, and often confusing. The reader would be well advised to keep Table 1 close at hand. The source of conflict and confusion may be attributed in part to the character of each of the settings in which large-scale bed configurations occur. Hence, the descriptions from each setting are followed by discussion of the problems inherent in studying each setting.

LARGE-SCALE BED CONFIGURATIONS IN NATURAL ENVIRONMENTS

Large-scale bed configurations can form wherever an effectively unidirectional flow of sufficient strength and depth transports sediments coarser than 0.1 to 0.2 mm. They are found in fluvial environments and in marine environments from tidal creeks to the outer continental shelf, and even in the deep ocean. Ranging in size from 50 cm to 20 m high and 70 cm to greater than 1000 meters in spacing, large-scale bed forms occur in flow depths of 0.5 to 250 m. Tables 2 and 3 specify the conditions of occurrence of these bed forms in the fluvial and marine environments.

The majority of detailed data comes from studies in the intertidal environment; it is from these studies that the

TABLE 2

LARGE-SCALE BED FORMS IN FLUVIAL ENVIRONMENTS

	Setting	Depth Range (m)	Mean Velocity (cm / s)	Sediment Size (mm)	Bed-Form Height (m)	Bed-Form Spacing (m)
Coleman ('69)						
Megaripples	Braided River	3-27	61-213	Fine sand	0.3-1.5	3-153
Dunes		3-30	152-213	& silt	1.5-7.6	43-488
Collinson ('70)						
Linguoid Bars	Braided River	0.4-1.1	Discharge 250-1500 m^3/s	Coarse-Medium sand	0.5-2.0	200-300
Dunes					0.1-0.4	1-20
Karcz ('72)						
Dunes	Desert Wadi	0.5-0.75	60-75	0.4	0.1-0.3	0.75-1.8
Neill ('69)						
Major	Meandering River	0.3-3.6	57-118	0.35	0.3-1.5	305 (aver.)
Minor		0.9-3.6	57-137		0.3-1.8	2.5-21.3
Singh & Kumar ('74)						
Sand Waves	Meandering River	8-10	(peak)	0.26	0.2	40-50
Dunes			300		0.3-0.7	8-10
Smith ('71)						
Tranverse Bars	Braided River	N/R	N/R	0.24-	0.03-1.0	10-51
Diminished Dunes				0.62	0.01-0.05	20-100
Dunes					0.03-0.25	45-75

TABLE 3

LARGE-SCALE BED FORMS IN MARINE ENVIRONMENTS

	Setting	Depth Range (m)	Mean Velocity (cm / s)	Sediment Size (mm)	Bed-Form Height (m)	Bed-Form Spacing (m)
Allen & Friend ('76)						
Dunes	Tidal	greater than	> 78	0.25	0.8-0.12	1-2
Sand Waves		2.8	>60		0.14-0.25	5-10
Belderson & Stride ('66)						
Dunes	Shallow	88	75-102	0.3	0.75-1.25	10
Sand Waves	Subtidal				8 (aver.)	300
Boothroyd & Hubbard ('75)						
Megaripples	Intertidal; Shallow	2-5	60-100	0.44	0.08-0.04	1.5-4
Sand Waves	Subtidal		40-80	0.31	0.15-0.40	8-20
Dalrymple ('77)						
Megaripples	Intertidal	0-11.9	100-200	0.19-0.55	0.05-0.65	1-10
Sand Waves			80-110	0.22-1.8	0.05-1.3	2.26
Green ('75)						
Dunes	Estuary (tide-	2-6	85	0.20	0.2	2-3
Sand Waves	dominated)				0.6-0.9	10-15

TABLE 3 (CONTINUED)

	Setting	Depth Range (m)	Mean Velocity (cm / s)	Sediment Size (mm)	Bed-Form Height (m)	Bed-Form Spacing (m)
Hine ('75)						
Linear Megaripples		5-7	60-80	0.35	0.05-0.2	0.4-4
Cuspate MRs	Shallow Subtidal				0.03-0.2	1-3.5
Sand Waves					0.06-0.2	5-20
Klein ('70)						
Dunes	Inter-tidal	2-6	60-100	0.27-1.8	0.16-0.53	2.4-7.6
Sand Waves		3.7-6	45-95	0.4-0.57	0.17-1.77	13-50
Knight ('72)						
Megaripples	Inter-tidal	0.5-7.9	51-142	Coarse-Medium sand	0.10-0.30	1-4
Sand Waves		0.3-8.3	45-138		1.0(aver.)	35(aver.)
Kumar & Sanders ('74)						
Dunes	Tidal inlet	4.5-10		0.40	0.5	20-30
Sand Waves			120		0.5-2.0	60-100
Ludwick ('72)	Estuary (tide-dominated)					
Dunes		5-7.3	57-93	0.25	0.3	10
Sand Waves					1.9	270
McCave ('71)						
Megaripples	Shallow Tidal Sea	18	60	0.31-0.45	1-2	10-20
Sand Waves				0.20-0.45	7.4	200-500

properties of these forms will be described here. Although fluvial settings do not allow such close observation of bed forms, what data there are indicate that these general descriptions from the intertidal environments hold for fluvial environments as well (Bluck, 1971; Bridge and Jarvis, 1976; Carey and Keller, 1957; Coleman, 1969; Collinson, 1970; Jackson, 1975a; Neill, 1969; Pretorious and Blench, 1951; Smith, 1971).

In shallow intertidal flows, two kinds of large-scale bed forms are observed: dunes (megaripples) and sand waves. They are grossly similar in shape to bed forms seen in flume, but they are at least an order of magnitude larger. Workers investigating modern tidal sediments (Reineck, 1963; Klein, 1970; McCave, 1971; Boothroyd and Hubbard, 1975) distinguish these two types of large-scale bed configurations most commonly on the basis of a spacing criterion, and on their external morphology. A full list of criteria and bed configurations recognized is contained in Table 4.

Dunes

Dunes appear less regular than sand waves. They are commonly sinuous-crested, but straight, lunate, and catenary varieties also occur. Strongly developed scour pits immediately downstream of dune crests result in an irregular elevation of troughs and crestlines. Dunes are much steeper than sand waves in profile, with a lee face at or near the angle or repose of the sediment.

TABLE 4 -- Bed-Form Classification Criteria

Study	Bed Forms Recognized	-Classification Criteria- Spacing	Height	Steepness(L/H)	Morphology of:
Allen&Collinson (1974)	R (< 60 cm) MR (>60 cm)	X			
Boothroyd & Hubbard (1975)	R, MR, SW	X			
Bridge & Jarvis (1976)	R, D	X			
Collinson (1970)	R, D	X			Stoss slope; Crestline
Dalrymple et al. (1978)	R, D, SW	X	X	X	Lee slope; Crestline
Hine (1975)	R, D, SW	X	X		
Klein (1970)	R, D, SW	X			Lee slope; Crestline
Knight (1981)	R, D, SW	X	X		
McCave (1971)	R, D, SW		X		Stoss slope
Neill (1969)	R, D, SW	X	X		
Rubin & McCulloch (1980)	R, D+SW	X	X		Crestline

R = Ripples; MR = Megaripples; D = Dunes; SW = Sand Waves

Due to their simple avalanche faces, dunes display a relatively simple internal stratification. A single set of cross-beds with tangential foreset laminae resting on an erosional surface is the most common structure. Reactivation structures are often seen interrupting the cross-bedding.

Some field investigators, for example, Dalrymple (1977), subdivide dunes into two varieties: Type 1 megaripples and Type 2 megaripples. There is a continuous gradation between Type 1 megaripples and Type 2 megaripples: no single morphologic characteristic can be used to distinguish between them.

Type 1 megaripples are long and low forms, very "two-dimensional" in plan, with straight to sinuous crests. The crests are laterally continuous and of uniform height due to a lack of scour pits in the troughs. They average 6 meters in spacing (range 1 - 25 m) and 18 cm in height (range 5 - 50 cm). Spacing-to-height ratios are generally greater than 20, and their heights and spacings correlate poorly.

Type 2 megaripples are shorter and higher, and more "three-dimensional" and complex in appearance. Their crests are sinuous to lunate in plan and vary in height considerably along the crestline. This variation in height is caused by well-developed scour pits in the troughs. Dimensions of Type 2 megaripples range from 0.5 to 14 m long (4.3 m average) and 5 to 70 cm high (28 cm average); spacing-to-height ratios average less than 20. Their spacings and heights are well correlated.

Type 1 megaripples form at lower flow velocities than Type 2 megaripples. The Type 1 megaripples appear abruptly when the flow velocity increases above the ripple stability field. With continuing increases in velocity, they become more "three-dimensional" and grade into Type 2 megaripples. Thus it may be seen that Type 1 and Type 2 megaripples are end members in a continuum of bed forms, intermediate in scale between ripples and sand waves, with a lee face at the angle of repose of the sediment during active migration.

Careful examination of studies in other environments shows the presence of these "two-dimensional" and "three-dimensional" dunes in ephemeral streams (Karcz, 1972) and in mesotidal estuaries (Hine, 1975; Boothroyd and Hubbard, 1975; Allen and Friend, 1976a).

Sand Waves

Sand waves appear much more regular than dunes, being straight to sinuous crested in plan view. Elevations of crests and troughs are very even, due to a complete lack of scour pits in their troughs. Sand waves are as large as, or larger than, associated dunes, and always appear less steep. Most of the larger sand waves have lee face slopes of about 20 degrees (Klein, 1970; Dalrymple et al., 1978) -- considerably less than the angle of repose.

Both ripples and dunes are seen superimposed upon sand waves; Dalrymple (1977) notes that sand waves with superimposed dunes are larger than those with only ripples

superimposed. The superimposition of these forms, plus the common lack of a slipface, results in an intricate, compound internal structure. Bipolar, herringbone, and ripple-drift cross-stratification can be found in sand waves.

Another setting that displays large-scale transverse bed forms is the open continental shelf. Examples of large-scale bed forms on continental shelves are found world-wide; the most extensive work has been carried out on the shelf around the British Isles. Workers in the North Sea area, starting with Van Veen in 1935 and continuing to the present (Cartwright and Stride, 1958; Stride, 1963; Houboult, 1968; McCabe, 1971; Langhorne, 1973, 1981), have described these features as sand waves, found alone or in trains. These sand waves average 5 meters in height, and range from 30 to 500 meters in spacing. They migrate under steady currents and currents generated by storms and tides. Sand waves possess varying degrees of profile asymmetry, closely correlated with the nature of the local tidal cycle (McCave, 1971).

Though most studies are carried out by sonic depth sounding (profile and side-scan) with some direct observation, investigators are able to discern the effects of grain size upon the bed forms. McCave (1971) noted that dunes are found superimposed on sand waves only in sediments coarser than 0.3 mm diameter. This is in accord with the results of Dalrymple et al. (1978), who found that dunes in the Bay of Fundy are present only on the coarser-grained sand waves (diameter greater

than 0.31 mm). Briggs (1979) also saw dunes on sand waves only in sediments coarser than 0.34 mm (in Vineyard Sound -- shallow subtidal flow).

Where better observations of the surficial sediments are available, more specific influences of the grain-size distributions may be discerned. In eastern Long Island Sound, Bokuniewicz, Gordon, and Kastens (1977) found that sand waves did not form if the sediments have a large content of fines or of coarse sand (> 10% mud or > 12% coarse sand).

Depending on their setting, sand waves in the marine environment may show net migration, on the scale of a tidal cycle (Jones et al., 1965; Bokuniewicz, 1977; Dalrymple, 1977), or on a seasonal basis (McCave, 1971), or may exhibit little net transport. Langhorne (1973) reports that individual crests may shift ("flex") up to 25 meters on a yearly scale with little or no net migration. Briggs (1979) reports a similar flexing of crestlines at the confluence of ebb-dominated and flood-dominated sand waves.

Differentiating Dunes From Sand Waves

In the literature there is some debate about the existence of two different types of bed configurations larger than ripples. Some investigators of natural flows (Neill, 1969; Collinson, 1970) are unsure that all scales of bed forms are active and migrate at the same time. That is, they may observe two or more orders of bed forms; whether all scales are in equilibrium with the particular flow is the question. This

uncertainty may result from the methods of study used: low-resolution sonic profiling and aerial photography. Their methods may have sufficient spatial resolution, but the time between observations is so long that individual bed forms cannot be traced in successive profiles or photographs.

There are both empirical and theoretical models which support the viewpoint that dunes and sand waves are but one bed configuration. Several of these models are examined in this section, and all have serious shortcomings.

Empirical Models

It has been generally accepted that size of large-scale bed forms depends on the flow depth, with a continuum of large bed forms (similar in shape) increasing in size from those formed in the intertidal zone to those produced on the open shelf. This idea rests upon the mathematical models developed by Yalin (1964) and by Allen (1970). Careful examination of these models shows them to be based on unrealistic or unproven assumptions.

Yalin (1964) was the first to model mathematically the height and spacing of sand waves formed on a cohesionless, mobile bed under a uniform, tranquil flow with a free surface. Using an inductive approach, he examined the value of the shear stress acting in the trough of the sand wave. He stated that the shear stress at the lowest point (B) in the trough can be expressed as:

$$\tau_B = \tau_o \, k_1 \, (H/d) \qquad (1)$$

where:

τ_o = average total shear stress

H = bed-form height

d = flow depth

k_1 = constant of proportionality

He then equated τ_B with τ_{cr}, the critical shear stress for entrainment corresponding to the fluid and bed material under consideration. The variation of the shear stress was assumed to be totally controlled by the flow depth:

$$\tau_o/\tau_{cr} = d/d_{cr} \qquad (2)$$

Eq. (2) is substituted into Eq. (1) and the constant of proportionality determined empirically from experimental data:

$$H/d = 1/6(1 - d_{cr}/d) \; . \qquad (3)$$

There are several problems with this model. First, Eq. (1) is stated without proof or derivation. Yalin assumes that H/d is an explicit function of τ_o/τ_{cr}, which makes H/d an implicit function of the fluid density and viscosity, sediment size and density, and the acceleration of gravity. He then makes the shear stress an explicit function of the flow depth only. Second, although Eq. (3) follows the trend of the experimental data, the scatter about this line, in some cases more than 100%, is enormous. This was attributed to "experimental error".

Gill (1971) in his re-examination of Yalin's work calls this explanation "plausible, [but] it is not sufficient". He was able to derive Yalin's equation from Exner's (1925) hydraulic model only by additionally assuming that the hydraulic resistance of the flow does not vary with the flow velocity. Of this, Gill said:

> The assumption of constant resistance is drastic indeed. Recent studies (Raudkivi, 1967) show that the hydraulic resistance of alluvial channels varies appreciably with velocity and the intensity of sediment transport. It is almost certain that the scatter of Yalin's diagram is due mainly to the inapplicability of this assumption ...

Allen (1970), using dimensional reasoning, suggests that the spacing of dunes is a function of the ratio of flow depth to grain diameter, and of a dimensionless sediment transport rate. From this, according to Allen, it may be deduced that the spacing is approximately equal to five times the flow depth. This was the whole of his theoretical development of the subject. He fitted a linear curve to experimental observations and determined that "the constant of proportionality is nearer 10 than 5." The range of depths represented in his experiments was limited; field observations suggested that dune spacing follows the relation $L = 1.16\ d^{1.55}$, where d is the flow depth. Using the same data, he showed that dune height varied with water water depth as: $H = 0.086\ d^{1.19}$.

Once again, the empirical curve clearly follows the trend of the data, but with a large amount of scatter. Data available

from the literature, plotted in Figs. 1 and 2, shows little dependence of bed-form size on flow depth (Allen and Friend, 1976; Belderson and Stride, 1966; Boggs, 1974; Bokuniewicz, et al., 1977; Boothroyd and Hubbard, 1975; D'Anglejean, 1971; Dingle, 1965; Dyer, 1971; Green, 1975; Harvey, 1966; Hine, 1975; James and Stanley, 1968; Karcz, 1972; Keller and Richardson, 1967; Knebel and Folger, 1976; Kumar and Sanders, 1974; Loring, Nota, Chesterman, and Wong, 1970; Ludwick, 1972; Rubin and McCulloch, 1980; Singh and Kumar, 1974; So, Pierce, and Siegel, 1974; Southard, 1975; Stride, 1970; Terwindt, 1970; Visher and Howard, 1974). In specific environments, other investigators mention this lack of depth control on bed-form size (Boggs, 1974; Bokuniewicz et al., 1977; Briggs, 1979; Coleman, 1969; Jackson, 1975a; Stride, 1970; Terwindt, 1970; Werner and Newton, 1975).

What, then, controls the ultimate height and spacing of a bed form? This is a complex problem, not fully understood; the treatment of the hydraulic resistance of mobile sand beds is not fully developed, and an explicit evaluation is not yet possible. Gill (1971) extended his examination of Yalin's model and allowed the hydraulic resistance to vary. The ratio of bed-form height to flow depth then becomes an intricate function of Froude number, critical and total shear stress, a bed-form shape factor, the velocity and friction factor, and the rate of change of these variables.

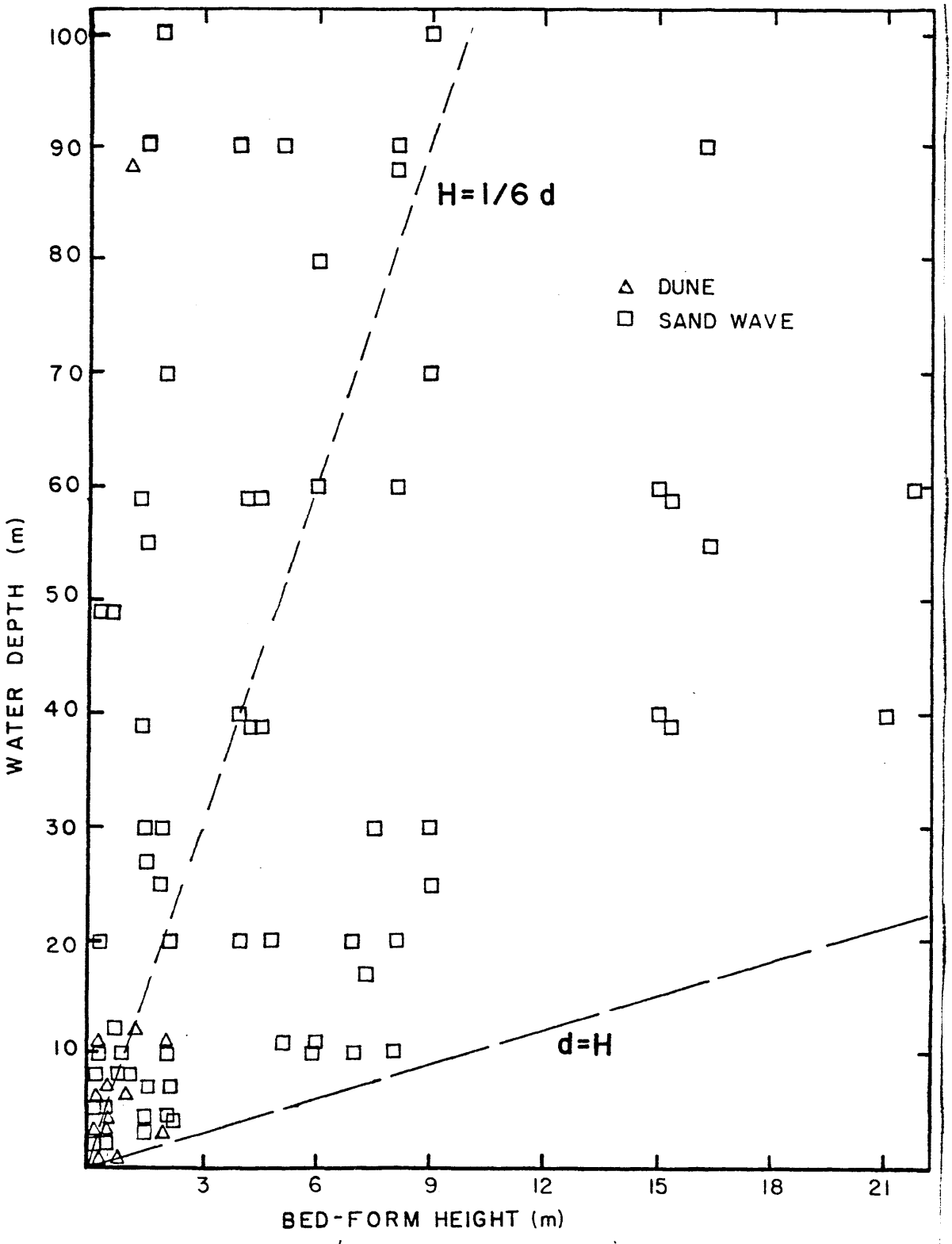

FIGURE 1 -- Flow depth versus bed-form height for field data cited in the text.

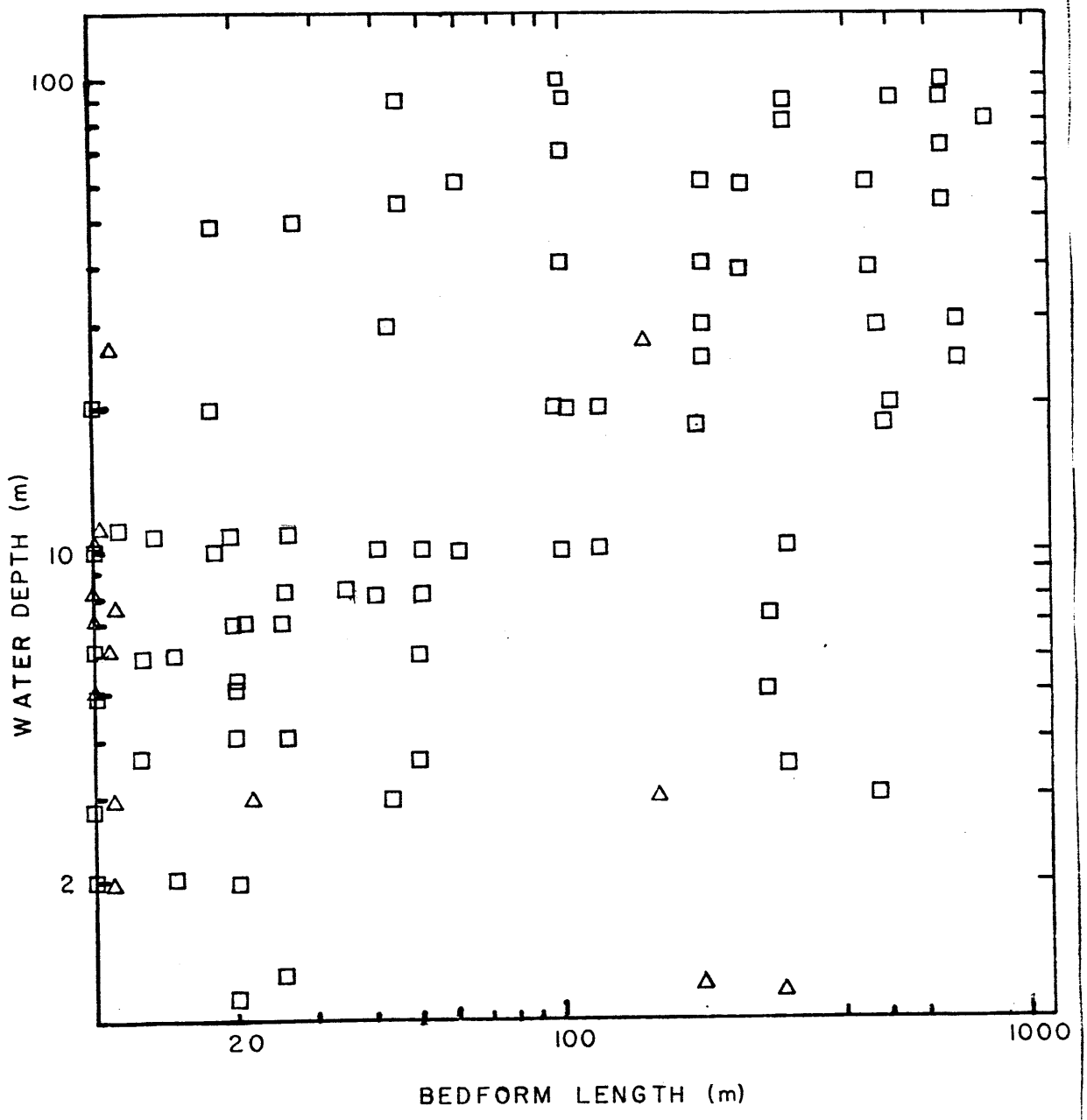

FIGURE 2 -- Flow depth versus bed-form spacing for field data cited in the text. (Triangles = Dunes; Squares = Sand Waves)

Fredsøe (1979), although primarily concerned with unsteady flow, derived a model for the equilibrium states of dune height and water depth. For a river with constant water discharge, he found that the dimensions of the bed forms are uniquely determined by the water-surface slope and the sediment properties (size, sorting, and fall velocity). The model was tested against the results of Gee's (1975) experiments on suddenly varied flow and found to be in reasonable agreement.

Fredsøe (1981) extended his earlier analysis to include the change in dune height at high sediment transport rates, where suspended-load transport is significant. His model predicts that if the bed shear stress is increased, the bed load would try to increase dune height, while the suspended load acts oppositely, trying to destroy the dune.

These more complete analyses of the bed-form height problem show that many factors affect bed-form size. Flow depth is one variable, important only as it acts in concert with other system variables to control the bed shear stress, and ultimately the bed-form height.

Theoretical Models

Theoretical investigations (Yalin, 1964; Richards, 1981) have led to models of steady, unidirectional flow over a cohesionless bed of sediment that produce only two types of transverse forms with avalanche faces. At a length of 60 cm, ripples

are separated from dunes, each the result of a distinct mode of instability in the two-phase flow system.

An instability in the flow of sediment generates ripples whose dimensions are governed by the local bed properties, most notably the grain roughness. Ripple size is independent of flow depth in these models.

The second mode of instability has a wavelength that depends primarily on the depth of flow. Dunes are the corresponding bed configuration, their height growing with increasing flow depth.

Jackson (1976a) proposed a similar two-scale bed form hierarchy. Its bipartite nature was suggested by flow-visualization experiments (Kline, Reynolds, Schraub, and Runstadler, 1967; Offen and Kline, 1975). These experiments indicated that the turbulent boundary layer can be divided into two zones: an inner zone, whose properties scale with the boundary variables; and an outer zone, whose characteristics scale with the hydrodynamic variables of the entire flow.

Ripples are the bed configuration ("microform") governed by the turbulent structure of the inner zone (the viscous sublayer). The size and spacing of ripples scale with the inner variables (shear velocity, kinematic viscosity, and grain roughness). When the grain roughness exceeds a certain size, the inner zone is disrupted, and microforms (ripples) cannot form. In this way

the model explains the disappearance of the ripple bed configuration with increasing grain size (as seen by Southard and Boguchwal, 1973).

Dunes and sand waves (grouped as a class called "mesoforms") scale with the outer variables (free-stream velocity and boundary-layer thickness) and reflect the hydrodynamic regime in the outer zone. The mean spacing of the mesoforms is proportional to the boundary-layer thickness; the spacing of these "dune-like large-scale ripples" equals the length scale formed by the product of the free-stream velocity and a turbulent time scale (Jackson, 1976a).

Jackson compared turbulence measurements in field settings with laboratory experiments and found that they "suggested" a preservation of similarity. He also found that time scales of on the free surface of rivers is comparable to that of the bursting period seen in flumes.

There are several problems with Jackson's model. The turbulent flow structure that is the basis for his theory has been seen only over smooth, immobile beds. In experiments with a mobile bed, Gust and Southard (in prep.) showed that the viscous sublayer does not exist. Dune spacing is taken to be determined by the generation and spacing of boils and kolks. Jackson attributes these effects on the free surface to "bursting and lift-ups" without taking into account the effects of flow separation over the dune crests. Thus the experimental

systems on which Jackson based his model may have little kinematic or dynamic similarity to natural systems.

Allen and Collinson (1974) addressed the problems of classifying large-scale bed forms under unidirectional aqueous flows from an observational viewpoint. They cite theoretical investigations and laboratory observations of bed forms of several scales. All scales are active at the same time only under "nominally" steady flow. The term "nominally" is never defined; that is, how unsteady a flow may be and still be termed "steady" is not addressed. Allen and Collinson conclude from their study of natural unidirectional flows that superimposition of large-scale bed forms occurs where there are rapid and large flow changes.

Allen and Collinson (1974) believe that under fluvial flows (typically unsteady) only one hydrodynamically distinct kind of large bed form is present in the cases of bed-form superimposition reported. Where two or more orders of bed forms are observed, only the smallest members are active. Hence, they classify all large transverse bed forms found under unsteady flows as dunes.

Evidence to the contrary, for two types of large-scale bed configurations, was cited in the previous section, and is discussed in the next section. There are sufficient differences in the morphology and kinematic behavior of dunes and sand waves to warrant the distinction. The different types of internal

structures generated by the two forms make it geologically important to distinguish dunes from sand waves.

Observational Differences Between Dunes and Sand Waves

Sand waves and dunes are differentiated by most investigators on the basis of spacing criterion. This is generally due to the methods of data collection (mainly sonic depth profiling). It sometimes reveals a gap in bed-form spacing, distinguishing dunes from sand waves (Klein, 1970; Boothroyd and Hubbard, 1975; Hine, 1975). Where a three-dimensional picture of the bed forms is available, the spacing criterion is often coupled with general morphologic criteria. These may include lee-face slope, crestline morphology, and superimposed bed forms. Several field studies indicate that sand waves and dunes may be divided on the basis of internal structure (Klein, 1970; Harms, Southard, Spearing, and Walker, 1975; Knight, 1977).

Dalrymple (1977) was able to divide sand waves (occurring on an intertidal sand bar) on a bivariate plot of height against spacing. He finds that this plot permits almost perfect separation of these two configurations by the line:

$$H = (0.072)\ L - 0.210$$

when he plotted H and L in meters. Dunes, the shorter and steeper form, fall to the left of this line, while the long and low sand waves cluster to the right. Unfortunately, such a graph is seen to be system-specific, as it merely quantifies the steepness criterion mentioned by other researchers (Boothroyd

and Hubbard, 1975; Klein, 1970; Hine, 1975). That is, although a line may be drawn dividing dunes and sand waves in a particular setting, that dividing line will be different in each setting and is not applicable to other areas.

A plot involving more general parameters that specify the condition of the system would be of greater use in deciphering the dynamics of the bed forms. Such a plot has been proposed by Southard (1971; see also Vanoni, 1974) and used by several investigators (Costello, 1974; Boguchwal, 1977; Dalrymple et al., 1978; Rubin and McCulloch, 1980). This diagram is based on the properties of the sediment, fluid, and flow. It has the property that each point on the diagram corresponds to one and only one bed state. As all important system variables are included, there is no overlapping of bed-phase stability fields.

There are seven independent variables (of first-order importance) in the system under consideration:

U = mean flow velocity
d = mean flow depth
D = mean sediment size
ρ_s = sediment density
ρ = fluid density
u = dynamic fluid viscosity
g = acceleration of gravity

Of these, only the first three vary appreciably in natural systems. Hence, two plots (depth-velocity, and velocity-size) serve to display all the pertinent relations. Figures 3, 4, and 5 display the data from Tables 2 and 3 (for bed forms in marine and fluvial environments).

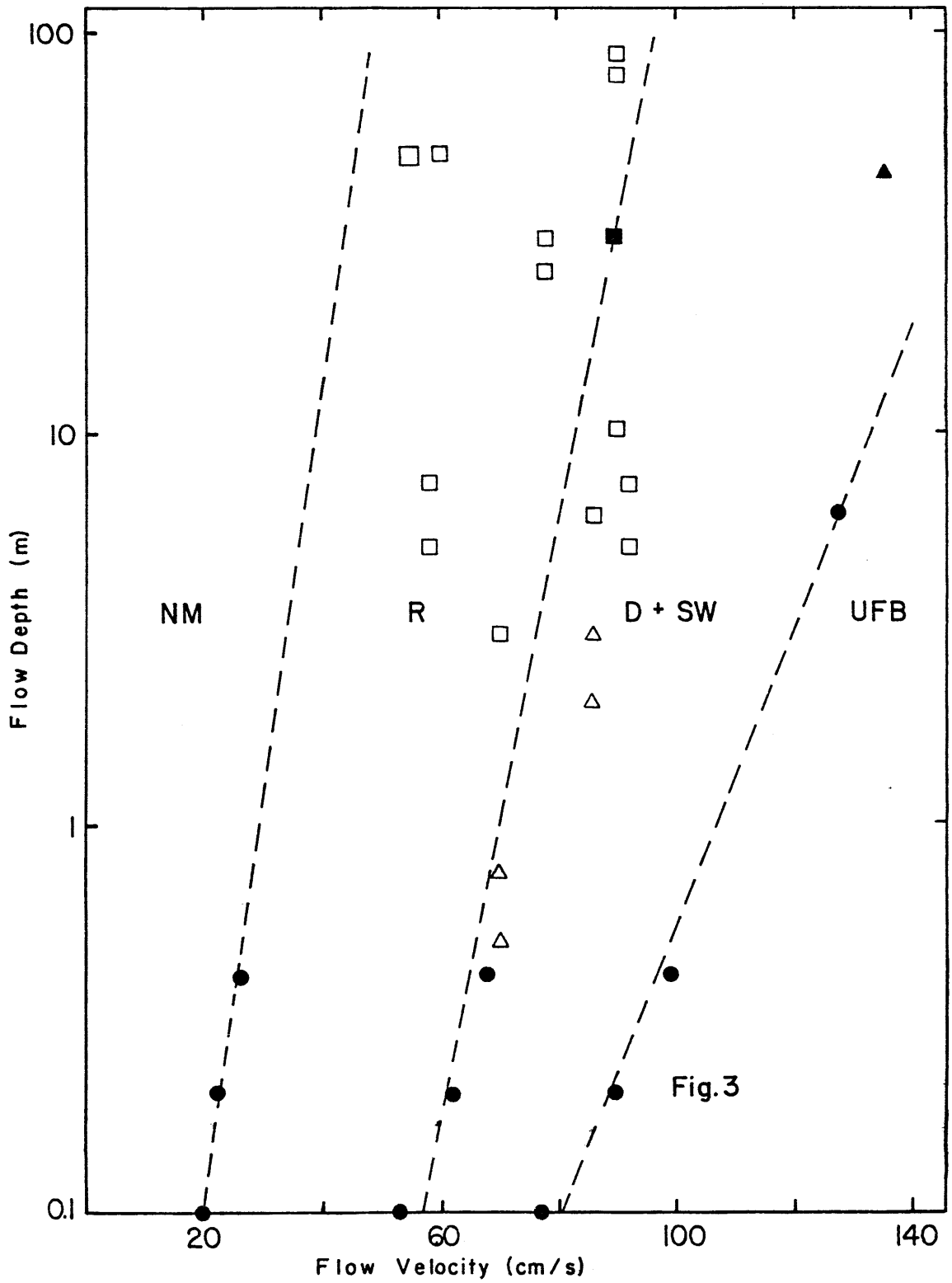

FIGURE 3 -- Flow depth versus flow velocity for fine sand from field data cited in the text. (Boundaries and blacked-in points from Rubin and McCulloch, 1980; Triangles = Dunes, Squares = Sand Waves)

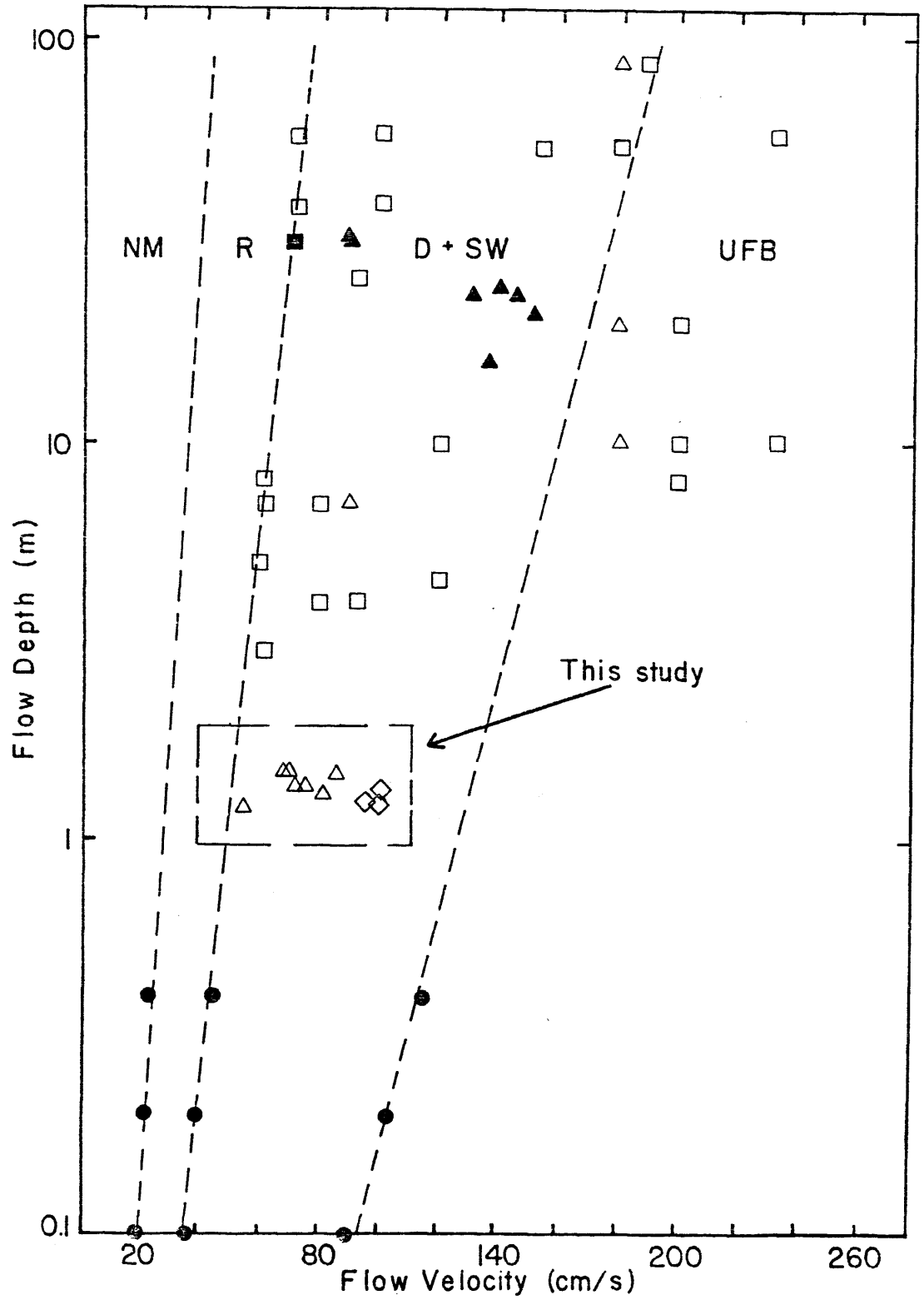

FIGURE 4 -- Flow depth versus flow velocity for medium to coarse sand from field data cited in text; includes bed forms generated in this study. (Boundaries and blacked-in points from Rubin and McCulloch, 1980; Triangles = dunes, Squares = sand waves, Diamonds = higher velocity dunes.)

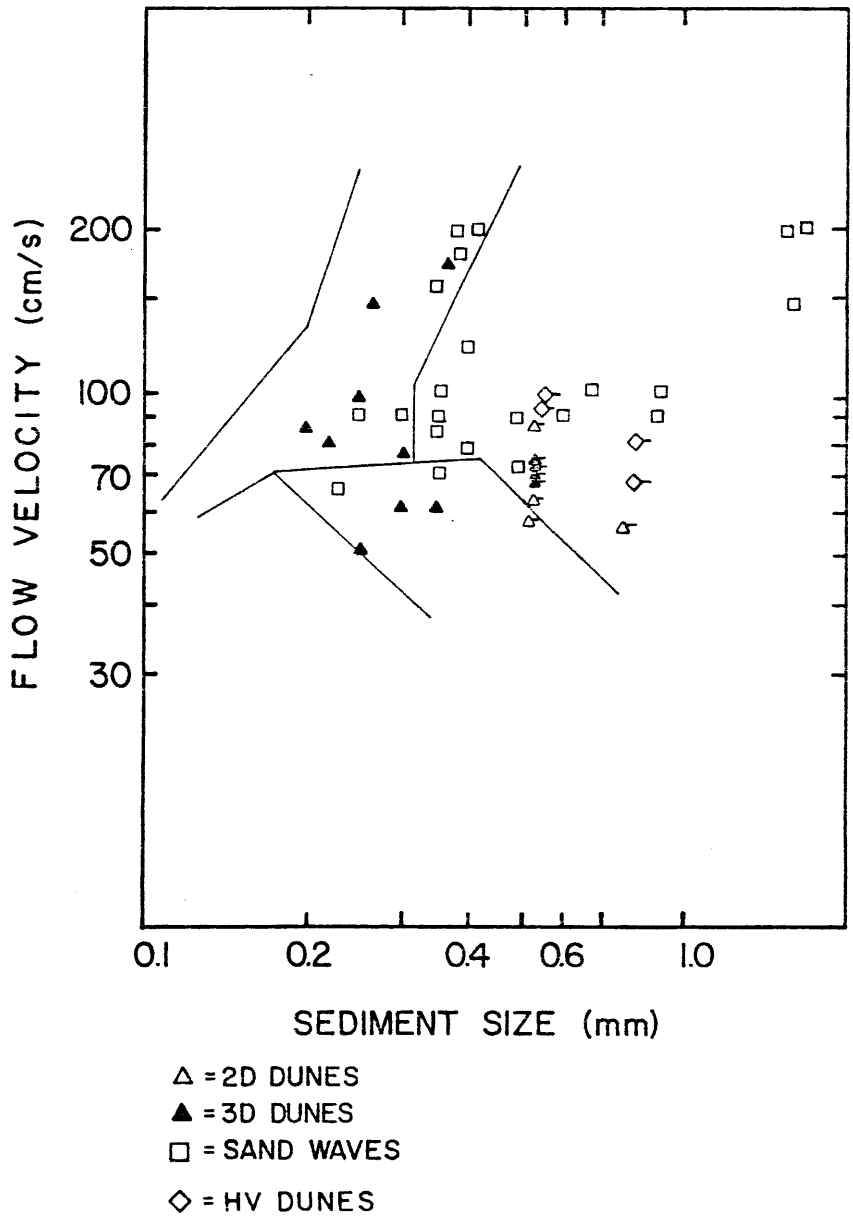

FIGURE 5 -- Flow velocity versus sediment size for flow depths greater than 1.0 m. Data are from field studies cited in the text; points with ticks are from this study. (Phase boundaries from Dalrymple et al., 1978)

Sand waves, originally defined on the basis of their geometry, have a well defined stability field in the velocity-size diagram, distinct from dunes. The depth-velocity diagrams show more scatter, with the fields for dunes and sand waves overlapping to a large degree. This agrees with the findings of Dalrymple et al. (1978); they also were able to break out Type 2 megaripples from sand waves only in a velocity-size plot. The graphs presented here extend their findings (from the intertidal environment) to many environments (shallow marine, fluvial, and large flume).

Problems with Field Studies

Observational Difficulties

From the data presented above, one can see a number of problems with field studies. First is the difficulty in actually seeing what is happening. In rivers, the water is seldom clear enough for direct observation or photography during active bed-form migration. Often bed forms are studied at low stages of the river, permitting direct access but giving rise to problems of low-flow modification.

Marine bed forms are often studied in the intertidal or shallow subtidal zone. Here, the water is often sufficiently clear for direct observation of bed forms and their migration.

The bed forms may also be examined if exposed at low tide, although they may be partially or completely modified by the ebb flow.

In deeper water, on the open shelf, direct observation is seldom workable, and most data come from sonic depth sounding, both profile and side-scan. Depth sounding has a number of problems. Its resolution may not be sufficient to discern bed forms superimposed on the major bed features. To study this problem, Bouma and others (1980) compared data from side-scan sonar, high-resolution sonic profiling , bottom television, and bottom sampling. They found that interpretations of bed-form and bottom characteristics based solely on sonographs can be in error. The quality of sonar records is strongly influenced by the amount of ship pitching, sea state, and the direction of the current with regard to the ship's heading. This study demonstrates the need to integrate multi-scale observations and sampling in order to correctly classify the bottom characteristics.

Disequilibrium Effects

The effect of unsteady flow upon the bed state in natural environments causes two areas of concern: the extent of disequilibrium (between the bed state and the superjacent flow) and its effects; and whether two or more orders of bed forms may migrate at equilibrium under the same flow.

A completely equilibrium reference state is usually lacking, hence it is difficult to assess the consequences of bed-state disequilibrium in natural flows. It has been implicitly assumed by most investigators that changes in bed state lag behind changes in flow conditions.

Allen (1974, 1976a, 1976b, 1978a, 1978b) has specifically addressed this subject at great length. Bed forms under natural flows are not in instantaneous equilibrium with the prevailing processes because (Allen, 1976a):

(1) a change in the character of the forms necessitates sediment and/or solute transport, which is a measure of process intensity and proceeds at a finite rate.

(2) natural process act unsteadily.

Bed forms can exhibit stable patterns of adjustment to processes of changing intensity, provided that the process intensities vary in a more or less regular sequence or pattern. The characteristics of these forms then respond to changing process intensity "according to a stable limit cycle" (Allen, 1976b). The phase and range of this cycle depends on the time scale of the process variation and of the bed-form response. The relative magnitude of the two time scales determines the extent of bed-state disequilibrium.

Southard (1975) divides the extent of disequilibrium into three ranges, based on the rate of change of flow conditions relative to the response rate of the bed forms:

(1) bed forms that are only slightly out of equilibrium with variations in the flow;

(2) bed forms that are generated and modified by a single flow event (e.g., a tidal cycle, a storm generated current, a flood in a river), but are always markedly out of equilibrium with the flow;

(3) bed forms that are large enough relative to modifying effects of changing flow depths that they are changed little by a given flow event; if such flow events are repetitive, a particular set of intermediate flow conditions might then characterize the bed configuration.

How far out of equilibrium a bed configuration may be in a given situation is governed by the size of the bed form ($\propto$ volume of sediment to be moved), the velocity range under which the bed form migrates ($\propto$ sediment transport rate), and the time scale of the flow ($\propto$ sediment flux). In most tidal environments marked by asymmetry of ebb and flood currents, these factors are such that ripples are never far out of equilibrium. Dunes may be initiated, grow, and be completely reworked over single tidal cycles, though always lagging somewhat behind the changing flow conditions. Sand waves, while showing net migration, persist almost unchanged over many tidal cycles, being in equilibrium with the "average" flow.

The degree of disequilibrium depends upon its time-discharge curve; that is, on the magnitude and duration of high-stage flow. Except in the smallest rivers, ripples and dunes are largely in equilibrium with the flow. Sand waves typically lag somewhat behind the changing flow, being "undersized" on the rising stage and "oversized" on the falling stage (Allen, 1974; Pretorious and Blench, 1951).

Whether assemblages of bed forms are an equilibrium phenomenon is the second problem. Dunes may be found superimposed upon sand waves in many environments. Some investigators attribute this to lag effects (Allen and Collinson, 1974), while others clearly see both these forms as being in simultaneous equilibrium with the superjacent flow (Harms et al., 1975; Dalrymple, 1977; Jackson, 1976b).

In the Bay of Fundy, virtually all sand waves have dunes (generally Type 2 megaripples) superimposed upon their stoss slopes; echo-sounder records show this to represent an equilibrium assemblage. Ripples on sand waves are a relatively rare assemblage, suggested by Dalrymple et al. (1978) to be a disequilibrium form of megarippled sand wave because it almost always occurs in situations of decelerating flow. Also, the stability field for rippled sand waves in Fig. 6 is seen to overlap considerably with that of Type 1 megaripples and megarippled sand waves. Thus, Dalrymple et al. (1978) propose that the sequence of bed configurations with increasing flow velocity is:

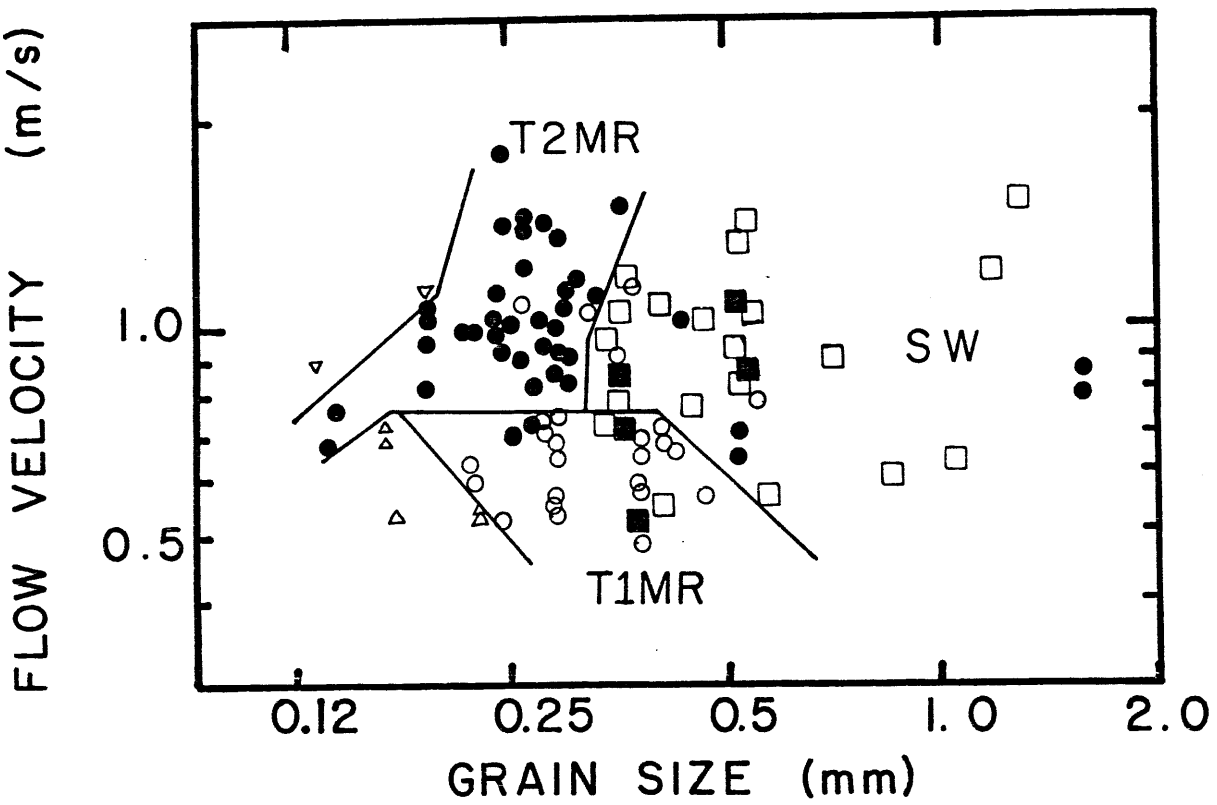

FIGURE 6 -- Flow velocity versus grain size (Data from Dalrymple et al., 1978, Bay of Fundy study); their phase boundaries).

Triangles =	Ripples
Inverted Triangles =	Upper Plane Bed
Circles, open =	Type 1 Megaripples
Circles, closed =	Type 2 Megaripples
Squares, open =	Megarippled Sand Waves
Squares, closed =	Rippled Sand Waves

Ripples → TlMR (2D Dunes) ↗ T2MR (3D Dunes) - in medium sands

Ripples → TlMR (2D Dunes) ↘ Megarippled SW - in coarse sands

With decreasing flow strength the sequence would be:

Megarippled SW → Rippled SW → TlMR - in coarse sands

This area of disequilibrium effects has been little studied, and a general bed-configuration sequence with increasing and decreasing flow is unknown.

Differences In Environments

Field data on large-scale bed forms come from a variety of environments. This variety itself may be a major source of scatter in the data, beyond the different data-collection problems each poses.

This variation in settings has been explicitly addressed by Boothroyd (1978) for the tidal nearshore environment - one of the major sources of data (Boothroyd and Hubbard, 1975; Dalrymple, 1977; Dalrymple et al., 1978; Hine, 1975; Klein and Whaley, 1972; Knight, 1972; Langhorne, 1973). Davies (1964) classified shorelines on the basis of tidal range: microtidal (range less than 2 m); mesotidal (range 3 to 4 m); and macrotidal (range greater than 4 m). From a study of worldwide coastal charts, Hayes (1975) related variations in the morphology of depositional shorelines to variations in tidal range. This variation is reflected in the bed-form patterns, sedimentary structures,

detailed morphology, and stratigraphic sequences of these areas. Factors accounting for this variability are tidal range, type of tide, amplitude difference between spring and neap tides, and the relative importance of tidal energy and wave energy. The most direct effect of tidal range is the volume of water moving in and out of the system in a given time. This is directly proportional to the velocity of the current generated. Its other first-order effect is the actual depth of water available for the growth and migration of the bed forms.

The type of tide -- diurnal, semidiurnal, or mixed -- sets the time scale of the flow, affecting the strength and duration of the currents. It also has an important effect on the time-velocity asymmetry of the tidal currents.

Amplitude difference between spring and neap tides controls the variability of the tidal prism. Increased amplitude means an increased tidal prism; a larger tidal prism means that more water must move in and out of the system in the same amount of time, hence increased current velocities. This monthly cycle sets a second time scale for the system; the time history of the current affects the equilibrium of the major bed forms.

Waves, the other source of energy, have a major effect on microtidal coasts. Their influence is considered to be minor on macrotidal coasts, where tidal currents dominate the energy spectrum. Waves and tides are of subequal importance in mesotidal systems. Commonly waves and tides switch dominance in

this environment from season to season, or due to the passage of storms.

Problems with field studies resolve themselves into two primary areas: observational difficulties, and system variability (most notably disequilibrium effects). Advances in data collection allowing integration of multi-scale observations will improve the data base. Unsteady flow will continue to obscure the basic nature of the bed configurations with complex secondary effects.

LARGE-SCALE BED CONFIGURATIONS IN FLUMES

Most of our basic knowledge of the dynamics and kinematics of bed forms is the result of flume studies (Gilbert, 1914; Vanoni and Brooks, 1957; Simons and Richardson, 1962, 1963; Guy, Simons, and Richardson, 1966). This is due to the ease of observation and control of system variables possible in this setting.

Classically, a flume run starts with a flat bed of sediment, and the flow velocity is increased in increments at a constant flow depth. The flow is kept at each velocity step until the bed state is in equilibrium with the flow. Flume studies have been carried out at flow depths of 5 - 50 cm, in sediment that ranges from coarse silt to gravel. Most studies, and all concerned with bed-form behavior, have used quartz or quartz-density sand. Table 5 contains a representative sample of experimental observations.

TABLE 5 -- Laboratory observations of large-scale bed forms

	Flume Length (m)	Flume Width (b)	Depth Range (h)	h/b	Mean Velocity (cm/s)	Sediment Size (mm)	Bed-Form Height (cm)	Bed-Form Spacing (cm)
Costello (1974)	11.5	91.5cm				0.51-0.79		
Bars			14.6-15.9	0.16-0.17	34.4-45.1		0.05-4.6	20-190
Dunes			14.6-15.6	0.16-0.17	46.6-50.3		0.60-6.6	20-110
Costello (1974)	5.5	17cm						
Bars			5.4-5.8cm	0.32-0.34	42.0-46.0	1.14	Combined with	
Dunes			4.9-5.2cm	0.29-0.30	47.0-57.0		11.5 m flume data	
Pratt (1971)	21.3	137cm				0.49		
Flattened Dunes			7.6-45.7	0.05-0.33	32.6-59.4		0.58-5.8	13-130
Dunes			7.6-30.5	0.05-0.22	39.9-70.1		0.55-5.5	16-114
Chauvin & Chabert (1963)	21	80cm	< 70 cm	N/R	N/R			
Bancs						0.96-2.72	N/R	N/R
Dunes						0.45-2.72	N/R	N/R
Boguchwal (1977)	27	2.7m				0.11-0.25		
Sand Waves			46.0-51.0	0.17-0.19	55.0-68.0		3.0-13.0	20-230
Dunes			45.0-53.5	0.17-0.20	60.0-86.0		10-37	75-520

In fine to medium sands, the bed-configuration sequence with increasing flow velocity is: no movement -- ripples -- dunes -- flat bed (Simons and Richardson, 1966). Ripples are not formed in sands coarser than 0.7 mm diameter (Southard and Boguchwal, 1973).

Dunes

The dune configuration may be divided into two subphases: two-dimensional (2D) dunes and three-dimensional (3D) dunes (Costello and Southard, 1981).

Two-dimensional dunes are long and low, with generally staight, continuous crests, showing little scour downstream of the slipface. Variously termed "bancs" (Chabert and Chauvin, 1963), "bars" (Costello and Southard, 1971; Costello, 1974), or "flattened dunes" (Pratt, 1971), they are formed at relatively low flow velocities. Two-dimensional dunes are similar in spacing and height to the classic type of dune and with increasing flow velocity become more and more dunelikein geometry.

Two-dimensional dunes appear when the flow velocity is such that there is general grain motion on the bed (Costello, 1974). They appear as small areas of higher bed elevation, forming a slipface with relief of two to three grain diameters. Behaving like sediment "waves", they grow and then quickly attenuate downstream. Their rate of advance varies inversely with height; smaller waves overtake larger, slower waves, merging to produce higher slipfaces (up to 6 mm high). Only by this merging

process do 2D dunes grow, otherwise they tend to dissipate downstream. The spacing between consecutive slipfaces may be irregular or regular. At higher velocities these long and low forms grow to occupy the entire width of the channel. Boguchwal (1977) states that often the body of a 2D dune is not readily recognizable. In all cases, however, 2D dunes are associated with flat, unscoured troughs. This type of trough is diagnostic of the 2D dune bed configuration.

Three-dimensional dunes are more irregular than 2D dunes, being higher and shorter, and consistently associated with a scoop-shaped trough downstream of the slipface. In plan view their crestlines are sinuous, not extending across the full width of the flume. 3D dunes are quasi-periodic in spacing (Yalin, 1972). Sediment is transported over the backs of 3D dunes in strong, sheet-like flow, with much sediment thrown into suspension at the crest. Crests of 2D dunes are marked by simple avalanching of the sediment down the slipface.

The geometrical properties of 2D and 3D dunes allow them to be differentiated in several ways. Costello (1974) reported that 2D dunes have a large range of spacings (Fig. 7). The range of spacings of 3D dunes overlap that of 2D dunes, but has a different mode and not so great a spread of values. 3D dunes have larger heights, with 2D dunes again showing a wide range of heights. Hence, 2D dunes are characterized as long and low forms displaying a great (almost random) variation in spacing.

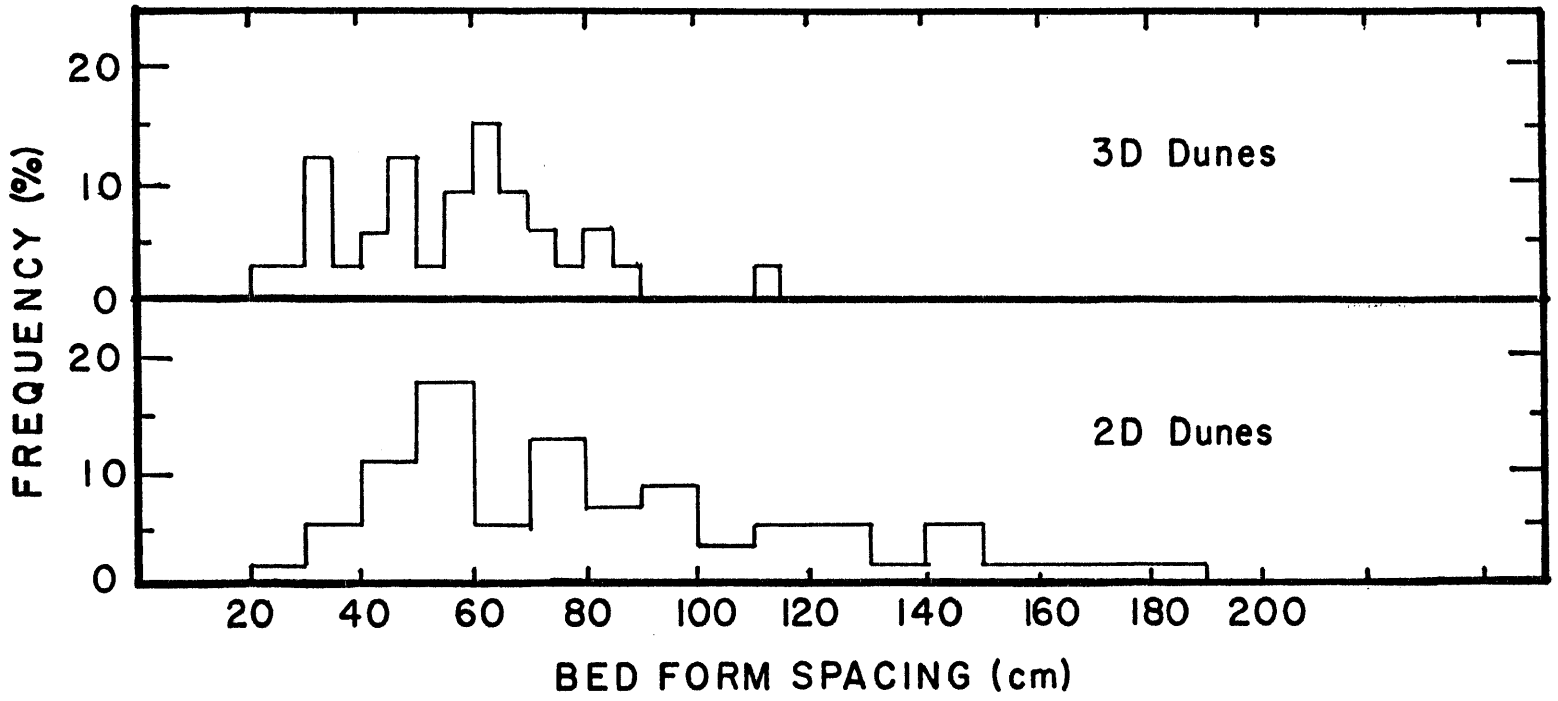

FIGURE 7 -- Histograms of bed-form spacing (after Costello, 1974)

3D dunes have greater and more variable heights, and large but fairly regular spacings.

The development of the different bed phases can also be delimited in terms of the mean flow properties (Pratt, 1971). The development of 2D dunes is marked by a lower rate of increase in energy slope with increasing velocity than for ripples (Fig. 8a). The range of mean velocity for which 2D dunes develop in coarse sands is marked by a decreasing bed friction factor ($f_b = 8(u*/U)^2$, where $u* = (\tau/\rho)^{1/2}$, the shear velocity, and U = mean flow velocity). The 3D dune range shows a trend of increasing bed friction factor (Fig. 8b). These two hydraulic characteristics of 2D and 3D dunes emphasize that the two superficially similar bed configurations are indeed hydraulically different. Costello (1974) concluded that the differences in form and hydraulics of the two subphases reflect different mechanisms of formation. Costello and Southard (1981) view all dunes as kinematic shock waves; the subphase differences are attributed to the different relative importance of shock-wave coupling and of sediment transport in bed-form troughs.

Problems With Flume Studies

Existing flume studies are not the total self-contained answer to the problems of the kinematics and dynamics of large-scale bed forms. The problems arise from the actual physical scale of the flumes used, along with their rigid boundaries.

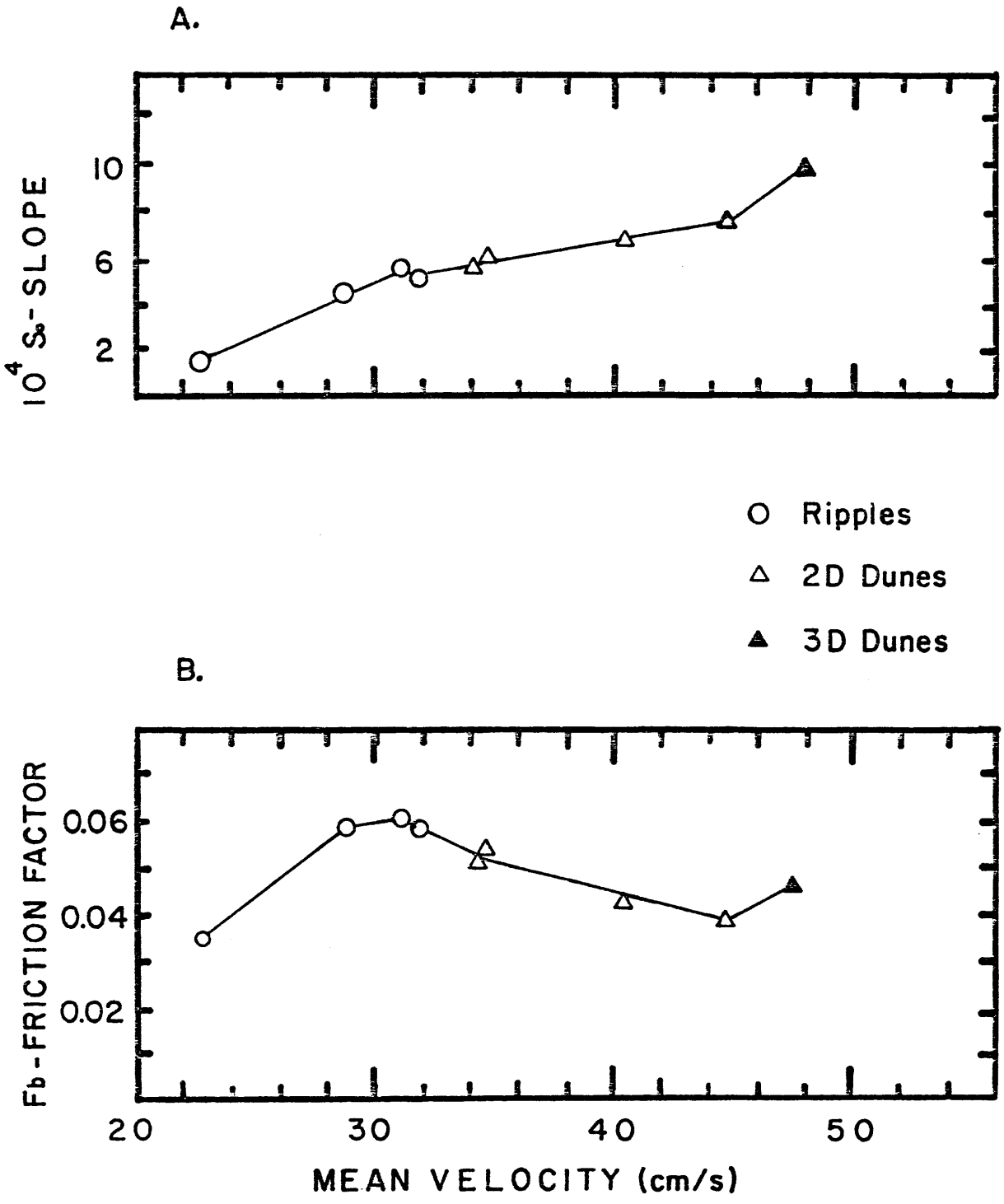

FIGURE 8 -- A. Energy slope versus flow velocity (after Costello, 1974).

B. Friction factor versus flow velocity (after Costello, 1974).

The length scales are often too small. Dunes and sand waves may not have enough room to grow in height; the crests become planed off. There may not be a sufficient working length of uniform flow conditions for the bed forms to develop. The presence of side walls constricts bed-form development in the cross-stream direction. Specifically, the development of three-dimensionality is restricted when the crest length is short relative to the bed-form spacing. Also, the depths and discharges achievable in flumes are fairly limited (see Fig. 12). The cross-stream restriction on the bed-form geometry and the narrow range of conditions attainable are the two major drawbacks to flume studies.

The rigid boundaries also affect the flow pattern and shear-stress distribution. Data from a series of experiments on the effect of channel width in flume studies reveal two competing trends (Williams, 1970). (In Williams's experiments, the flume width was varied from 7.5 to 119 cm in flow depths of up to 21 cm; the bed was covered with dunes.) For a given depth and flow velocity, decreasing the flow width increased the water surface slope. However, the rate of decrease of the hydraulic radius relative to the increasing water surface slope was such that the boundary shear stress decreased. (In uniform flow the boundary shear stress is proportional to the product of the hydraulic radius and the slope.) As the width decreases, the walls form a larger portion of the wetted perimeter. Being much smoother than the sand bed, the walls generate less resistance to the flow.

Hence, the boundary shear stress decreases with decreasing width for a given flow depth and velocity. Using a small width-to-depth ratio in a given set of experiments will yield smaller shear stresses than those which would be determined for "two-dimensional" flow. Most investigators recognize these problems and try to generate as nearly two-dimensional flow as possible. It is advantageous, however, to use a small width-to-depth ratio in order to attain deeper flow depths. This may shift the bed-phase boundaries somewhat, but will not alter the basic existence and overall geometry of the bed forms. Thus, one must balance the two-dimensionality of the flow against the flow depth; inaccuracy in shear-stress determination seems a small price to pay to attain a larger range of depths.

Distribution of the boundary shear stress is nonuniform across the flume cross-section. This causes secondary currents with helical flow patterns. The secondary flow has only minor effects because the magnitude of these cross-stream currents is only a small fraction of the mean velocity. When the bed forms are large and robust, secondary circulation is unimportant: the mean current and the transverse vortices generated to the lee of the bed forms overpower the secondary currents.

Flumes and rivers behave differently in the way that the bottom shear stress and the flow adjust to change. Flumes are usually constructed to operate with constant depth and discharge and a variable slope. In rivers (for a particular reach, at a particular time) the energy slope and discharge are constant,

and the depth varies. In natural flows the depth and discharge may vary over relatively short periods of time.

Although the temporal variability of natural environments can be simulated in the laboratory, the major constraint is still the length scale. What is needed is either a much larger flume or a nondistorting scale model.

EXTRAPOLATION OF FLUME DATA TO FIELD CASES

Extrapolation of flume data to natural environments is possible only in a general way. The two major differences in these settings is flow depth and disequilibrium effects found in the field. As Costello and Southard (1981) note, "... Owing mainly to difficulties of observing such bedforms [in the field] and sorting out effects of changing flow conditions, as well as to the impracticality of generating large-scale bed forms in the laboratory, there is not yet any general agreement about how to classify large-scale bed forms."

There is the problem of how one studies the bed forms in each setting. The kinematic and hydraulic characteristics seen in the flume are not readily discernible in the field. Internal structures used to differentiate among the bed configurations in the field have not been explicitly studied in the laboratory.

These problems are especially acute for very-large-scale bed forms. Due to the large mass of sediment contained, sand waves are the bed configuration most likely to lag behind

changes in flow conditions. At the shallow depths of flumes, 2D dunes are about the same size as 3D dunes. They become strikingly differentiated only at depths greater than the upper limit of existing flume data.

One may seek to compare the diverse natural settings with flume data in a dimensionless depth-velocity-size diagram (Southard, 1971). Rubin and McCulloch (1980) generated such graphs, combining flume data with their own observations of the floor of central San Francisco Bay. They found good agreement between the field data and the bed-phase boundaries determined from flume studies. Critical shear velocities calculated for the transitions from ripples to sand waves and from sand waves to upper-regime flat bed in flows tens of meters deep were within 10% of those observed for the same transitions in flumes. However, Rubin and McCulloch lump dunes and sand waves together do not discuss in detail on the extrapolation of bed-configuration sequences from flumes to field settings.

Figures 9, 10, and 11 are depth-velocity graphs (for fine, medium, and coarse sands) that compare data from flume studies (Pratt and Smith, 1972; Pratt, 1973; Southard and Boguchwal, 1973; Costello, 1974) and field studies (Neill, 1969; Klein, 1970; Sternberg, 1971; Boothroyd and Hubbard, 1975; Knight, 1972; Dalrymple, 1977). The position of the boundaries between ripples, dunes, and sand waves thus established show very good agreement between field and flume data. This would tend to indicate that 2D dunes are small-scale equivalents of sand waves.

FIGURE 9

FLOW DEPTH VS. FLOW VELOCITY FOR FINE SAND

R = Ripples
SW = Sand Waves
D = 2D Dunes
D = 3D Dunes
UFB = Upper Flat Bed

Data From:

Barton and Lin, 1955
Dalrymple, 1977
Guy, et al., 1966
Nordin, 1976
Vandi and Brooks, 1957

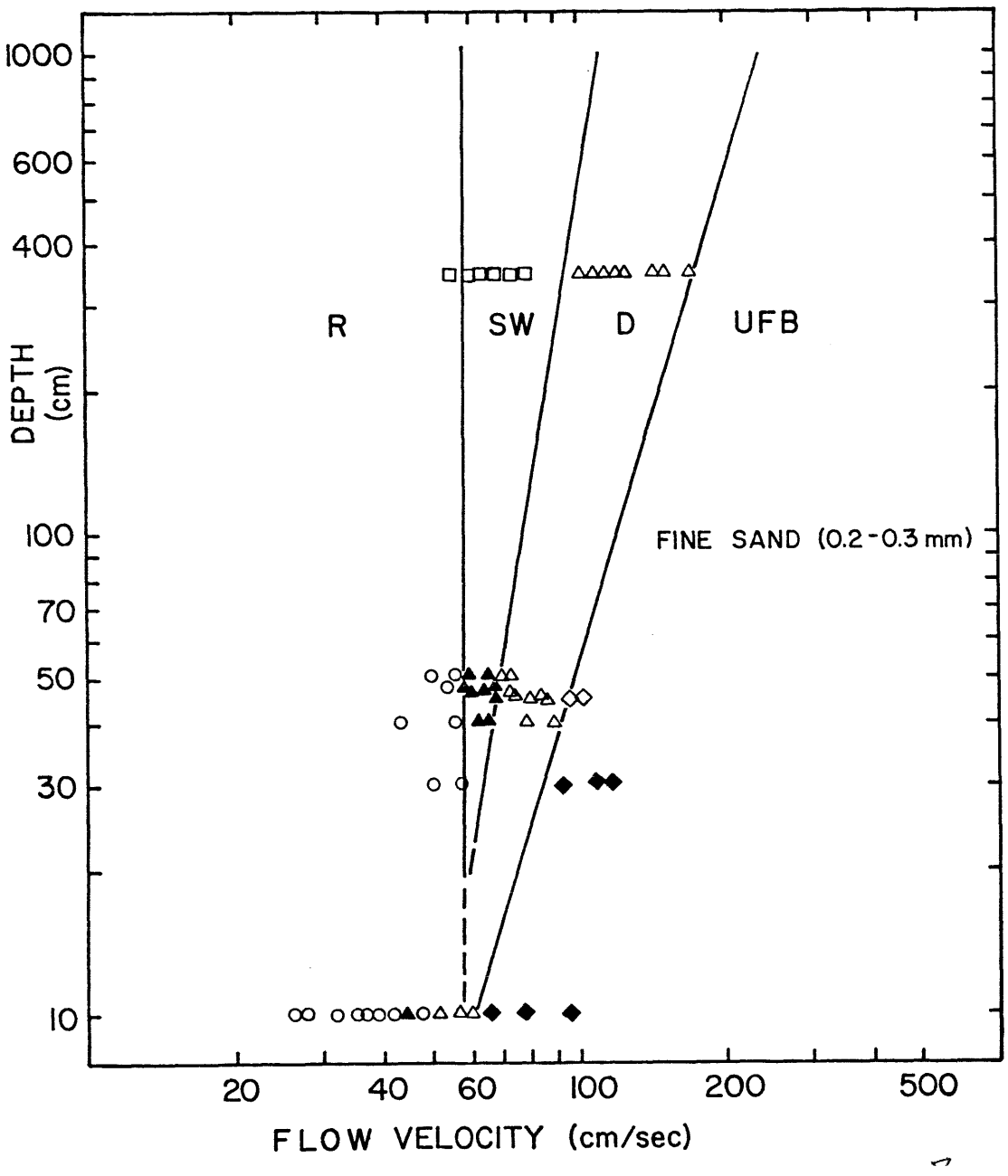

FIGURE 9 -- Flow depth versus flow velocity for field and flume data on bed configurations in fine sand cited in the text. Flume data are for flow depths less than 50 cm.

Open circles: ripples
Open triangles: 2D dunes
Solid triangles: 3D dunes
Squares: sand waves
Diamonds: upper flat bed

Data sources: Barton and Lin (1955), Dalrymple (1977), etc.

FIGURE 10

FLOW DEPTH VS. FLOW VELOCITY FOR MEDIUM SAND

NM = No Movement
R = Ripples
SW = Sand Waves
D = 2D Dunes
D = 3D Dunes

Data From:

Boothroyd and Hubbard, 1972
Dalrymple, 1977
Knight, 1972

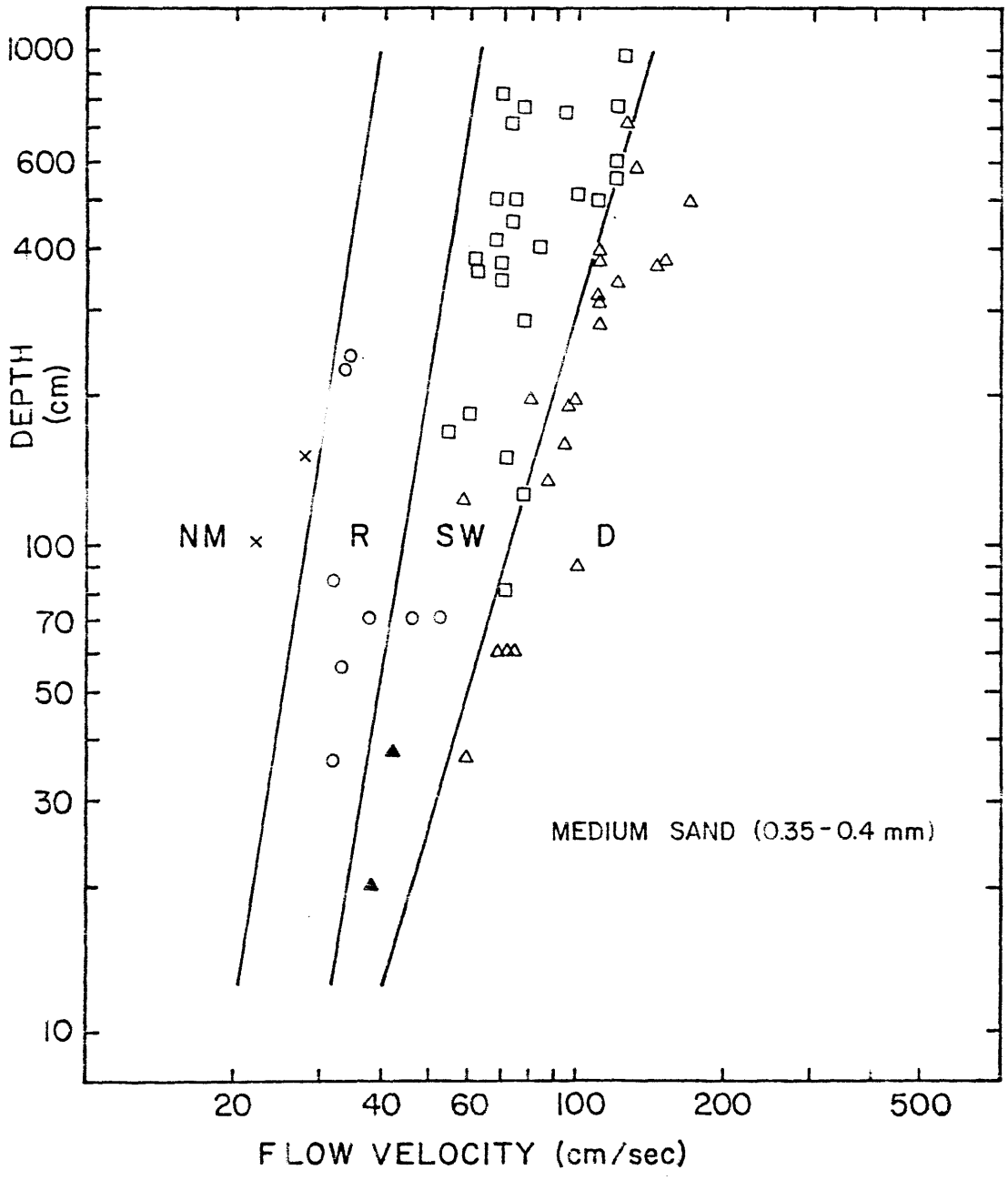

FIGURE 10 -- Flow depth versus flow velocity for field and flume data on bed configurations in medium sand cited in the text. Flume data are for flow depths less than 50 cm.

Crosses: no movement
Circles: ripples
Closed triangles: 2D dunes
Open triangles: 3D dunes
Squares: sand waves

Data sources: Barton and Lin (1955), Dalrymple (1977), etc.

FIGURE 11

FLOW DEPTH VS. FLOW VELOCITY FOR COARSE SAND

NM = No Movement
R = Ripples
SW = Sand Waves
D = 2D Dunes
D = 3D Dunes

Data From:

Costello, 1974
Klein and Whaley, 1972
Neill, 1969
Pratt, 1971
Pratt and Smith, 1972
Sternberg, 1971

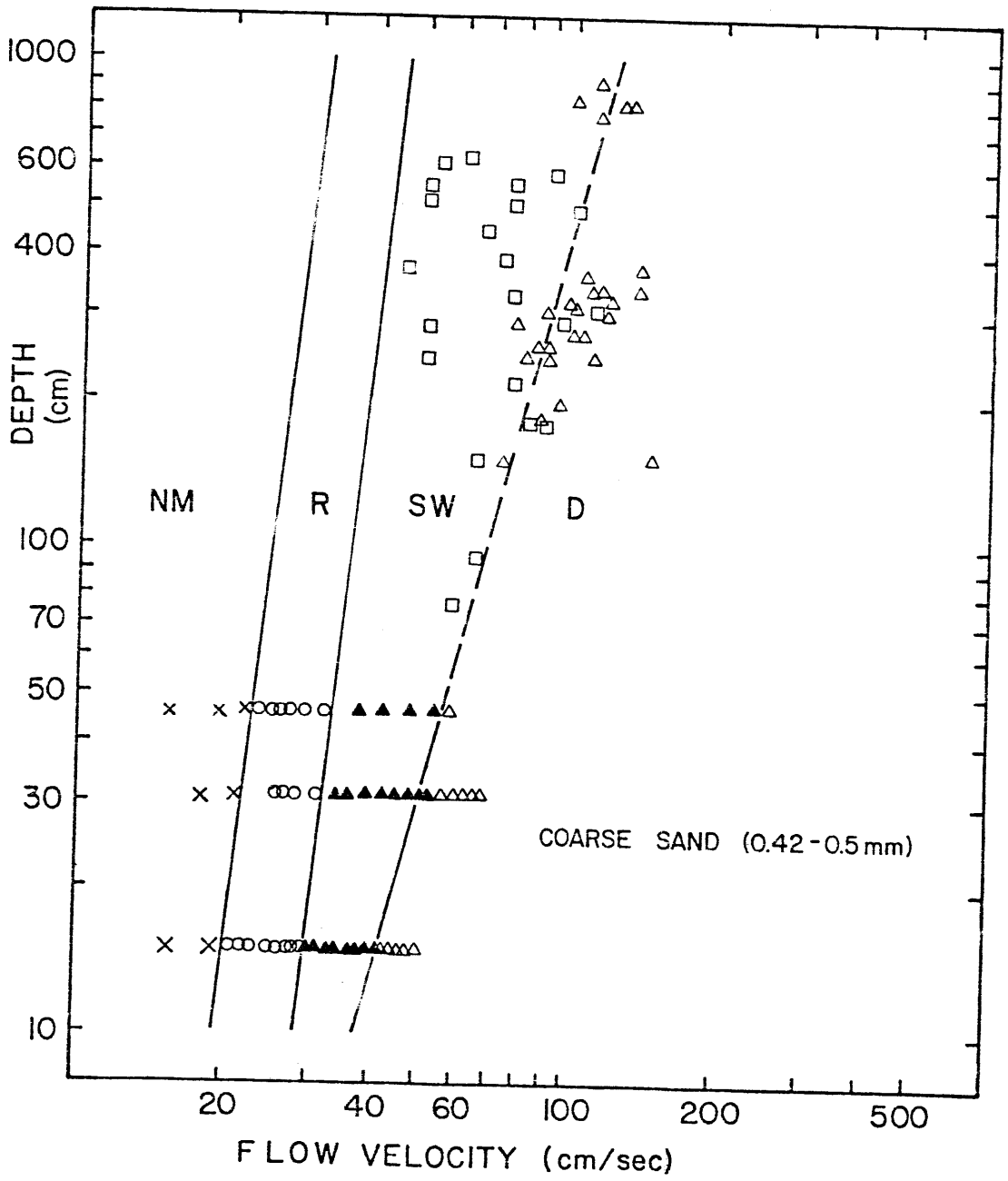

FIGURE 11 -- Flow depth versus flow velocity for field and flume data on bed configurations in coarse sand cited in the text. Flume data are for flow depths less than 50 cm.

Crosses: no movement
Circles: ripples
Closed triangles: 2D dunes
Open triangles: 3D dunes
Squares: sand waves

Data sources: Barton and Lin (1955), Dalrymple (1977), etc.

Problems with this interpretation are: size -- all forms are similar in flumes, sand waves are substantially larger than dunes in natural environments; stability fields -- 2D dunes occur at lower flow velocities (for the same depth) than dunes in the flume; dunes are seen superimposed upon sand waves in the field, apparently in equilibrium; dynamics/kinematics of establishment and growth -- ripples abruptly organize into 2D dunes which then grade into 3D dunes with increasing velocity in the flume; detailed kinematics are unknown at flow depths greater than 0.5 meters. It is precisely these problems which this study seeks to resolve.

CHAPTER 3

EXPERIMENTAL APPARATUS AND PROCEDURES

By use of the hot-water scale modeling technique in a large flume, scaled flow depths of 1.5 to 2 meters -- depths comparable to some natural flows -- can be achieved. This allows large-scale bed forms to achieve equilibrium on the scale of sedimentologically interesting flows and can fill the gap extant between studies in the flume and in the field. By providing detailed information on dunes and sand waves in the depth range where they become well differentiated, this study seeks to establish the relation between 2D dunes and sand waves.

Two series of flume runs were made to study the basic geometry and kinematics of large-scale bed forms at equilibrium. Hydraulic and sediment parameters were varied and tabulated to delimit the stability fields of these forms in terms of depth, mean flow velocity, and mean sediment size (after Southard, 1971). In doing so, this study endeavours to provide a basic observational framework or an equilibrium reference state to serve as a basis for interpreting bed forms in more complex natural environments.

The flume described herein was jointly maintained and operated by Kevin Bohacs and William Corea. Both spent many hours covered with grease to keep the system functioning. During individual runs, Corea concentrated on the sonic depth-profiling system, while Bohacs operated the photographic equipment and

recorded the hydraulic data. Compilation and reduction of the basic data was a cooperative effort. Interpretation and discussion of the data have been done separately.

As reported in Corea (1981), his main interest was in the internal structures of the bed forms. Using the bed profiles, he synthetically generated cross-stratification and compared it to the cross-strata actually produced. The main thrust of this study is to detail the kinematics and dynamics of the large-scale bed forms: their behavior under differing conditions.

MODELING CONSIDERATIONS

Due to the complex nature of turbulent flow and concomitant sediment transport, problems of bed-form dynamics do not admit of exact mathematical solutions. The study of these phenomena is, of necessity, empirically based. Field studies of bed forms seldom allow easy observation and never permit control of the diverse variables of the system. Laboratory studies obviate these problems and ensure that the bed states observed are in equilibrium with the flow. The degree of similitude attainable in such models is limited largely by the width and depth of flumes. The fixed channel walls restrict the development of large-scale bed forms, and side wall effects generate smaller-than-natural shear stresses -- especially when the width-to-depth ratio is less than about 5:1 (Williams, 1970). Even with an acceptable width-to-depth ratio, laboratory flow depths are still much less than those in natural flows (see Fig. 12).

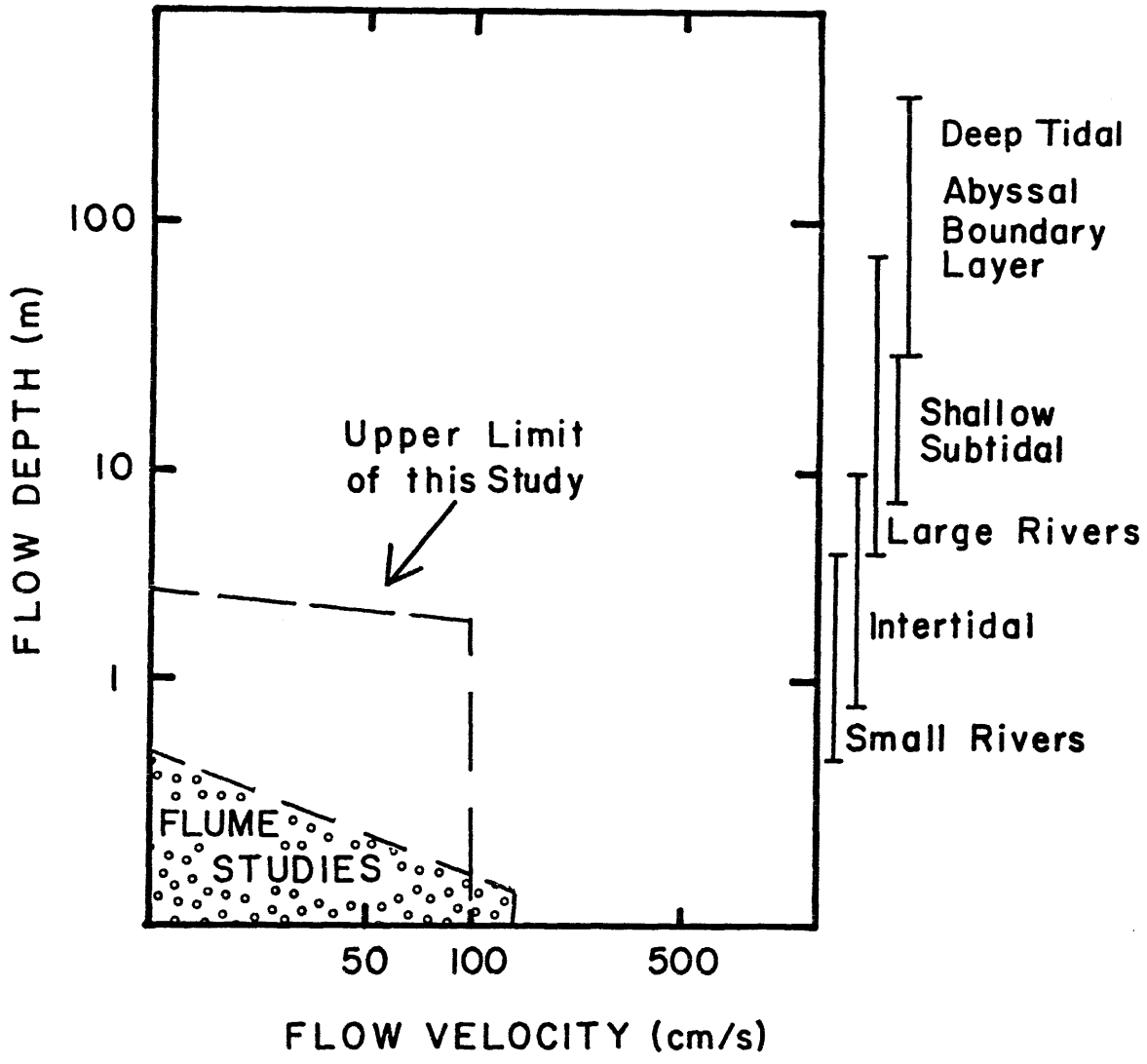

FIGURE 12 -- Schematic diagram of flow depth versus flow velocity comparing flume studies to natural environments (after Middleton and Southard, 1977).

Hence, it is not possible to extrapolate directly the relations observed in flumes to natural environments.

What is needed is a nondistorting scale model, practically achievable in the laboratory, which simulates flows of sedimentological interest. A nondistorting model is both geometrically and dynamically similar to its prototype. Geometric similitude (identical shape, different size) is easily attainable. For the model and prototype to be dynamically similar, corresponding forces must be in the same ratio in the two. The forces of interest in open-channel flow are those due to gravity (F_g = mg $\cong$ ρ L^3 g), viscosity (F_V = $\mu(du/dy)$ $\cong$ $\mu(V/L)L^2$ = μVL), and inertia (F_I = ma $\cong$ ρ $L^3(L/T^2)$ = ρ $L^2(L^2/T^2)$ = ρ L^2V^2). Dynamic similitude of the model (flume) and the prototype (natural flow) is achieved if:

$$\frac{F_{g(p)}}{F_{g(m)}} = \frac{F_{v(p)}}{F_{v(m)}} = \frac{F_{I(p)}}{F_{I(m)}} = 1 \qquad (4)$$

where the subscripts p and m refer to prototype and model. One may express these relations as:

$$(F_I/F_V)_p = (F_I/F_V)_m \; ; \quad (F_I/F_g)_p = (F_I/F_g)_m \qquad (5a, 5b)$$

Each of these combinations is dimensionless and when recast into a slightly different form are equivalent to the well known parameters:

$$\frac{F_I}{F_g} = \frac{\rho L^2 V^2}{\rho g\ L^3} = \frac{V^2}{g\ L} = \text{the square of the Froude number} \qquad (6)$$

$$\frac{F_I}{F_V} = \frac{L^2V^2\rho}{LV\mu} = \frac{\rho LV}{\mu} = \frac{VL}{\nu} = \text{the Reynolds number} \qquad (7)$$

Hence a dynamically similar model of open-channel flow requires that the Reynolds number and Froude number of the model and prototype be equal:

$$Fr_m = Fr_p \ , \ Fr_p/Fr_m = 1 \ ; \qquad Re_m = Re_p \ , \ Re_p/Re_m = 1.$$

Hence:

$$Fr_p/Fr_m = Re_p/Re_m \qquad (8)$$

or

$$L_p/L_m = (\nu_p/\nu_m)^{2/3} \qquad (9)$$

In most models either friction or gravity is taken to be the most important force, and the other force is determined empirically or fudged away in some manner. Both gravity and viscosity are important variables in the flow of water transporting sediment in open channels, thus the difficulty in scale modeling. The normal manner of dealing with the dilemma is to posit fluid friction as being independent of the Reynolds number (for fully developed turbulence) and to model on the basis of Froude-number similarity.

The present study requires complete similitude of forces, so additional modeling criteria are required. Many sets of variables, discussed at length in Middleton and Southard (1977) and Boguchwal (1977), have been proposed to characterize sediment transport on the scale of bed configurations.

Boguchwal (1977) has demonstrated that the set of seven variables proposed by Southard (1971) completely specifies bed configurations and that dynamic scale modeling of these forms is possible (see also Southard, Boguchwal, and Romea, 1980). The seven independent variables are:

d = mean flow depth

U = mean flow velocity

D = mean sediment size

ρ_s = sediment density

ρ = fluid density

μ = fluid viscosity

g = the acceleration of gravity

As in most problems in fluid dynamics, the study of bed configurations may be approached by a mathematical technique known as dimensional analysis. By grouping the physical parameters which influence a system into dimensionless combinations a better understanding of the phenomena is possible. Dimensional analysis is particularly useful in experimental work because as these dimensionless combinations provide a guide to those variables which significantly influence the system and act as a guide to the direction in which experimental work should go. It is an alternate, but equivalent, approach to that discussed in the first part of this section.

The Buckingham (1914) Pi therorem states that if there are n independent, fundamental variables (which fully characterize a system), described by m fundamental dimensions, they may be grouped into n-m dimensional groups. As in most physical problems, there are three fundamental dimensions: mass, length, and time. Hence, open-channel flow generating bed configurations can be fully specified by four dimensionless parameters. There are infinitely many sets of these four dimensionless groupings. Each set is equivalent to any other, since each parameter could be multiplied by another dimensionless parameter and still retain its dimensionless character. (This is permitted only if dimensions are not eliminated, thereby leaving some aspect of the system unspecified.) To achieve dynamic similitude the value of the corresponding dimensionless parameters in the model and prototype must be equal.

The classic set of dimensionless groups is: $U\,d/\nu$, a Reynolds number based on flow depth ; $U/(gd)^{1/2}$, $U/\sqrt{gd}$, the Froude number; ρ/ρ_s, the ratio of fluid and sediment densities; and d/D, a ratio of system length scales. Dynamic similitude requires that these parameters be equal in model and prototype. Algebraic manipulation of these equalities yields the equations governing dynamic similitude for the generation of bed configurations:

$$\frac{L_p}{L_m} = \left[\frac{(\nu_p/\nu_m)^2}{g_p/g_m}\right]^{1/3} \qquad (10)$$

$$\left[\frac{\rho}{\rho_s}\right]_\rho = \left[\frac{\rho}{\rho_s}\right]_m \qquad (11)$$

For models constructed on Earth, Eq. (10) becomes:

$$L_p/L_m = (\nu_p/\nu_m)^{2/3} \qquad \text{(recognized as Eq. (9))}$$

The limiting factor for modeling this system is the choice of the model fluid.

Almost all fluids with a kinematic viscosity substantially lower than water (needed for even a modest scale ratio) are toxic, volatile, flammable, or otherwise unpleasant. Scale modeling has long been ignored by geologists and engineers for this and other reasons (discussed in Boguchwal, 1977).

However, for studies of sediment transport on the scale of bed configurations, even a scale ratio as modest as 2.5 would prove worthwhile. The depth range of such a model (up to 2.5 m) would overlap the depths found in intertidal and fluvial environments. Such a scale ratio is achievable in a large flume (depth = 1 m) by the use of water at a temperature of 80° C. As As can be seen from the accompanying diagram (Fig. 13) the scale ratio (relative to 10° C) attained is about 2.33 ($L_r = L_p/L_m = ((0.015/0.0042)^{2/3})$. The quotient ρ/ρ_s changes only by about 3%, hence quartz-density sand may be used in the model.

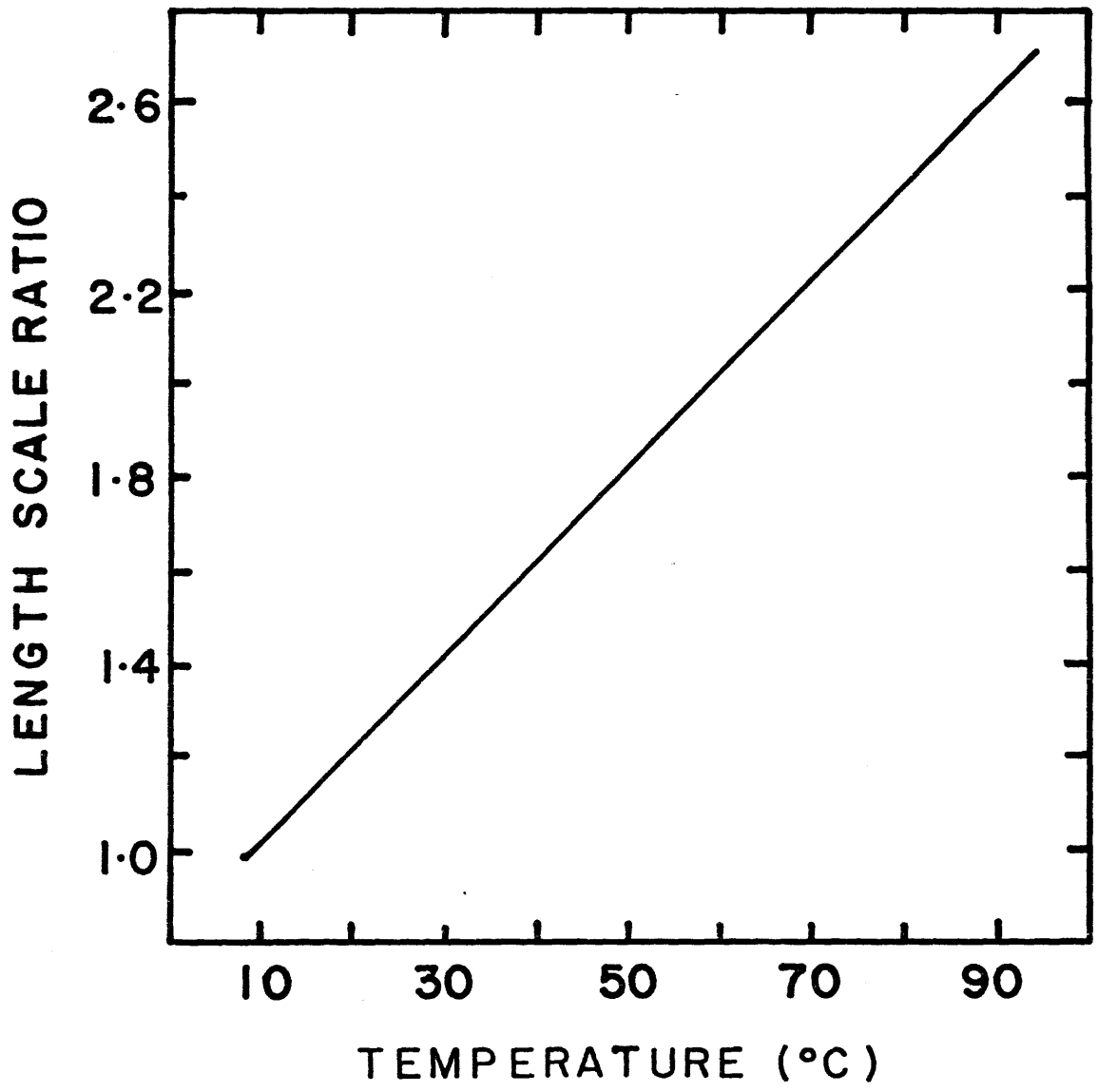

FIGURE 13 -- Length scale ratio versus water temperature, relative to 10° C. (Data from the Handbook of Chemistry and Physics, 1976).

EXPERIMENTAL APPARATUS

Flume

The experiments were conducted in a flume 60 meters long constructed as a large tank divided into two channels by a center partition (Fig. 14a). The channels thus formed were 2.2 meters wide and 1.5 meters deep, one for bed observations and one for return flow. The flume had a water capacity of about 400 m^3.

The channel walls, resting directly on the concrete laboratory floor, consisted of a sandwich of styrofoam panels between plywood sheets. The plywood facing the interior of the channel was coated with spun-glass cloth and polyester resin to form a water-resistant surface. One inch (2.54 cm) thick polystyrene foam sheets served to minimize heat loss to the surroundings. The exterior face of the wall was 3/4 inch plywood framed with 2" x 3" lumber and braced to the floor with 4" x 4" wood struts. (This system proved effective until late in the experimental program. A catastrophic failure of 30 meters of the wall necessitated bracing that part of the channel with 1/2 inch steel rods run across the tops of the channel walls.) The walls were bolted directly into the concrete floor. A water-resistant seal was formed by extending the glass cloth and resin 15 cm onto the floor. This flap was then coated with thick, heat-resistant grease and weighted down with sand bags and concrete paving blocks. These weights extended about 25 cm from the wall

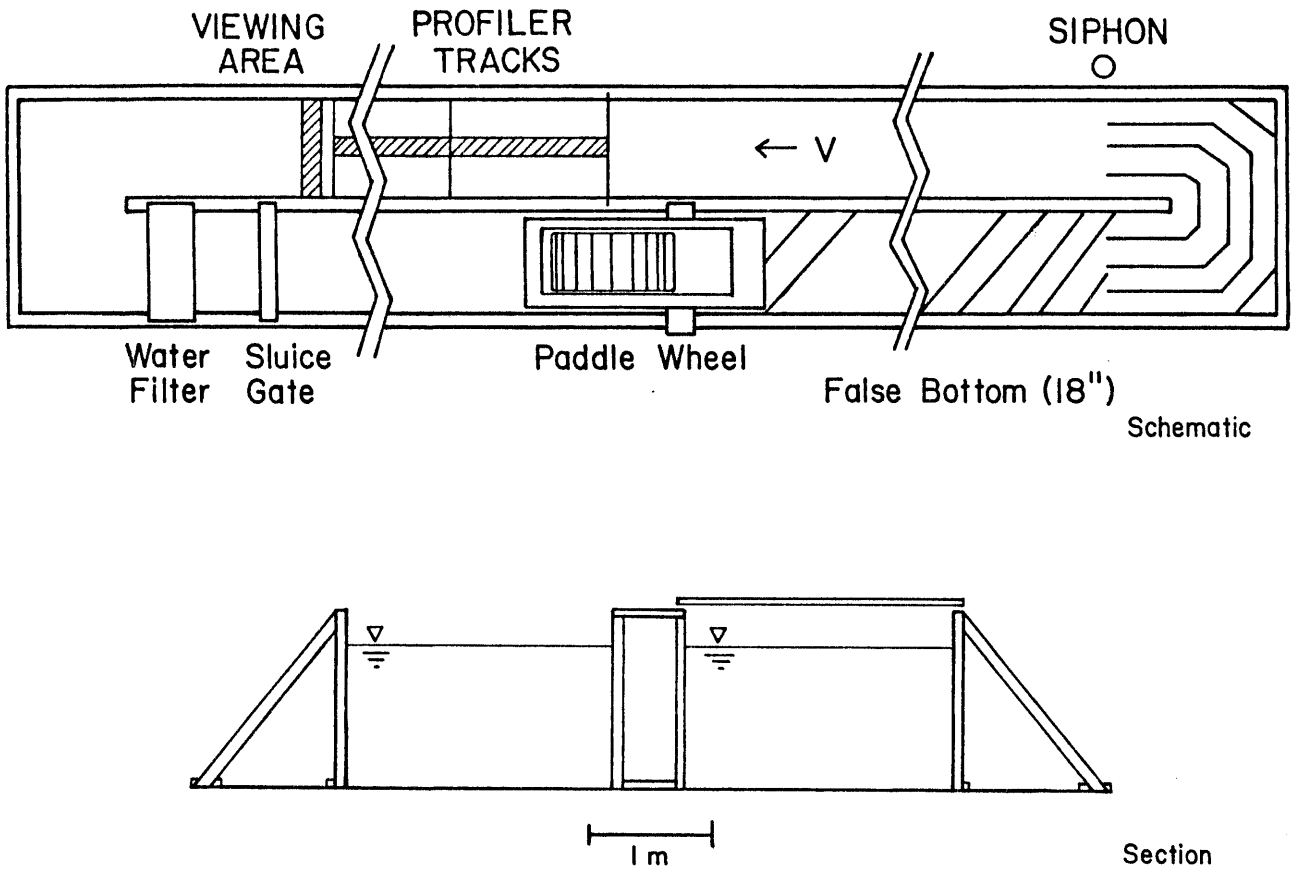

FIGURE 14a-- Schematic and section of the 60-meter flume used in these series of experiments.

into the channel and were about 10 cm high. They did not cause significant disruption to the flow because they were covered by the sand bed throughout most of the runs.

The top of the channel was covered with 4' x 8' removable panels constructed of 1/4" plywood, framed with 2" x 3" lumber, insulated with polystyrene foam, and covered with polyethylene sheet. Soft polyurethane foam along the panel edges minimized evaporation and heat losses.

Two viewing windows, made of 1/2" acrylic sheet, were set into the channel walls, one at 25 meters into the working section and the other at 50 meters. The downstream window, 2.3 meters long, served as the main observation point.

The flow was driven by a large paddle wheel or water wheel located at the midpoint of the return channel (Fig. 15). The water wheel, mounted on a horizontally pivoted steel frame, was 3 meters in diameter. It had 18 planar 4' x 8' paddles set at zero angle to the radius. The paddles were constructed of plywood and framing lumber coated with spun-glass mat and polyester resin. They were mounted in a steel spider framework encircled with two rims 30 cm wide and made of glass cloth and resin. The paddle wheel acted approximately as the inverse of an undershot water wheel used to generate power from streams with high velocity but small head differences.

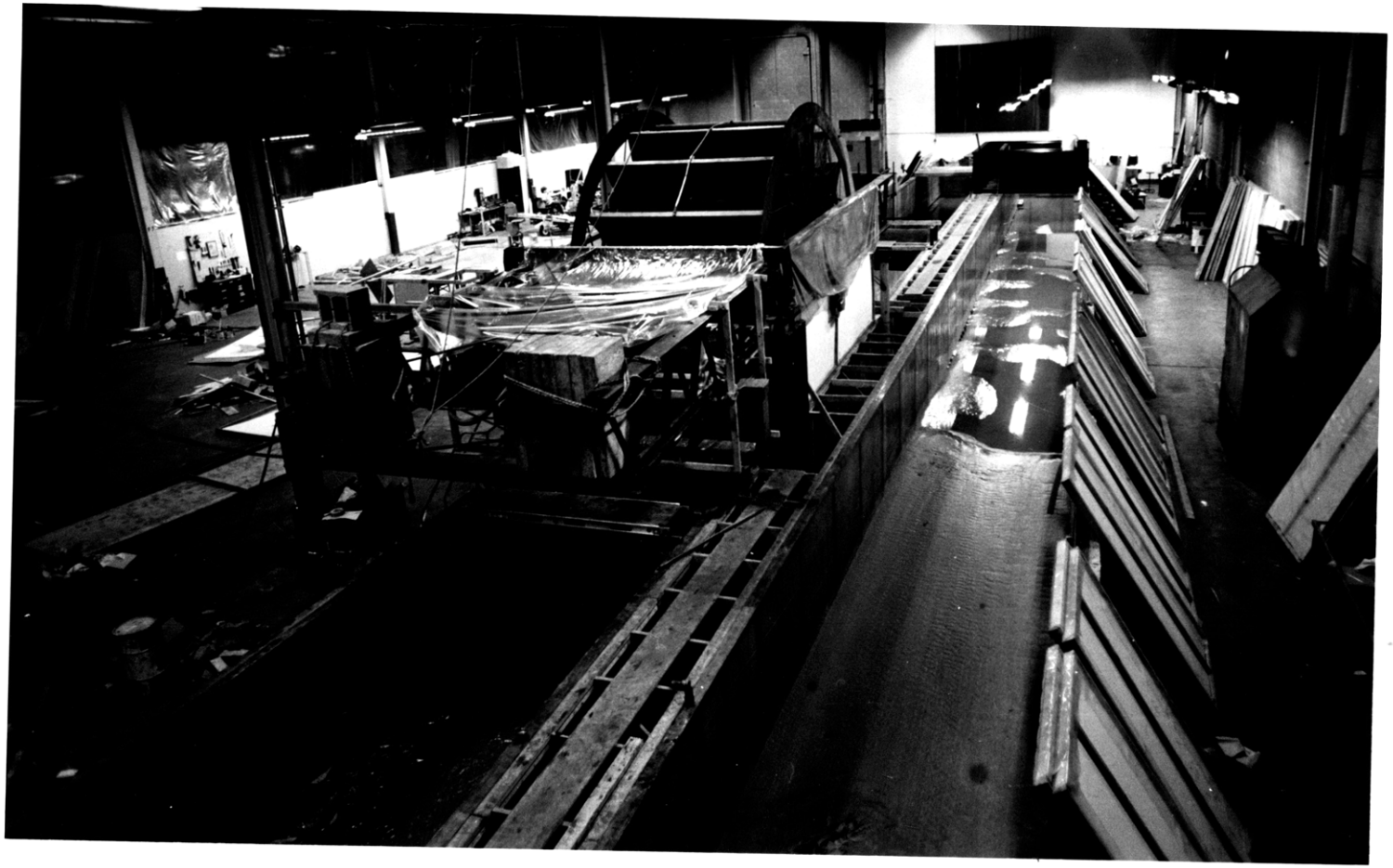

FIGURE 15 -- Photograph of the 60-meter flume and paddle wheel used in these experiments. (Channel width approximately 2 m)

Power was provided by a 40 horsepower constant-speed AC motor and transmitted to the wheel through a series of belt, chain, and gear drives. Ultimate delivery of power to the wheel was through a friction drive consisting of four rubber tires that gripped the wheel rims in pairs.

The entire steel structure supporting the wheel and drive system was pivoted horizontally. Thus the paddle wheel could be raised or lowered in the water by a large screw jack. This allowed a continuous variation in discharge from zero to a maximum of about 2.2 m^3/s (unscaled). The paddle wheel and its support structure were enclosed in a framework of plywood and framing lumber insulated with polystyrene foam and draped with polyethylene sheets. This reduced evaporation and minimized problems of noise and splashing.

To maximize the efficiency of the pumping system, minimal clearance (3 to 5 cm) was left between the paddle wheel and the channel walls, and a false bottom with the same curvature as the wheel was installed directly underneath the paddle wheel (Fig 14b). The false bottom, shaped like a segment of a circular cylinder, extended dowmstream through an arc of about 30 degrees from a line beneath the axis of the wheel and then horizontally for 1.5 meters. When the wheel was at its lowest position, for maximum discharge, there was 10 to 15 cm clearance radially between the edges of the paddles and the curved portion of the false bottom.

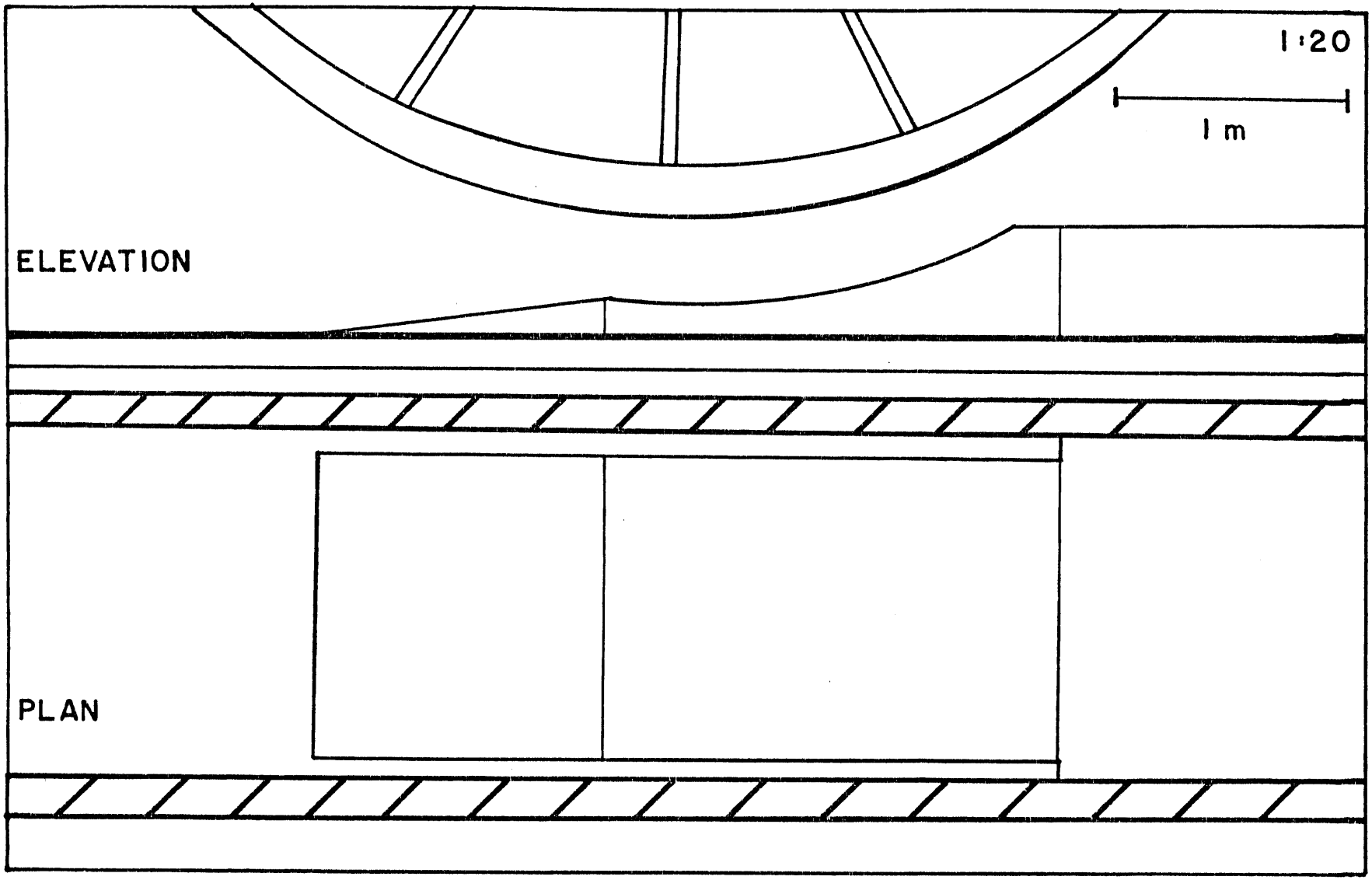

FIGURE 14b -- Plan and elevation of false bottom under paddle wheel.

Also, the false bottom was 20 cm narrower than the width of the flume to allow clearance for the rims of the paddle wheel.

A set of three turning vanes that divided the flow into four vertical sections of equal width were installed in the bend upstream of the working channel to suppress secondary flow and the pronounced flow separation that took place at the inner wall of the bend (Fig. 14a). Design of the vanes was more a matter of practical than theoretical considerations: they had to be sturdy and relatively easy to construct. The vanes extended the full depth of the flow and turned the flow in 45-degree increments. Their effectiveness was evident from the lack of the distinctive, grossly uneven pattern generated downstream when the vanes were not in place. Secondary circulations were also minimized by the hydraulic jump commonly formed at the upstream end of the test section just downstream of the bend. The large-scale bed forms showed no systematic cross-channel nonuniformity even near the upstream end of the working section.

Secondary flow was also a concern simply because of the method of pumping used. This turned out to be minimal due to the way the paddle wheel actually functioned: its action was more a lifting and piling up of the water rather than pushing it through. In this process, much turbulence was generated; all previously established flow patterns were broken up. Also, no sediment-accumulation patterns were maintained through the paddle wheel; in fact, little sediment ever accumulated or

resided in the section of the flume between the sluice gate and the paddle wheel.

A false bottom was also installed downstream of the paddle wheel to the 180-degree bend to keep the flow approaching the bend as uniform as possible and the reduce the total volume of sediment needed in the flume. It was formed of gravel fill to a height of 45 cm, covered with three sheets of polyethylene stretched tight and anchored all around. The surface thus formed was a coplanar extension of the downstream part of the false bottom beneath the paddle wheel. During most runs flow depth and velocity in this section were such that upper-regime flat bed was the mode of sediment transport, although Froude numbers were never greater than 0.5, so standing surface waves were not pronounced.

Hydraulic Characteristics of the Flume

It was advantageous in this flume to use a small width-to-depth ratio (1.5-2) as it allowed greater flow depths and thus larger-scale bed forms with only a modest increase in fluid discharge. (The ratio of flow discharge $Q = Vdb$, where b is the width of the channel, between prototype and model is $Q_r = V_r d_r b_r = L_r^{0.5} L_r L_r = L_r^{5/2} \cong 6{:}1$ where $L_r = 2.1$). As discussed in the section on problems with flume studies in Chapter 2, there are disadvantages with working at a small width-to-depth ratio. However, examination of the many sets of flume experiments reported

in the literature (e.g., Gilbert, 1914; Vanoni and Brooks, 1957; Simons and Richardson, 1962, 1963, 1966; Williams, 1970; Costello, 1974; Boguchwal, 1977) for the effects of width-to-depth ratio on both large-scale and small-scale bed features suggests that a small width/depth ratio, although affecting the details of bed-form geometry, does not alter essential characteristics such as existence, overall geometry, or relative scale of features. This is further suggested, by analogy, by an unpublished set of experiments on the effect of width/depth ratio in characteristics of small-scale current ripples (Southard, personal communication). In these experiments, the flow width was systematically varied from 1:1 to 5:1 at constant sediment size, flow velocity, and flow depth; geometric details of the ripples and stability-field boundaries varied somewhat, but no significant qualitative changes were found.

It may seem that a length of not more than 40 meters in the working channel might be too short for the development and study of features with a spacing of 2 to 4 meters. Observations of dunes in shallow tidal currents show that the upstream boundaries of fields of well-developed large-scale bed forms can be strikingly sharp (Bokuniewicz et al., 1977; Briggs, 1979; Hine, 1975; Dalrymple, 1977). A good generalization for flows in which bed-form height and flow depth are within an order of magnitude of each other is that bed forms reach equilibrium in an entrance length of no more than about five average bed-form spacings (Costello, 1974).

Thus the dunes produced by a flow of about one meter depth will reach full development halfway down the test section of the flume. In the present experiments, the large-scale bed forms became fully developed in the first 10 meters of the working section, or only 2 to 3 average bed-form spacings. While not ideal, this channel length in this flume is adequate for a basic study of the size, shape, kinematics, and interrelations of large-scale bed configurations.

Sand

The sands used in the experiments were commercial preparations supplied by the Holliston Sand and Gravel Company (Holliston, Massachusetts). The K series used AFS 50 foundary sand and the L series used Type 00 blasting sand. Both sands were supplied washed and partially sieved to remove the finer sediments. Derived from a glacial outwash sand, both were quartz-rich (greater than 90%), subrounded, and medium and coarse grained, respectively.

Several sieve analyses of each sediment were made to characterize the size distribution. The size fractions were separated on a set of 1/4-phi sieves; of phi = $-\log_2(D_{mm})$. Three samples of each sand were sieved for 15 minutes on a Tyler shaker. The sediment retained on each screen was weighed and its percentage plotted on arithmetic-probability paper (Fig. 16). From this plot the size statistics were derived following the methods of Folk (1974).

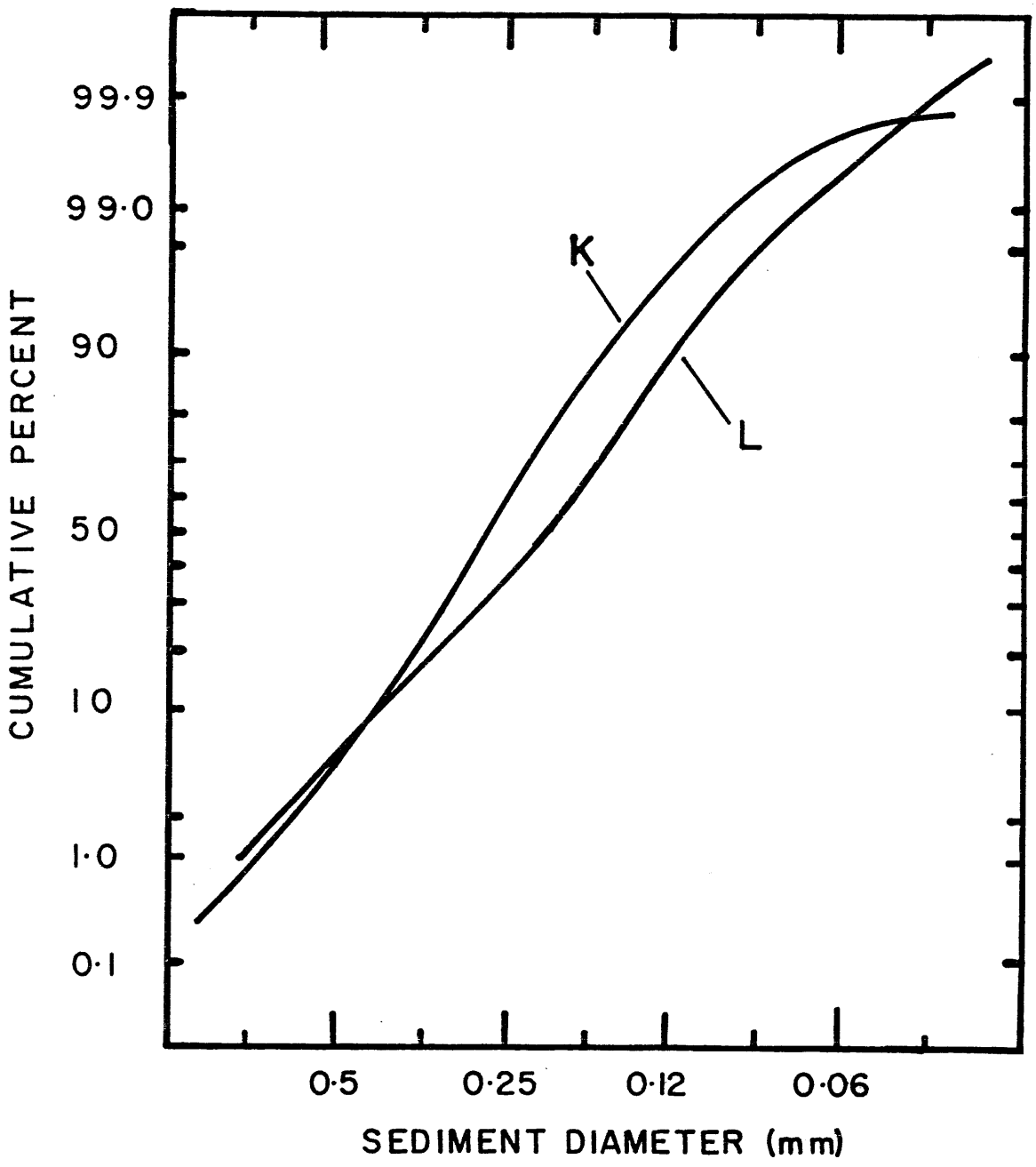

FIGURE 16 -- Grain-size distribution of the sands used in K and L series of experimental runs.

Shape, rounding, and mineralogy were determined by visual observation under a microscope. Data on each sand may be found in Table 6.

EXPERIMENTAL PROCEDURES

The scaled flow depth in the flume was chosen to allow the development of pronounced differences in the large-scale bed configurations. The differentiation of dune types was studied in a series of runs with unidirectional, steady flow. Each was planned to be sufficiently long to allow the bed state to come into equilibrium with the flow conditions. Technical difficulties seldom allowed a run to continue for the ideal (or planned) amount of time. All runs did last at least 8 hours (scaled; time scale factor = $L_r^{1/2}$), a time scale consonant with tidal flows.

Two series of experiments were made, each with a different grain size (scaled diameters of 0.54 mm and 1.7 mm) with a constant volume of water in the flume. The volume of sand in the flume made the average flow depth 60 to 70 cm, unscaled. Flow velocities ranged from 54 cm/s (scaled), just above the ripple stability field, to over 100 cm/s (scaled). All measurements of flow depth, flow velocity, and sediment size cited hereafter are scaled relative to 10° C. All flows were in the stability fields for large-scale bed configurations. A typical run went as follows. The flume was filled to the prescribed depth and heated to the highest temperature possible with a gas-fired heater. The

TABLE 6

- Properties of sands used in experiments -

Series K		Series L	
Mean = 0.27 mm		Mean = 0.44 mm	
Std. Dev. = 0.17 mm		Std. Dev. = 0.24 mm	
	- Mineralogy -		
Quartz	95%	Quartz	92%
Feldspar	3%	Feldspar	3%
Rock Fragments	2%	Rock Fragments	5%
(includes:		(includes:	
biotite;		biotite;	
magnetite;		garnet;	
muscovite;		tourmaline;	
tourmaline;		magnetite;	
metamorphic RFs)		igneous, sedimentary, & metamorphic RFS)	

paddle wheel was then started and lowered into the water by the screw jack to achieve the desired discharge. Discharge was measured by a drowned-underflow sluice gate. Depth and discharge thus being set, time was allowed for bed slope and shear stress to attain equilibrium. The time required for the bed forms to come into equilibrium was rather short; this finding will be discussed in a later section. In Runs K-1 to K-9 the flume was run at the specified conditions for 4 to 18 hours before data were taken. To specify the time to equilibrium and the behavior of bed forms under changing flow conditions, data were collected from the very start of Runs K-10 through K-12 and L-1 through L-3.

Unfortunately, the maximum sustainable temperature during a run was about 65° C. The paddle wheel proved to be quite effective in pumping air as well as water, and most of the heat that escaped from the system was carried by warm, moist air through the inevitable gaps in the covering around the paddle wheel. Heat losses due to evaporation and advection far outweighed losses due to conduction. Still, this allowed the system to attain a scale ratio of 2.1 (maximum scaled flow depths of about 1.5 m).

The bed forms generated were documented by visual observations and impressions, as well as still and time-lapse photography at the downstream viewing window. Bed profiling by a high-precision sonar unit was carried out in a reach 12 meters long immediately upstream of the main viewing window; for details, see Corea (1981).

DATA ACQUISITION

Bed-Form Measurements

Sixteen-millimeter time-lapse cinematography provided the primary means of characterizing the bed forms. Frames were shot once every 20 seconds. They were of a side view of the bed forms in the 2.3 m downstream viewing window. For reference, a clock and horizontal/vertical scale were kept in the field of view. Suspended-sediment concentrations (expecially in the K series) and general water murkiness prevented plan-view photographs except in still water after the flow was shut off for several hours. Several real-time segments were shot (at 18 frames per second) to document short-term characteristics of sediment transport. These films provided valuable information on bed-form height and migration rate, and behavior of superimposed bed forms; information on spacing suffered because the average bed-form spacing was longer than the observation window in seven of the fifteen runs. The time-lapse films emphasize aspects of geometry and migration not immediately perceptible from real-time observation.

The cinematography was supplemented with 35 mm still photography. This supplied information on a finer scale than the movies and permitted close-up pictures of small features. The bed forms were also subjected to careful visual observation and discrimination, tying together all the other data.

The photographic records of the bed forms were read by mounting the film in a 35 mm microfilm reader. As Boguchwal (1977) noted: "Thousands of frames were tediously scrutinized in dark corners of the library." Measurements of bed-form heights and crest positions, made every 30 frames (10 min), were marked on a sheet of graph paper and measured later. Bed-form spacing (as defined in Fig. 17, the distance between the lowest points in front of succesive bed-form crests; i.e., trough to trough) was measured whenever the entire bed form was in the field of view.

Due to the high temperature of the water, a closed system was necessary. The bed was profiled in a 12-meter reach by a high-precision sonic depth recorder. (The sections of sonar and visual observations did not overlap.) The recorder used a 4 MHz signal repeated at a 250 Hz rate. The measurements were accurate to at least 1 mm. A similar system was used by Dingler, Boylls, and Lowe (1977). For a full description of the present system, see Corea (1981).

The system produced an analog voltage that was plotted on a chart recorder. The horizontal scale was compressed four to one; the vertical scale varied from run to run. Calibration in the vertical scale was accomplished in two ways. First, series of voltage outputs were obtained from known depths. Second, the distribution of bed-form heights was calibrated against the distribution of heights of the same bed forms measured from the time-lapse films.

The horizontal distances thus determined were quite accurate (to within 0.5 cm); the vertical scale accuracy varied due to technical problems with the chart recorder. Examination of the records (sonar and photographic) indicates that most vertical distances were accurate to ± 1 cm.

The majority of the bed-form statistics were calculated from data derived from the profiles. For each bed form, the measurements detailed in Fig. 17 were recorded: bed-form height, trough-to-crest spacing, crest-to-trough spacing, and crest position. Also noted was the nature of the lee face and the presence and type of superimposed bed forms. Types of lee faces (as seen on the sonic profiles) were divided into those with a lee-face slope of close to 30 degrees, assumed to be at or near the angle of repose of the sediment, and those with a much lower slope.

The data are tabulated in Appendix 1 for each run. A program run on a hand-held computer corrected the data for change in horizontal and vertical scale, and, eventually, for the high-temperature scale factor.

Hydraulic Measurements

Water Discharge

Water discharge was measured with a drowned-underflow sluice gate. Such a sluice gate is simple to construct and reasonably well suited for measuring the range of discharges encountered. Its hydraulics may be analyzed as a case of "divided flow";

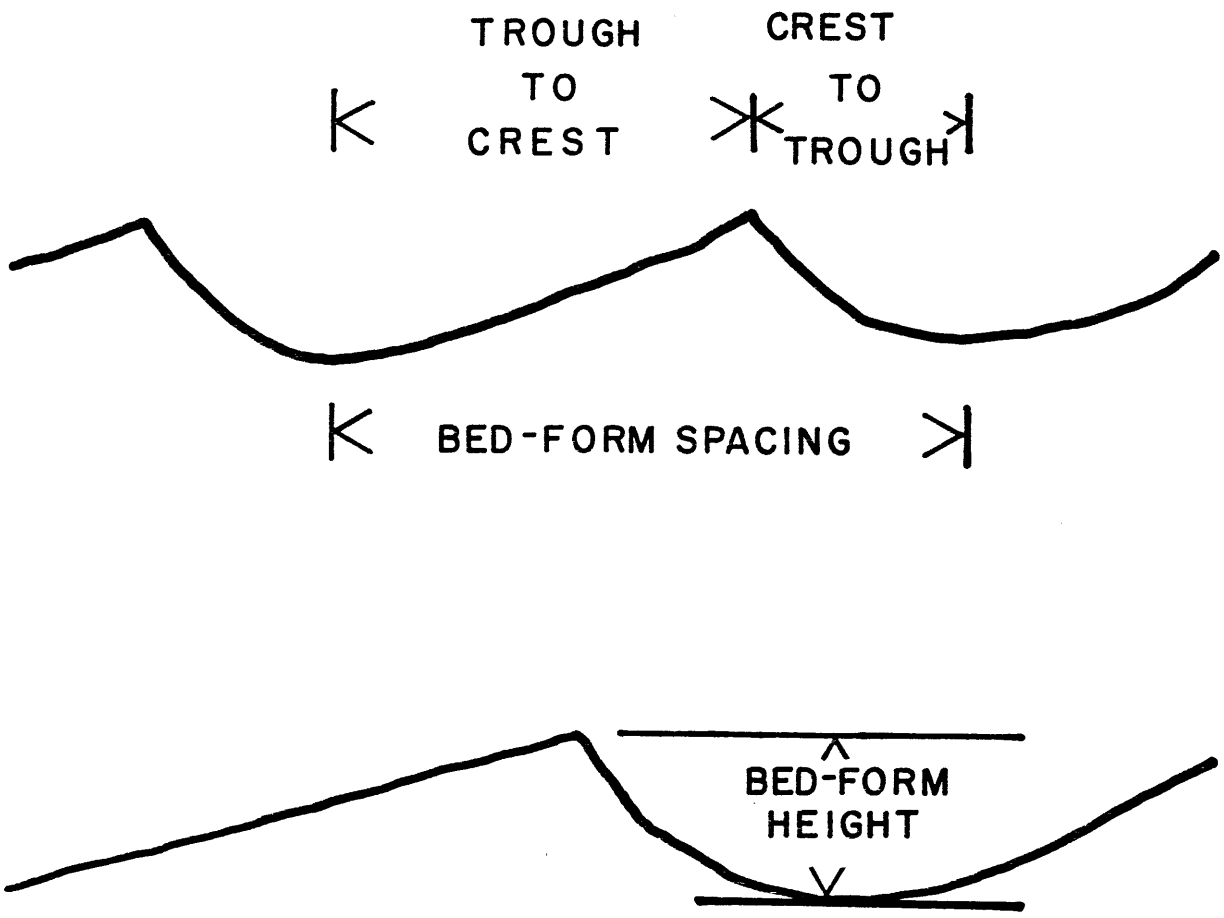

FIGURE 17 -- Definition sketch for bed-form measurements.

effectively the flow is that of a jet overlain by a mass of water with no net motion. Theoretical analysis and experimental investigations of this case reported in the literature agree to within 2 to 5 percent (Henderson, 1966). Agreement between the measured and calculated velocities in the present experiments ranged from 6% at the lowest discharges to 19% at the highest discharges. A complete analysis of the sluice-gate flow is given in Appendix 2.

Details of the construction of the sluice gate are shown in Fig. 18a. The gate, extending across the entire width of the flume, was suspended from two screw jacks. With the paddle wheel set to a discharge of about 1 m^3/s (in the middle of the discharge range), the height of the gate was adjusted to yield the maximum difference in water level across the gate. The gate was left at this height (43 cm above the bottom) in all subsequent calibration runs and experimental runs. At the beginning of the experimental program the head loss across the sluice gate was calibrated against discharge measured by the velocity-area method, at a section halfway down the working channel. This method involves measurement of the flow cross-section and the mean velocity of the flow through that section; the discharge is the product of the two quantities. The area of the flow cross-section was easily measured; the mean velocity was determined from a series of vertical velocity profiles. At the time of the calibration runs, only 30 of the 90 tons of sands eventually used in the experimental runs was in the flume. The bed forms during

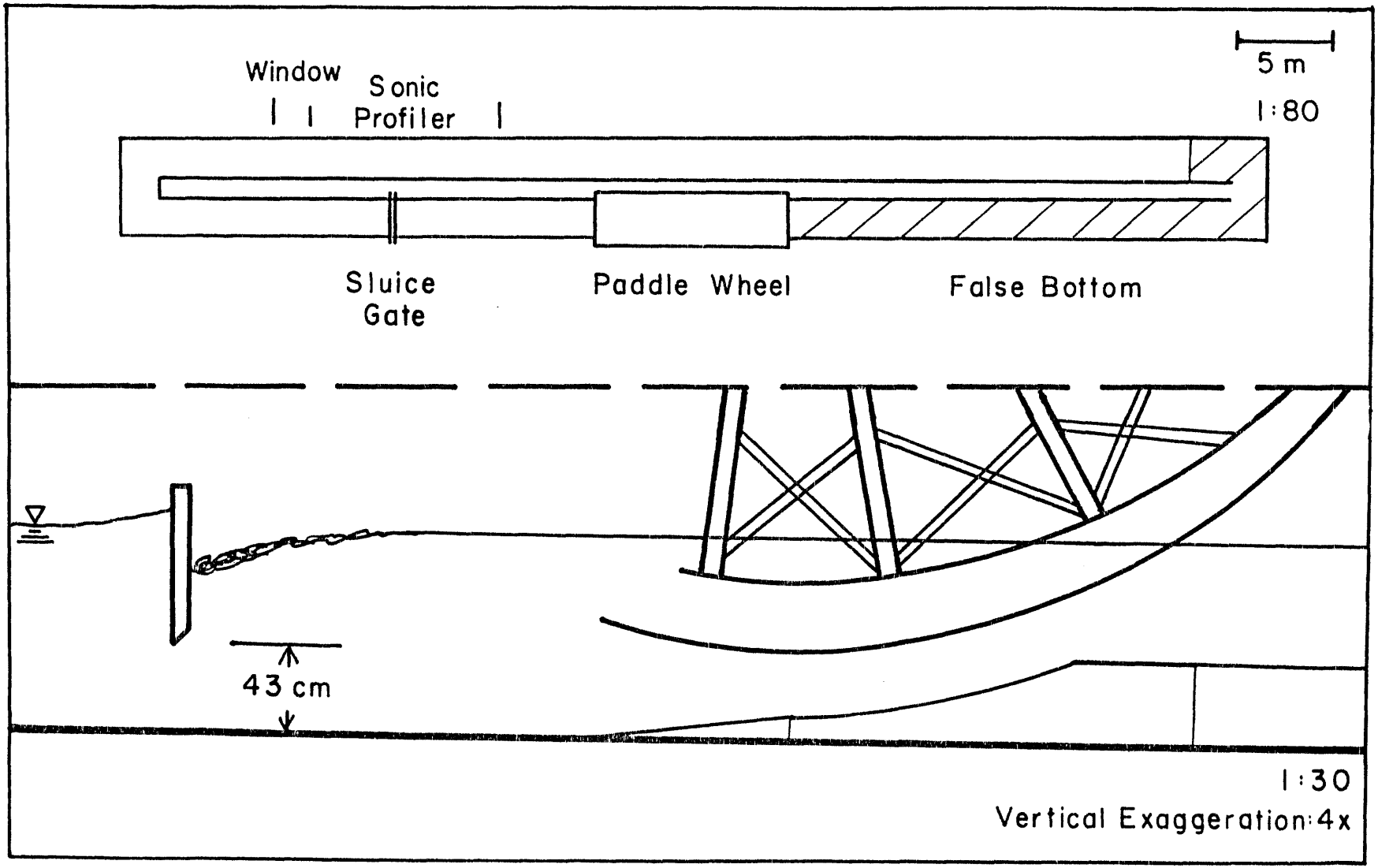

FIGURE 18a -- Details of sluice gate location and dimensions.

the calibration runs had a very flattened profile, with a maximum height of 15 cm. The crests were continuous and two-dimensional transverse to the flow; the concrete floor of the flume was often exposed in bed-form troughs. For each of six fixed discharges, covering the lower 75% of the discharge range, five vertical velocity profiles were taken with a Price current meter across the flow section. Readings were taken at 0.2, 0.4, 0.6, and 0.8 m below the water surface. Finer-scale measurements were not possible due to the size of the flow meter. Readings at each position were taken for five minutes and time-averaged. Typical performance of this type of current meter indicates that these velocities are accurate to 1.5 percent (Herschey, 1978).

The velocity measurements were taken at a position about halfway down the working channel. Each vertical profile took about 30 minutes to complete, and an entire discharge measurement required about 2.5 hours. In this period of time, two to four bed forms must have migrated past the measurement point. Thus the variations of the velocity profiles are systematic, and not due to the presence or absence of bed forms under the current meter. Two representative sets of profiles are shown in Figs. 19a and 19b. The profiles are taken from the middle and lower portions of the range of discharges. The highest discharges were not calibrated due to a protracted period of engineering difficulties with the paddle wheel after which the current meter was unavailable. This was not thought to be a major problem because the calibration curve was linear in the range of discharges measured, and the highest

uncalibrated discharge was only 25% greater than the highest calibrated discharge.

The velocity profiles were then graphically integrated (by plotting the profiles and measuring the area between the profile and the depth axis) to give the water discharge. Data on the flow cross-section and water discharge were used to compile a chart of fluid velocity versus water-level difference across the sluice gate (Fig. 18b) . The water levels on either side of the sluice gate were measured in glass-tube manometers that could be read to $\pm$ 2 mm. The two manometer taps were located 1 m upstream and 0.3 cm downstream of the gate. This rather low accuracy for water-level readings is the result of the design of the manometers. The manometers consisted of a 7 mm diameter glass sight tube connected to a fitting in the side wall of the flume with an opening of 3 mm. For most accurate readings, the opening should be small, and the sight tube large in relation to that opening. The present design was a non-optimal compromise and was the result of the hardware and materials readily available. Combining this uncertainty with the stated accuracy of the current meter, and of the velocity-area method, the measurements of flow velocity are taken to be accurate to ± 7% (calculated by the method of Herschey, 1978; see Appendix 2 for the calculations).

The nature of the flow approaching the sluice gate presented two complicating factors that may have affected the accuracy of the discharge measurements. As the flow rounded the bend at the downstream end of the working channel, a spiral flow was generated.

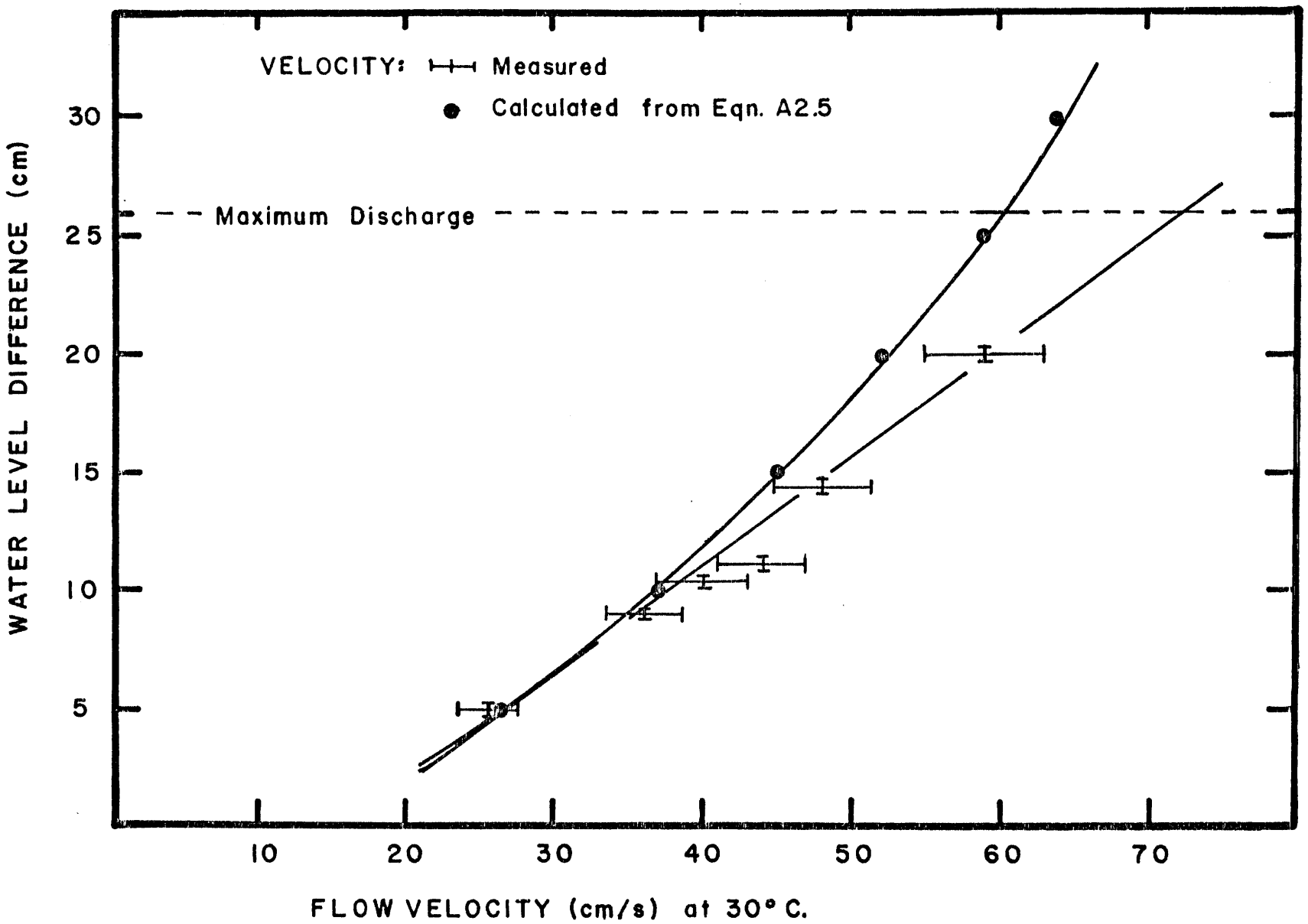

FIGURE 18b -- Water level difference versus flow velocity for calibration runs. Long-dashed line is the curve used to determine flow velocities in these experiments. Error bars are ± 7% for flow velocity, and ± 0.3 cm for water level difference. Solid parabola is for velocities calculated as in Appendix 2.

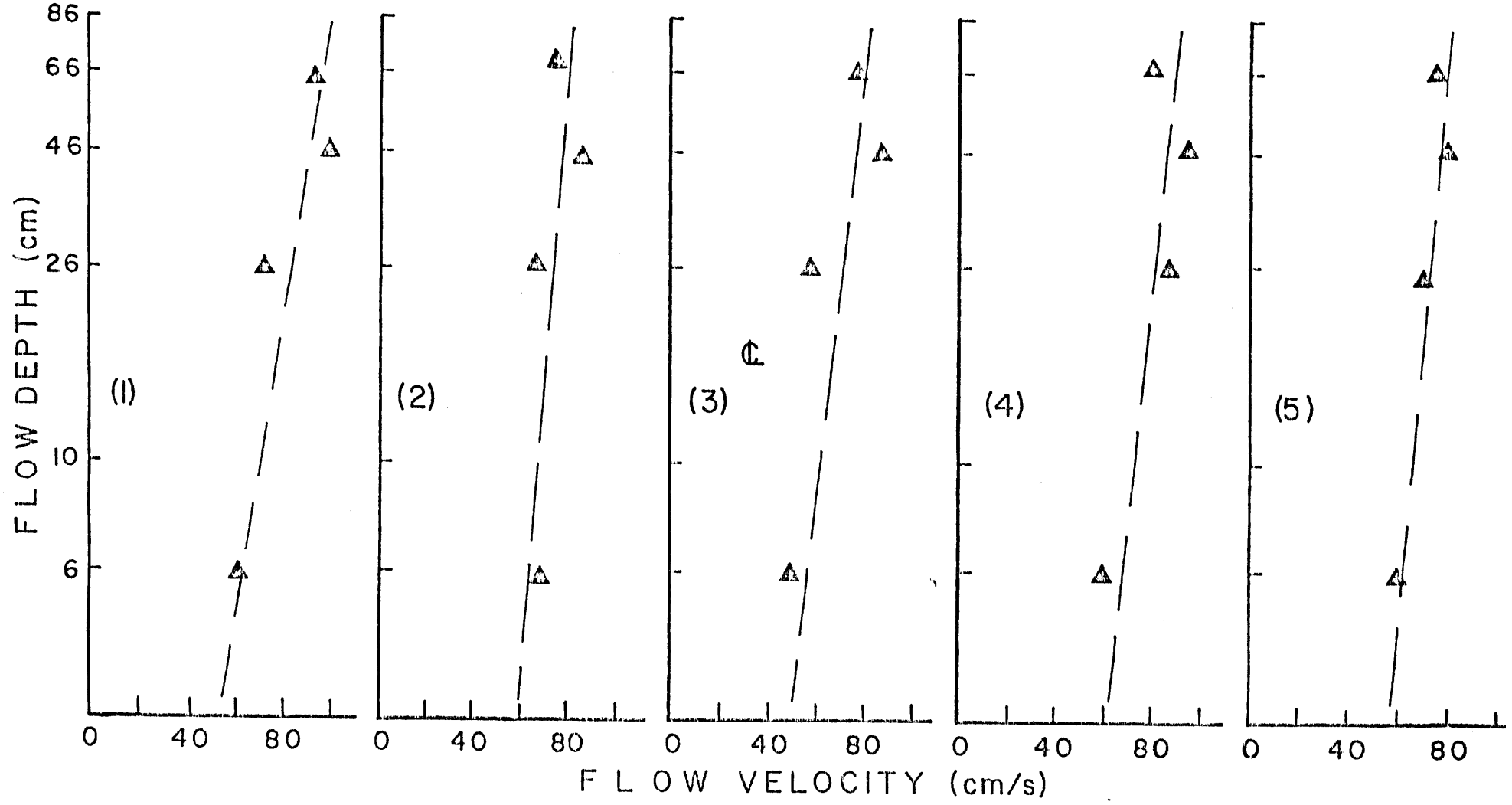

FIGURE 19a - Vertical velocity profiles taken with Price current meter at Five stations across the flume channel. Profile (1) at left side; profile (3) on centerline; profile (5) at right side of flume channel. Each point represents a five-minute average velocity.

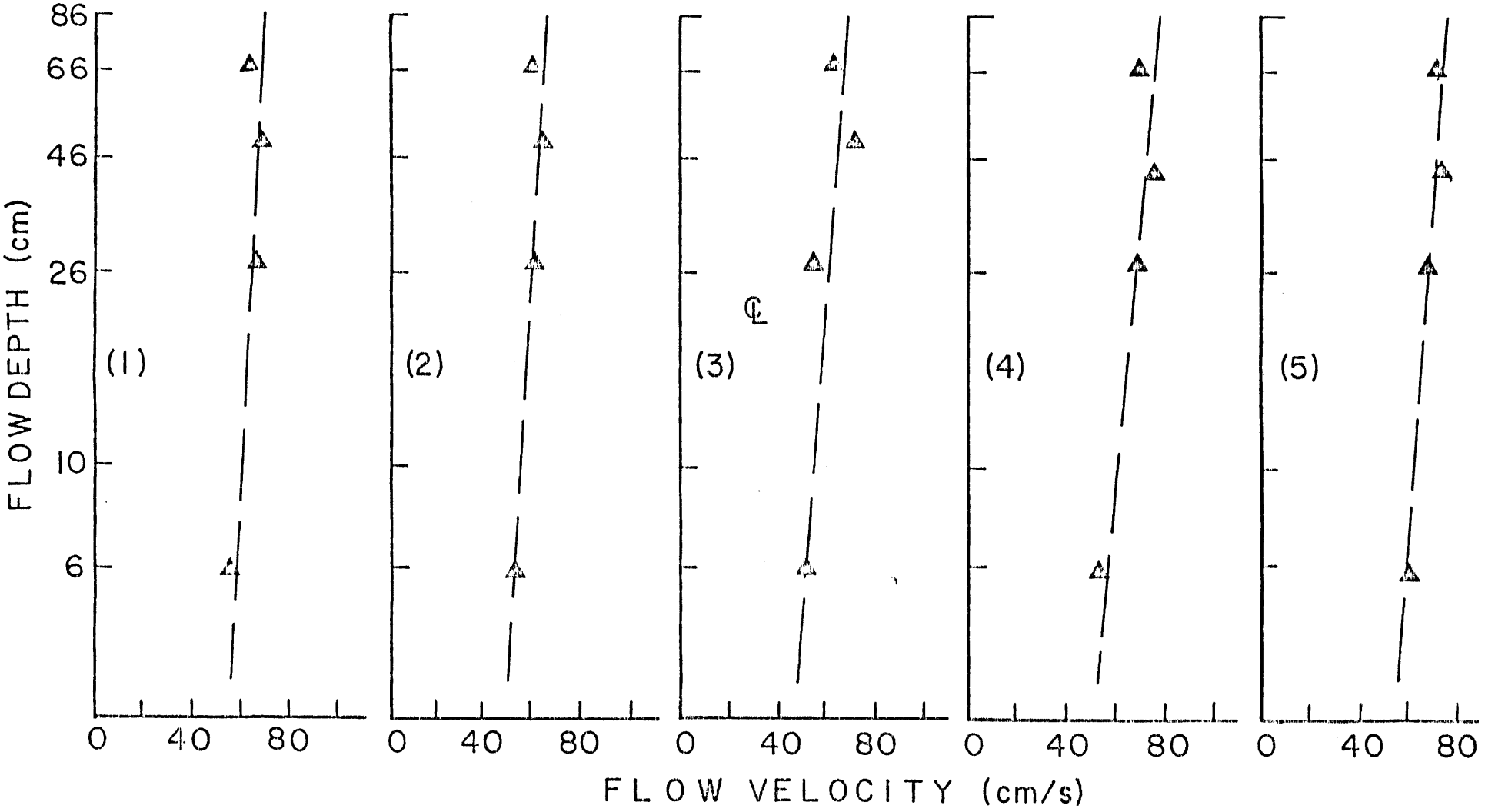

FIGURE 19b-- Vertical velocity profiles taken with Price current meter at five stations across the flume channel. Profile (1) at the left side; Profile (3) on centerline; Profile (5) at the right side of flume channel.. Each point represents a five-minute average velocity.

(There were no turning vanes at the downstream bend. Flow separation at this bend was not as pronounced as at the upstream bend because of the greater depth and smaller flow velocity. Hence, turning vanes were not considered to be essential there.) If the velocity distribution of the approaching flow was strongly distorted, there may have been an appreciable variation in water level across the sluice gate; this would have adversely affected the accuracy of the discharge measurements. To minimize this problem, the sluice gate was located six channel widths downstream of the turn. Although a longer distance would have been desirable, the upstream length had to be balanced against the downstream proximity to the paddle wheel, to minimize backwater effects from the paddle wheel. The pattern of sediment scour and of surface water movement one to two channel widths upstream of the sluice gate indicated that the approaching flow was relatively two-dimensional. Hence, the velocity distribution of the approaching flow probably had minimal deleterious effects on the accuracy of the discharge measurements.

The second complicating factor was the presence of a sediment bed in the reach between the bend and the sluice gate. (Downstream of the gate the sand bed was always less than 5 cm thick.) The volume of sediment in this reach varied little from run to run, with a maximum thickness of about 30 cm. The pattern of sediment accumulation in this reach remained fairly constant during all the runs. There was a pronounced scour pit along the inside of the bend, but the bed achieved an even cross-channel elevation by two

to three channel widths downstream of the bend. The bed forms in this reach tended to be subdued and not well developed. As expected due to the necessary acceleration of the approaching flow, there were no bed forms within one channel width upstream of the gate; the sediment surface sloped smoothly down to the flume bottom underneath the sluice gate. It was difficult to judge the effect of this upstream sediment accumulation, but no systematic variation with time in the water-level difference across the sluice gate was noted, as might have been expected if the approach of bed forms periodically altered the height of the bed just upstream of the sluice gate. Although the volume of sand in the flume was tripled between the calibration runs and experimental runs, there was no pronounced difference in the sediment distribution pattern in this reach. While the sediment flux through the reach increased, the local character of the sand deposition remained unchanged. This indicates that the calibration of the sluice gate was valid for the experimental runs.

An effort to check the calibration of the sluice gate was made by timing the passage of floats in a 10-meter reach of the working channel, starting at the velocity-profile measuring station halfway down the working section. This 10-meter reach overlapped for 5 meters with the upstream end of the sonic profiling section. As is commonly the case in open-channel flow, this measurement was difficult because often the floats found their way to a position near one or the other of the sidewalls. There was no preference for which sidewall the floats would approach; their somewhat less

than rectilinear motion seemed to be due to random interactions with large-scale turbulent eddies rather than to a systematic nonuniformity or residual secondary circulation from the upstream bend. The surface velocities thus determined agreed with the expected surface velocities to within 10-15%.

Careful examination of the velocity profiles reveals variations of up to 10 to 15 cm/s across the channel. Without more extensive velocity measurements it is difficult to precisely determine the source of the nonuniformity. These cross-stream variations arose from both the geometry of the flume and the small width-to-depth ratio. The turning vanes and the presence of the hydraulic jump just downstream of the vanes helped to minimize the effects of the flume geometry. Despite the inherent problems discussed in Chapter 2, a small width-to-depth ratio was chosen to allow greater flow depths for the development of the large-scale bed forms. And for a very practical reason: a wider flume would have required a disproportionate increase in time, effort,and money expended. This degree of nonuniformity was deemed acceptable because the focus of this study was the size, shape, and behavior of the bed forms. The hydraulic data are taken as representing the trends of the dynamics of the bed forms, and not as providing absolute values.

Water Temperature

Water temperature was measured in the inlet box to the water heater with a mercury thermometer reading to 0.25° C. A variety of internal and external factors (water-heater performance,

building temperature, and outside weather) caused the temperature to range from 55 to 65° C from run to run. Maximum variation in temperature within a single run was no more than 1° C.

Water-Surface Slope

Water-surface elevations were measured every 30 minutes at five stations during a run. The stations were located at 18, 27, 35, 43, and 48 meters from the upstream end of the working channel. Three of the stations were glass-tube stilling wells 7 mm in diameter connected to a 3-mm hole set flush into the side of the flume. The other two stations were at the upstream and downstream viewing windows. The datum for all measurements was established by filling the flume with about one meter of water (measured from the floor). Meter sticks at each station were then adjusted and set for one meter of depth, the floor then being the zero datum. The water-surface elevation could then be read to within ± 3 mm. This somewhat low accuracy was due to the design of the manometers, as discussed in the previous section. The water level in the manometers fluctuated on a time scale of 3-5 sec; the proper level could be determined by observing for 1 to 2 min because the fluctuations appeared evenly distributed about a mean value. The water level would often remain at that mean level for 10 to 20 sec, then fluctuate rapidly, and then return to the mean level, the entire cycle taking about 40 to 60 sec. The degree of accuracy attainable was determined by having five different observers read the water levels; their readings agreed to ± 3 mm.

Water-surface slope was determined by a linear regression program using the least-squares method. The correlation coefficient r^2 varied from 0.71 to 1.00 (r^2 = 1.00 being a perfect fit); r^2 values were mostly greater than 0.91.

Water Depth

Water depth was determined from the time-lapse films which could be read to within 1 to 2 cm. Measurements of the depth over the highest and lowest bed elevation in the field of view were made every 30 frames (10 min). All of the measurements were averaged together over the entire duration of the run:

$$\text{Average Depth} = \frac{\sum_{i=1}^{n} (d_{max} + d_{min})i}{n}$$

n = 2 [(duration of run)/(10 min)]

= total number of observations

Hence, the water depth determined was relative to the mean bed elevation. Results are listed in Table 7.

TABLE 7 -- Summary of Flume Runs

Run	Depth (cm)	Velocity (cm/s)	Temperature (^{o}C.)	Duration (hr)	Bed-Form Height	Bed-Form Length	Bed State
K-1	147	68.4	64.8	12.45	58 cm	390 cm	2D Dunes
K-2	145	73.4	65.0	12.93	47	289	3D Dunes
K-3	143	74.9	66.6	24.53	52	414	3D Dunes
K-4	133	61.5	61.9	32.06	19	157	2D Dunes
K-5	120	56.7	58.0	30.56	14	207	2D Dunes
K-6	140	98.6	62.0	36.21	--	---	HV Dunes
K-7	143	86.3	62.3	66.70	25	565	3D Dunes
K-8	134	100.8	59.9	14.70	61	783	HV Dunes
K-9	136	78.5	58.5	8.34	30	431	3D Dunes
K-10	129	82.6	56.2	16.40	59	517	3D Dunes
K-11	143	67.6	55.8	12.3	24	262	2D Dunes
K-12	130	99.1	55.1	19.14	35	461	HV Dunes
L-1	115	70.0	42.0	42.24	24	317	3D Dunes
L-2	117	57.5	52.0	9.40	25	240	3D Dunes
L-3	109	83.7	46.7	13.05	33	405	HV Dunes

*** All measurements are scaled to 10^{o} C. ***

CHAPTER 4

EXPERIMENTAL RESULTS

BED-CONFIGURATION SEQUENCE IN THE FLUME

All runs in the K and L series were in the stability fields for large-scale bed configurations. Dynamically, the runs all seem to manifest one overall bed phase. There is a steady and smooth progression of hydrodynamic variables with increasing flow velocity. The response of the bed forms also shows a general continuous trend. There is a smooth increase in bed-form size, both spacing and height, with increasing velocity, and the bed-form migration rates show an almost linear increase. Each of these bed-form parameters is discussed in the following sections.

Geometrically and kinematically, this single overall bed phase can be divided into three subphases: 2D dunes, 3D dunes, and higher-velocity dunes. The term higher-velocity (HV) dunes is introduced as a shorthand description for the type of dune that succeeds 3D dunes at higher flow velocities. HV dunes are large bed forms whose cross-stream development in these experiments was restricted by the size of the flume (see following section, Geometric Properties). They are generally larger than 3D dunes and have flat (almost horizontal) backs; they have been differentiated from 3D dunes because of these factors and because of their migration behavior. However, there is a considerable overlap in the properties of HV dunes and 3D dunes, and this may be an effect of flume size. The only unambiguous property that

separates HV dunes from 3D dunes is that HV dunes form at higher flow velocities than do 3D dunes.

It will become evident that HV dunes are equivalent to at least some sand waves found in natural flows. For the present, it is considered best that they be given a different name (at least on a provisional basis) until sufficient evidence can be collected and considered.

Each subphase (2D dunes, 3D dunes, and HV dunes) forms a distinct population (in terms of bed-form spacing, height, and spacing-to-height ratio). They can also be differentiated according to migration behavior -- the evolution of the bed-form shape as it proceeds downstream. This difference is significant geologically in that it affects the type and size of cross-strata deposited.

The classification of the bed forms -- the number of different bed configurations, whether to split or to lump -- depends upon one's point of view. In the ripples-to-dunes transition, there is no great jump in hydrodynamic variables, but there is a distinct change in the nature of the bed forms. In contrast, there are no distinct gaps in any of the bed-form properties in these experiments which would form a natural basis for division. Sufficient differences do exist among these large-scale bed forms that allow them to be readily differentiated, if one is interested in specifics of bed-form geometry and kinematics. The progressions in bed-form geometry and kinematics with increasing flow velocity may be related to the flow conditions of their occurrence; however,

there is no fundamental change in the dynamics of the bed forms in the range of velocities in these experiments. Hence, to the sediment transport engineer, they are all large-scale ripple-like bed forms; to the sedimentologist, they can be considered 2D dunes, 3D dunes, and HV dunes, each kind leaving its distinct mark upon the record.

GEOMETRIC PROPERTIES OF THE BED FORMS

An examination of the dimensions of the bed forms generated allows them to be divided into three types: 2D dunes, 3D dunes, and HV dunes. Figures 20, 21, and 22 are histograms of bed-form spacing, height, and spacing-to-height ratio for the K series.

Bed-form spacing is defined as the horizontal distance between successive troughs. (The lowest point in the trough could be determined more easily and consistently from profile to profile than the position of the crest because superimposed bed forms complicate the crest shape.) Bed-form height is the vertical distance between the crest (highest point on the bed form) and the lowest point in the trough immediately downstream. The dimensions plotted are for the major bed forms only, not for superimposed bed forms. It proved easy to distinguish the major bed forms on the profiles, as a 12-m reach could be examined as a whole, and the major forms could be recognized in successive profiles.

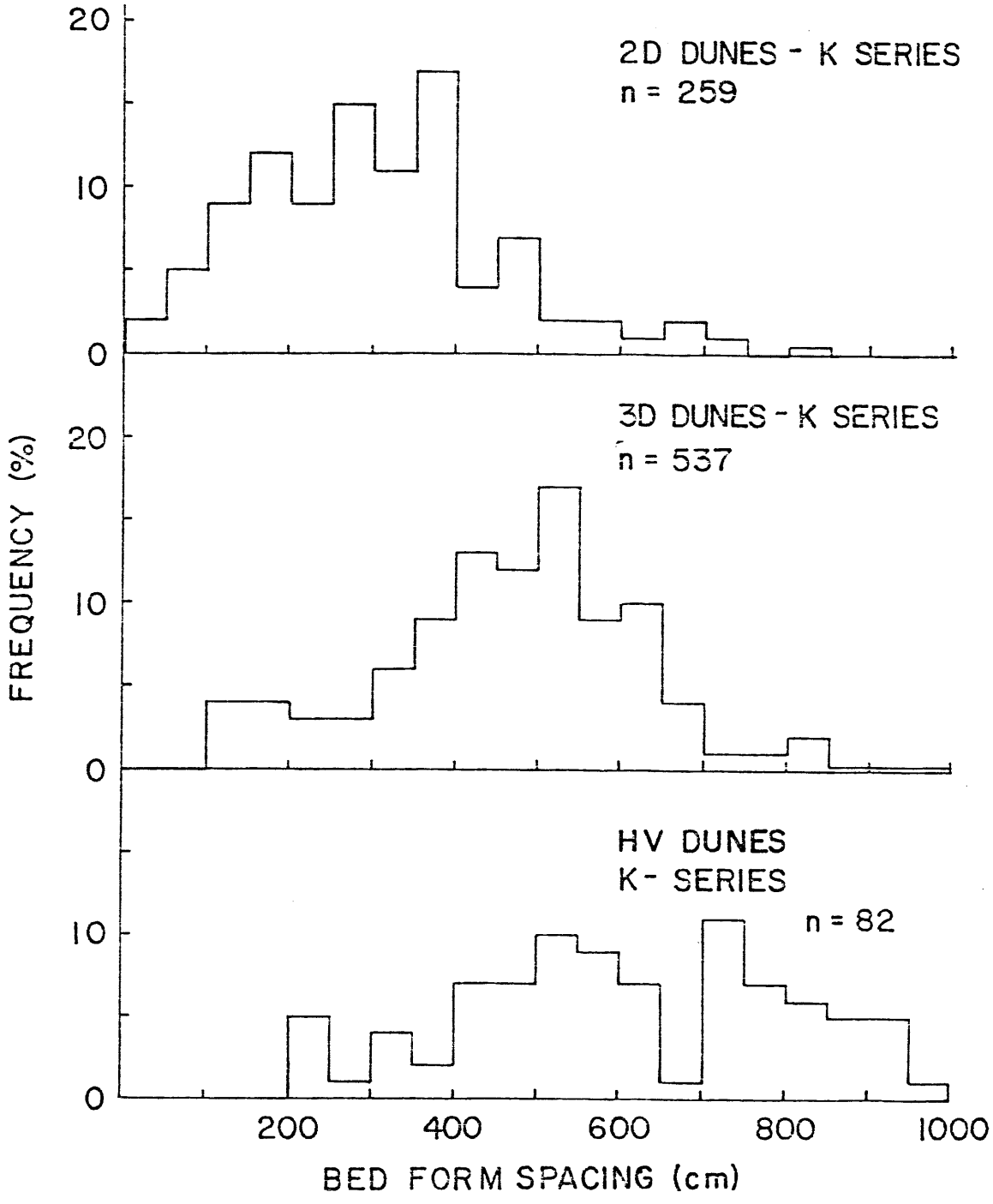

FIGURE 20 -- Histograms of bed-form spacing for K series (n = number of observations)

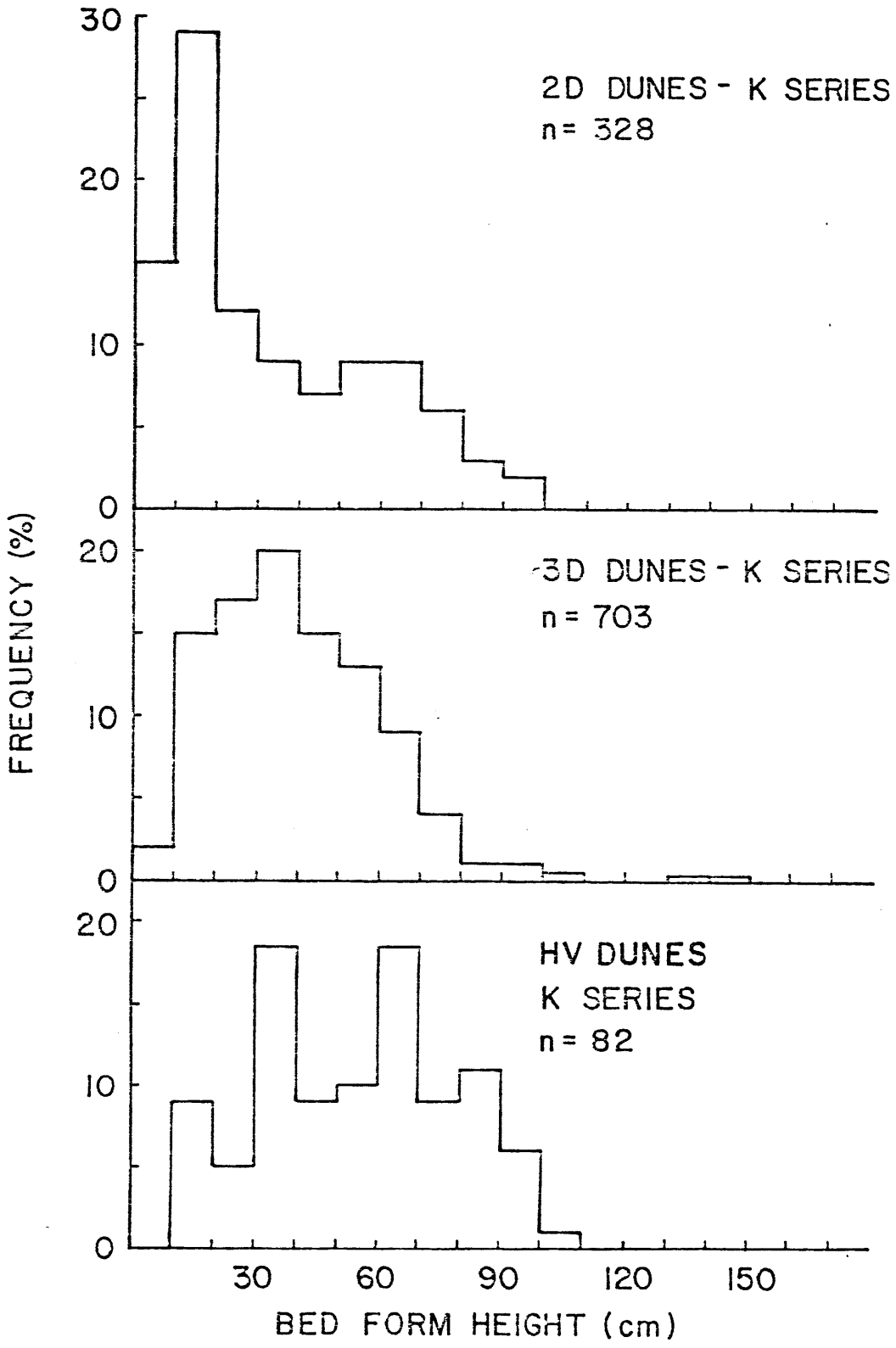

FIGURE 21 -- Histograms of bed-form height for K series (n = number of observations)

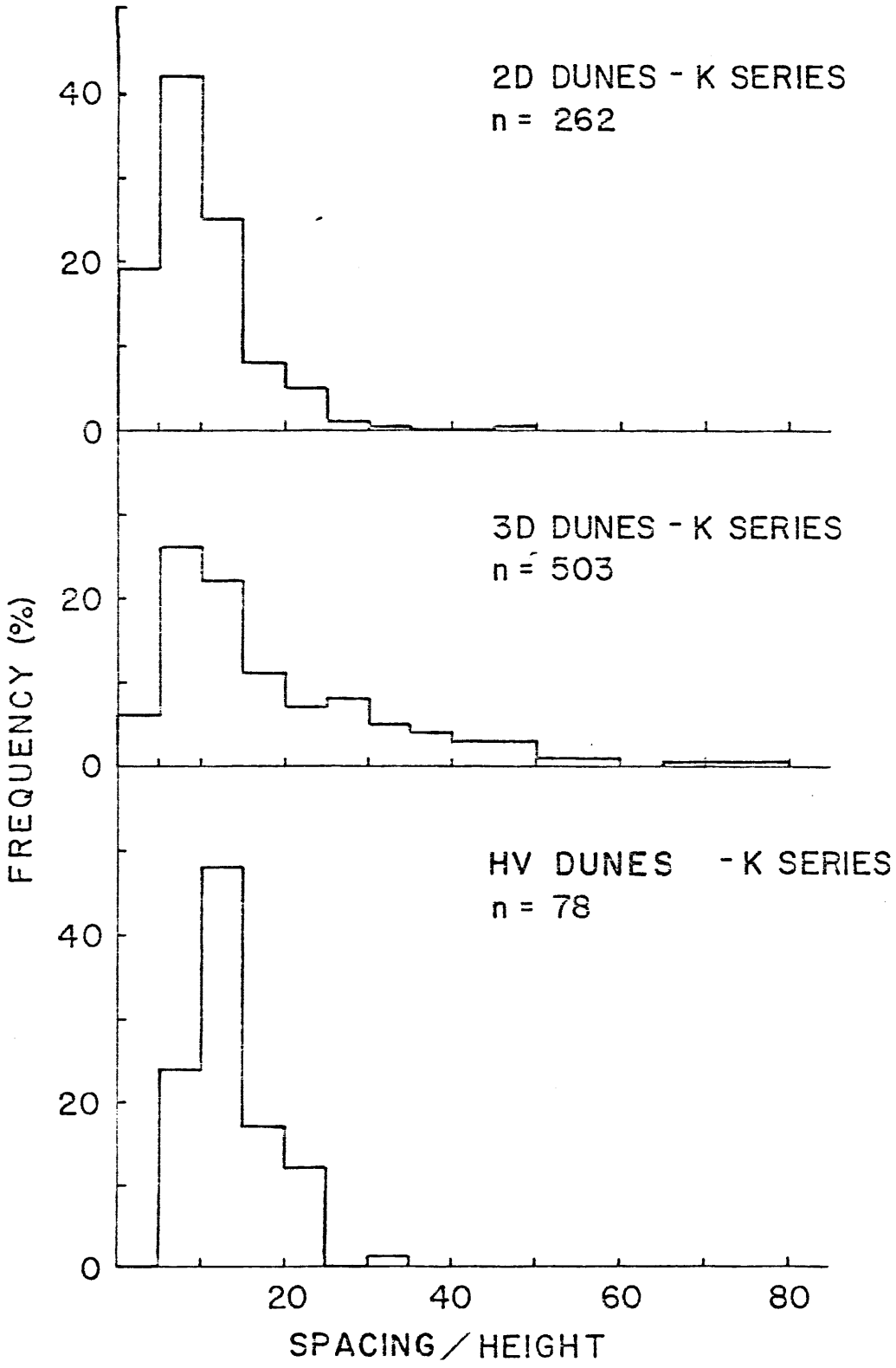

FIGURE 22 -- Histograms of bed-form spacing-to-height ratio for K series (n = number of observations)

Examination of the histograms of the spacings for the three kinds of bed forms emphasizes in differences among the three kinds of dunes. Two-dimensional dunes range in spacing from 10 to 750 cm and have a broadly unimodal distribution about a mode of 375 cm. Their distribution is asymmetric, skewed toward the shorter values. Three-dimensional dunes range in spacing from 100 to 800 cm. The spacings of 3D dunes are more symmetrically distributed about a fairly strong mode at 525 cm. Spacings of HV dunes range from 200 to 1025 cm, and are very broadly distributed, with several modes, the two strongest at 525 and 725 cm. The distributions of bed-form height follow the same general trends. Heights of HV dunes have a broad, polymodal distribution. The distributions of heights of 2D and 3D dunes are just as broad, but each subphase has a different, well-defined mode.

There is considerable overlap in the parameters of the three types of dunes; specifically, there is no obvious gap in spacing (as seen by Boothroyd and Hubbard, 1975; Jackson, 1975b), nor is there a marked difference in the distribution of height or spacing-to-height ratio (as seen by Costello, 1974, or by Dalrymple et al., 1978). Although data are not numerous enought to demonstrate it conclusively, there is probably a smooth progression in frequency distributions of height and spacing with increasing flow velocity throughout the dune range; differences in the histograms of Figs. 20 and 21 are a consequence of their composite nature. Still, one could readily differentiate among

2D, 3D, and HV dunes when observed in the flume, as discussed below.

The distinctions among the dune subphases were made on the basis of bed-form shape and behavior, parameters not easily expressed in numbers or reflected in the bed-form statistics. Quantification of easily measured variables may obscure and not enlighten the investigation. Careful observation and description can provide the key to the problem.

Two-Dimensional Dunes

Two-dimensional dunes have flat to slightly undulatory stoss slopes, with slope angles of about 7° (range 4° - 9°) (Fig. 23a). Ripples are the only bed form superimposed on these dunes. The lee face of 2D dunes always has a segment that lies at or near the angle of repose of the sediment. This slipface generally does not extend the full height of the bed form. The top of the slipface, where the avalanching of sediment begins, is defined as the brinkpoint. The bed-form crest is the locus of highest elevation (measured from the succeeding trough). In the 2D dune phase, the brinkpoint and crest are often not coincident; the crest may be 10 to 30 cm upstream of the brinkpoint (Fig. 23b). Thus the cross-beds generated by these forms are not as tall as the entire bed form. Crestlines of 2D dunes are even in elevation across the entire width of the flume. Their plan form is straight to slightly sinuous.

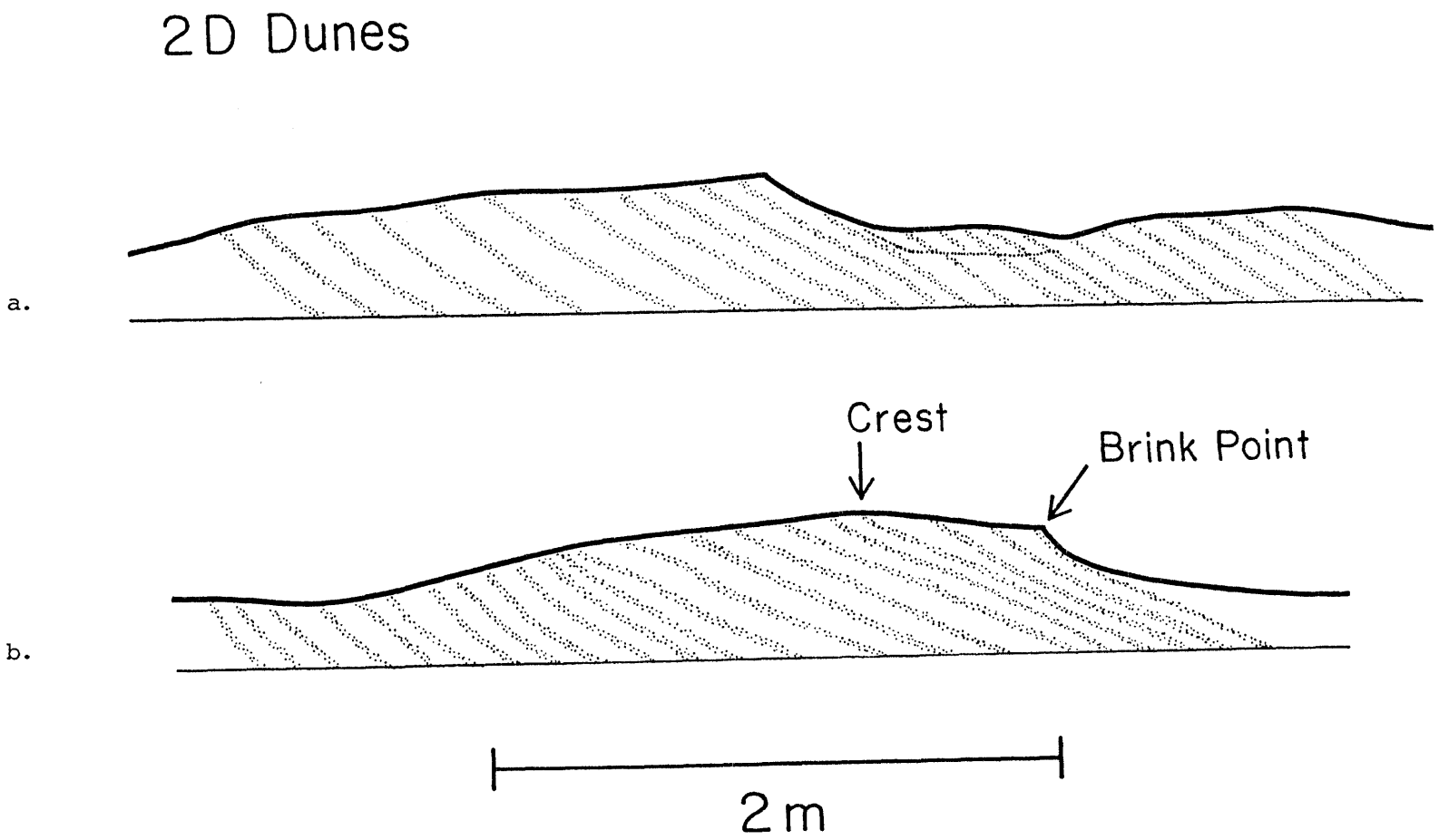

FIGURE 23a & 23b -- Morphology of two-dimensional dunes. (figures traced from 16mm films, cross-beds schematically represented.)

The internal structure of 2D dunes is shaped by their migration behavior, detailed below. Most commonly a 2D dune is composed of a stack of several tabular cross-sets, each 10 to 20 cm thick (Fig. 23c).

Three-Dimensional Dunes

Three-dimensional dunes have a "hump-back" appearance; the stoss slope is markedly convex upward in profile (Fig. 24a). Their backs are generally smooth with few superimposed bed forms. 3D dunes resemble ripples, having the classic triangular profile. The lee faces of 3D dunes lie at or near the angle of repose of the sediment. Crests and brinkpoints are usually coincident, hence the slipfaces extend to the full height of the bed forms (25 to 60 cm tall). Crestlines of three-dimensional dunes may be either even or uneven in elevation across the channel. Their form may be sinuous to lunate, sometimes with spurs extending 30 to 70 cm up the stoss slope of the downstream bed form.

Three-dimensional dunes usually leave deposits of large-scale trough cross-stratification with the sets extending to the full height of the bed form (Fig. 24b). When one dune overtakes and merges with another, the internal structure is composed of two or three smaller trough cross-sets (10-20 cm thick). The smaller sets may then progress downstream into a single set of cross-strata that forms the entire height of the the dune (Fig. 24c).

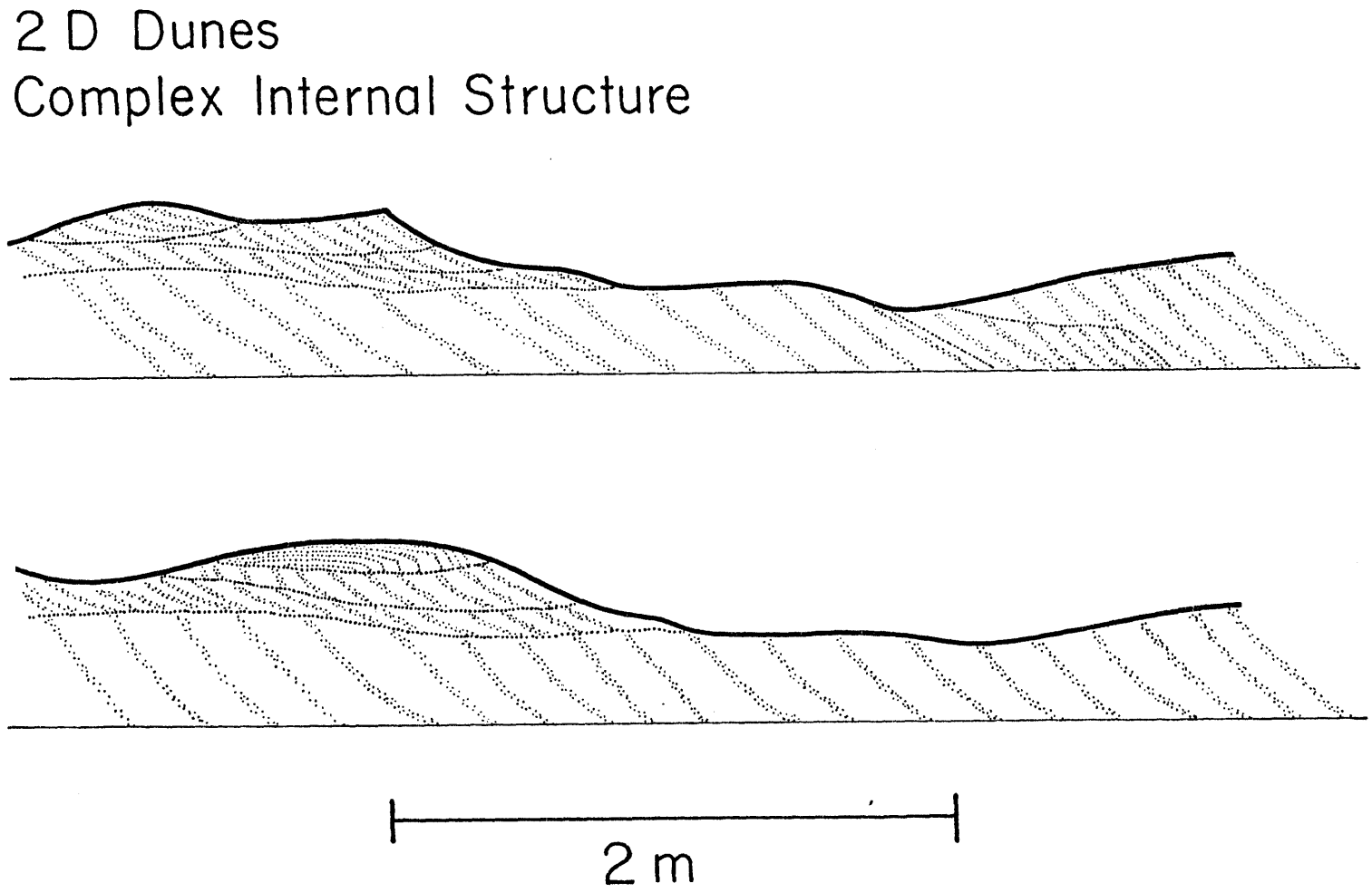

FIGURE 23c -- Internal structure of two-dimensional dunes. (Figures traced from 16 mm films, cross-beds schematically represented)

3D Dunes

Longitudinal Profiles

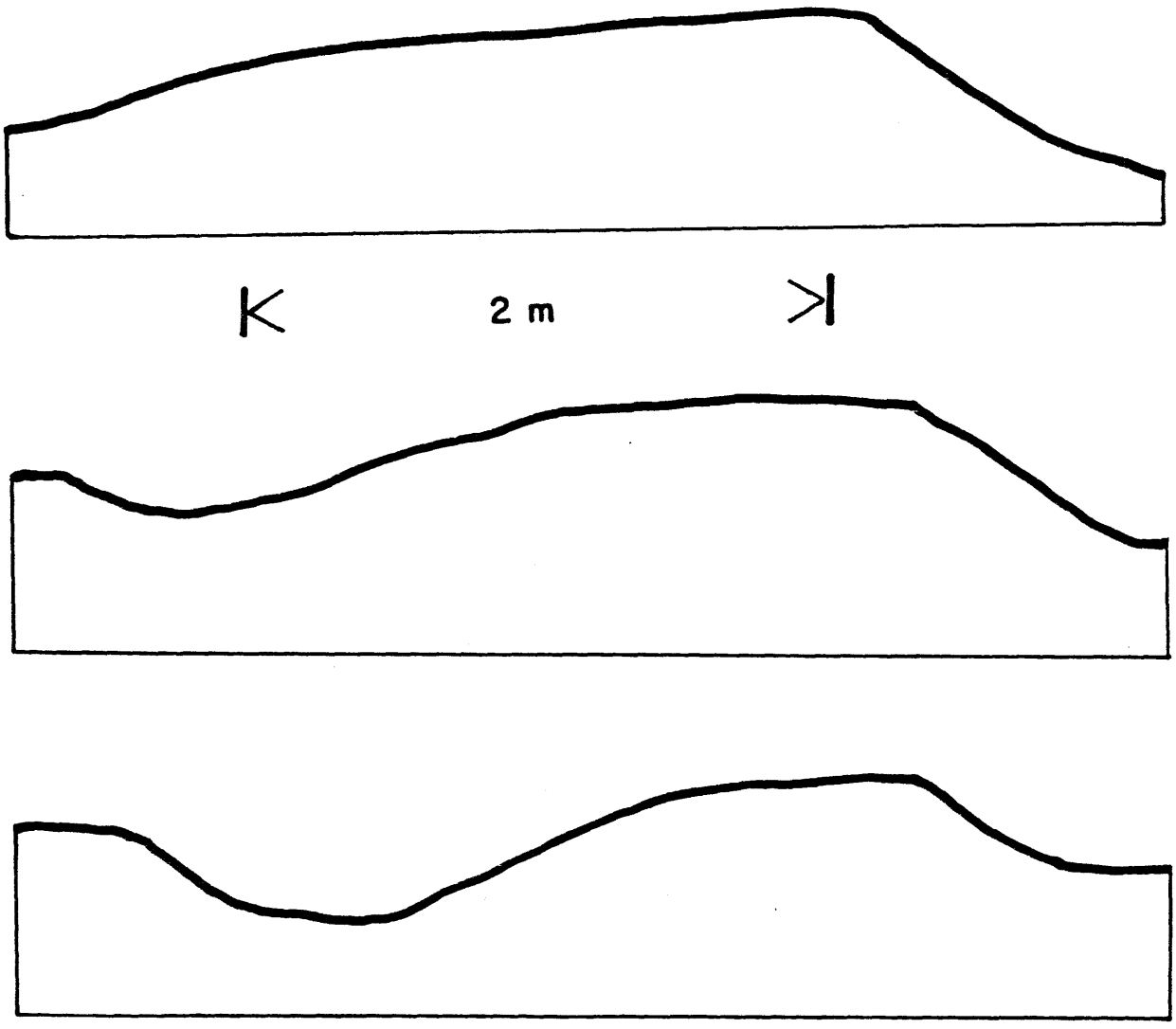

FIGURE 24a -- External morphology of three-dimensional dunes. (Profiles traced from 16 mm films)

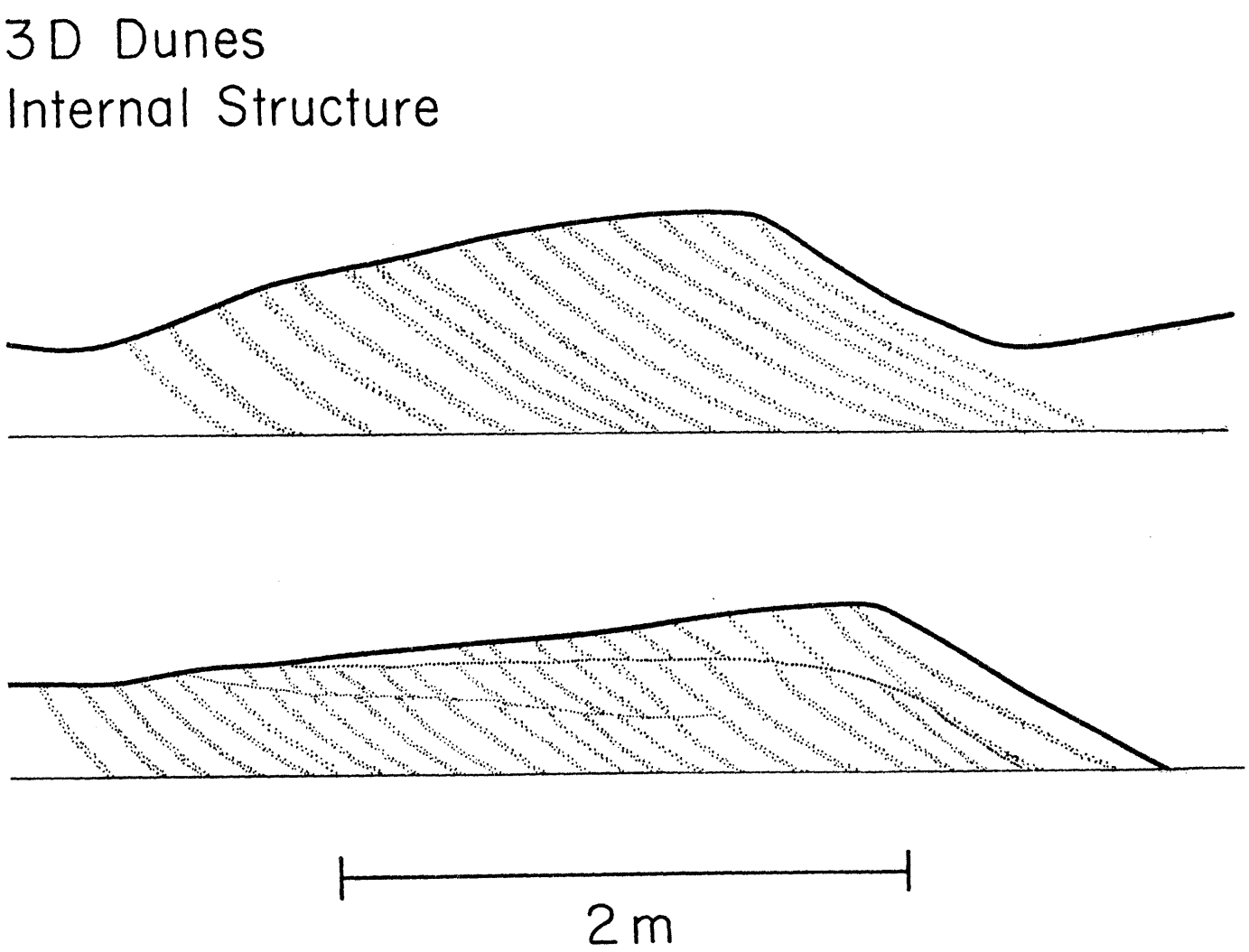

FIGURE 24b & 24c -- Internal structures of three-dimensional dunes. (Figure traced from 16 mm films, cross-beds schematically represented)

Higher-Velocity Dunes

Higher-velocity dunes have flat, almost horizontal, backs (average slope = 4°), extending over most of the stoss side (Fig. 25a). The stoss slope rises sharply out of the upstream trough and then flattens out to form the major part of the bed form. The initial stoss slope may be as steep as 23°, rising over a distance of 50 to 70 cm (about 1/6 to 1/10 of the entire length). This flat back is not due to a planing-off effect of the flow, as is seen in shallow flume experiments in which dunes "wash out" at high velocities (Simons and Richardson, 1963). The dune crests maintain a sharp break between stoss slope and slip-face. Even when the bed-form crest is about 60 cm high (flow depth over the crest = 40 cm) HV dunes maintain their normal shape and migrate in the same manner. This extreme condition occurred only once or twice in each HV-dune run, but indicates that flow constriction over the bed-form crest has little effect on the geometry of most HV dunes.

At least the downstream half of the HV dune is covered with smaller bed forms. These superimposed forms are small (4-8 cm high, 20-40 cm long), and subdued; they are not very asymmetric, and there is little flow separation over them. They resemble the "rollers" described by Pratt (1971). They travel quickly up the stoss slope, modifying the overall shape of the bed-form crest. Modification in crest shape involves switching from sharp and well-defined to rounded at a high rate (about every 3 to 5 min).

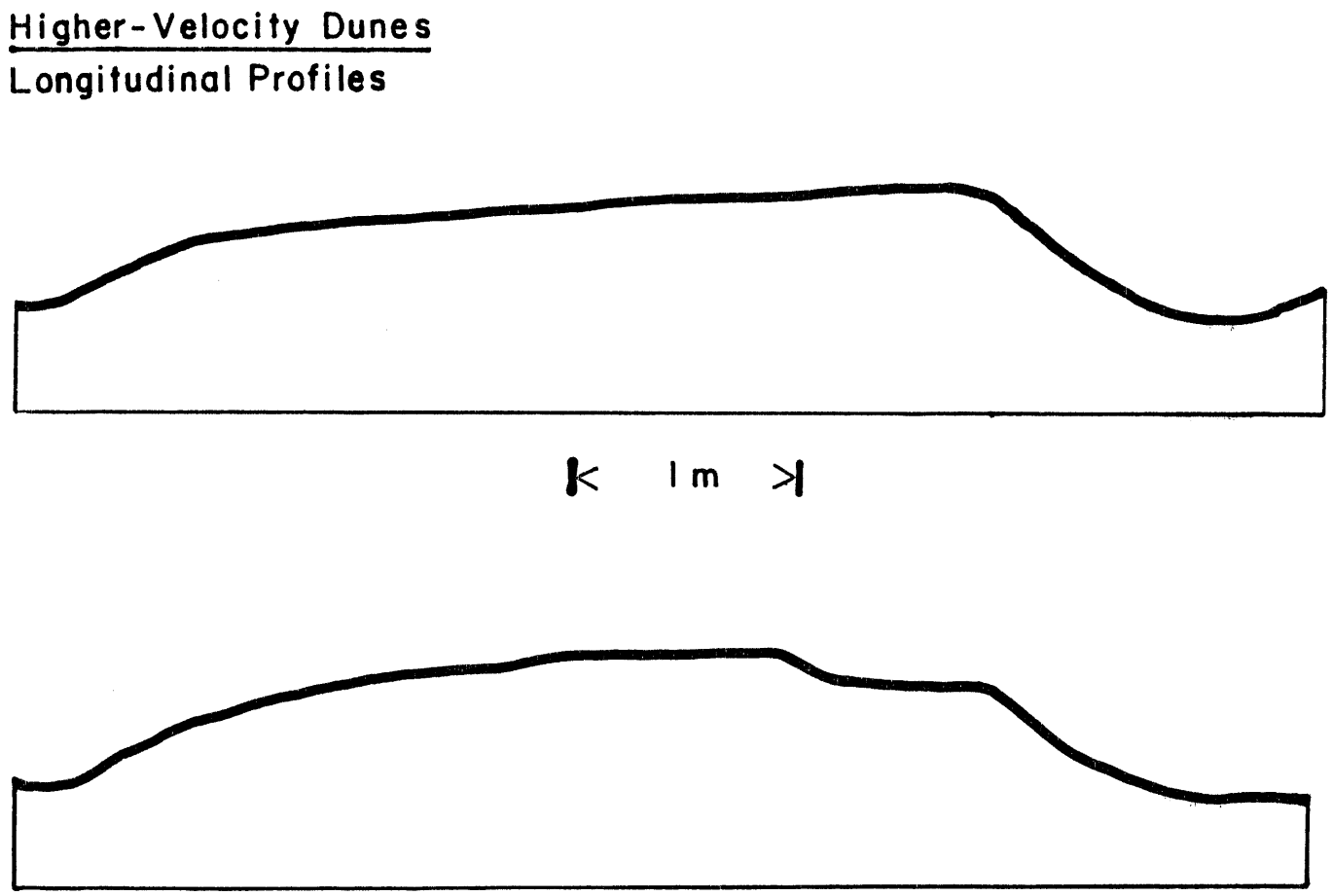

FIGURE 25a -- External morphology of higher-velocity dunes. (Profiles traced from 16 mm films)

The crest and brinkpoint may not be coincident, but the slipface always forms at least half of the height of the lee face. The upper part of the lee face may be rounded and deposit parallel laminations, grading downstream into angle-of-repose cross-sets, or the slipface may extend to the full height of the sand wave (Fig. 25b).

Crestline elevations are smooth across the width of the flume, but are generally higher on one side (Fig. 26). This indicates that the HV dunes are "too wide" for the channel: their cross-stream development is restricted by the walls. In plan, the crestlines are straight to sinuous and generally two-dimensional.

Higher-velocity dunes deposit large-scale tabular cross-strata that are almost the full height of the generating bed form. The top 5 to 10 cm of the deposit is composed of either parallel lamination (Fig. 27) or small-scale (ripple) trough cross-stratification.

BED-FORM KINEMATICS

The clearest distinctions among the three kinds of bed configurations generated in the experiments can be made on the basis of their kinematics. Their differences are reflected best in modes of migration, changes in crest shape, and types and behavior of superimposed bed forms.

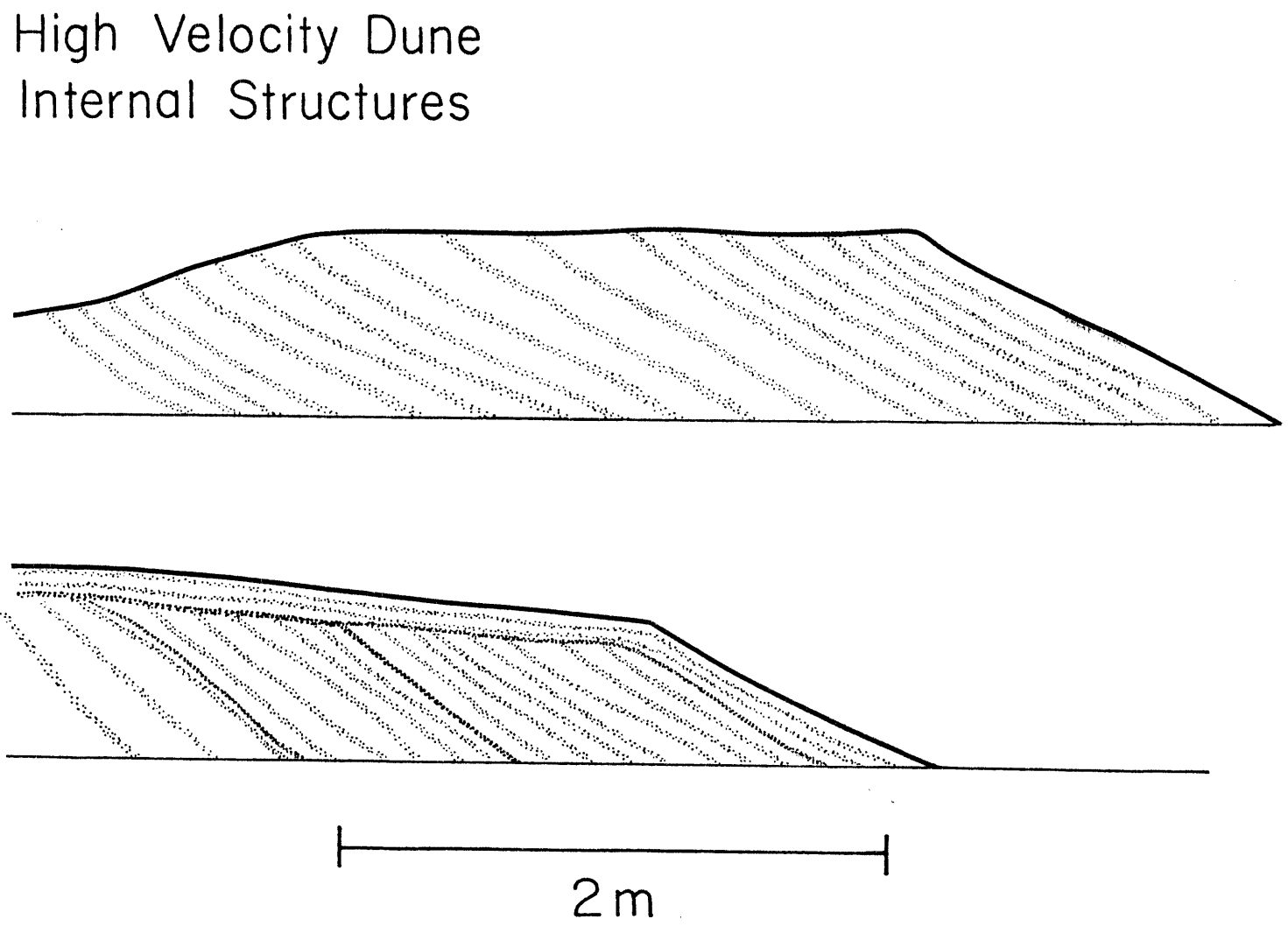

FIGURE 25b -- Internal structure of higher-velocity dunes. (Figure traced from 16 mm films, cross-beds schematically represented)

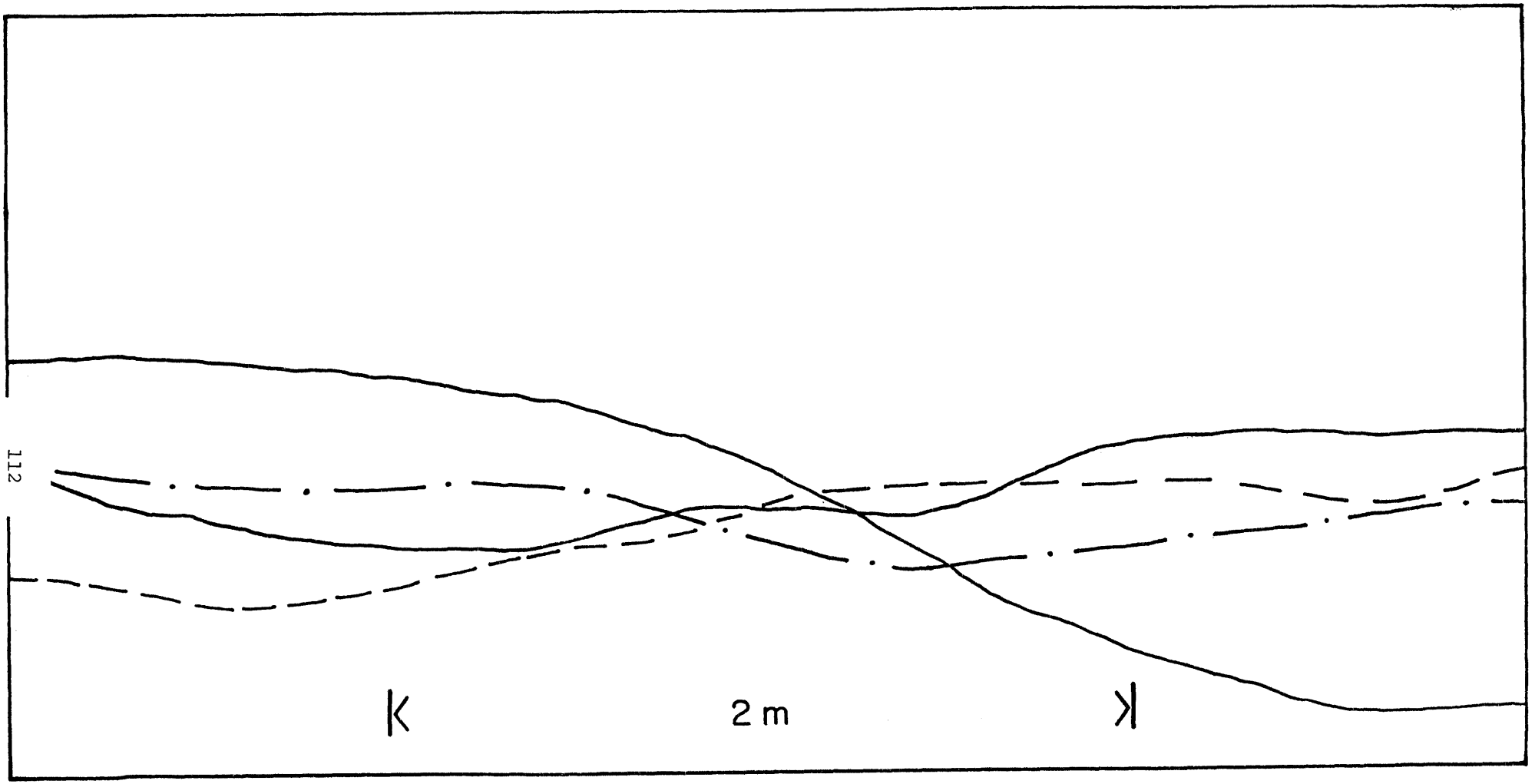

FIGURE 26 -- Transverse profiles of higher-velocity dunes (derived from sonic profiles, full channel width)

Higher-Velocity Dune Stratification

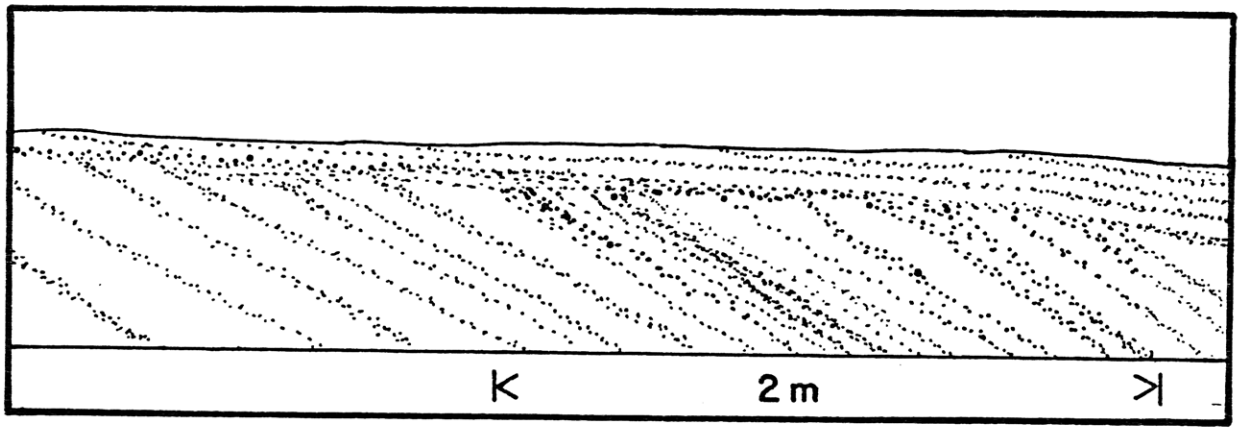

FIGURE 27 -- Stratification in higher-velocity dunes (bottom drawing is a schematic representation of the parallel lamination shown in the upper photograph).

Two-Dimensional Dunes

Two-dimensional dunes form in a range of flow velocities in which there is general, continuous grain motion. There is strong sediment transport as bed load, with little sand travelling in suspension.

Nearly all 2D dunes attenuate in height as they migrate downstream. Viewed in the observation window, most forms decrease 5 to 10 cm in this 2.3 meter reach. The 2D dunes maintain their form by the merging of successive dunes. The smaller 2D dunes travel faster than the larger ones, and overtake them. Several forms may do this, then combine into a single, larger 2D dune whose slipface extends the full height of the form. This larger dune migrates as a single unit until overtaken by other smaller forms, and the cycle repeats (Fig. 28).

In this overtaking and merging process, each smaller 2D dune progrades out over a thin (1-3 cm thick) unstratified layer (Fig. 29). This layer is sandwiched between two sets of cross-strata, and very much resembles a "reactivation structure" (Collinson, 1970). However, it is formed under uniform and steady flow conditions.

Similar reactivation structures to these were made by McCabe and Jones (1977), but only in a solitary delta-like form with superimposed ripples. In the present experiments there is proof that reactivation structures can be formed by the interaction of a series of migrating large-scale bed forms. This process is described in detail by Corea (1981).

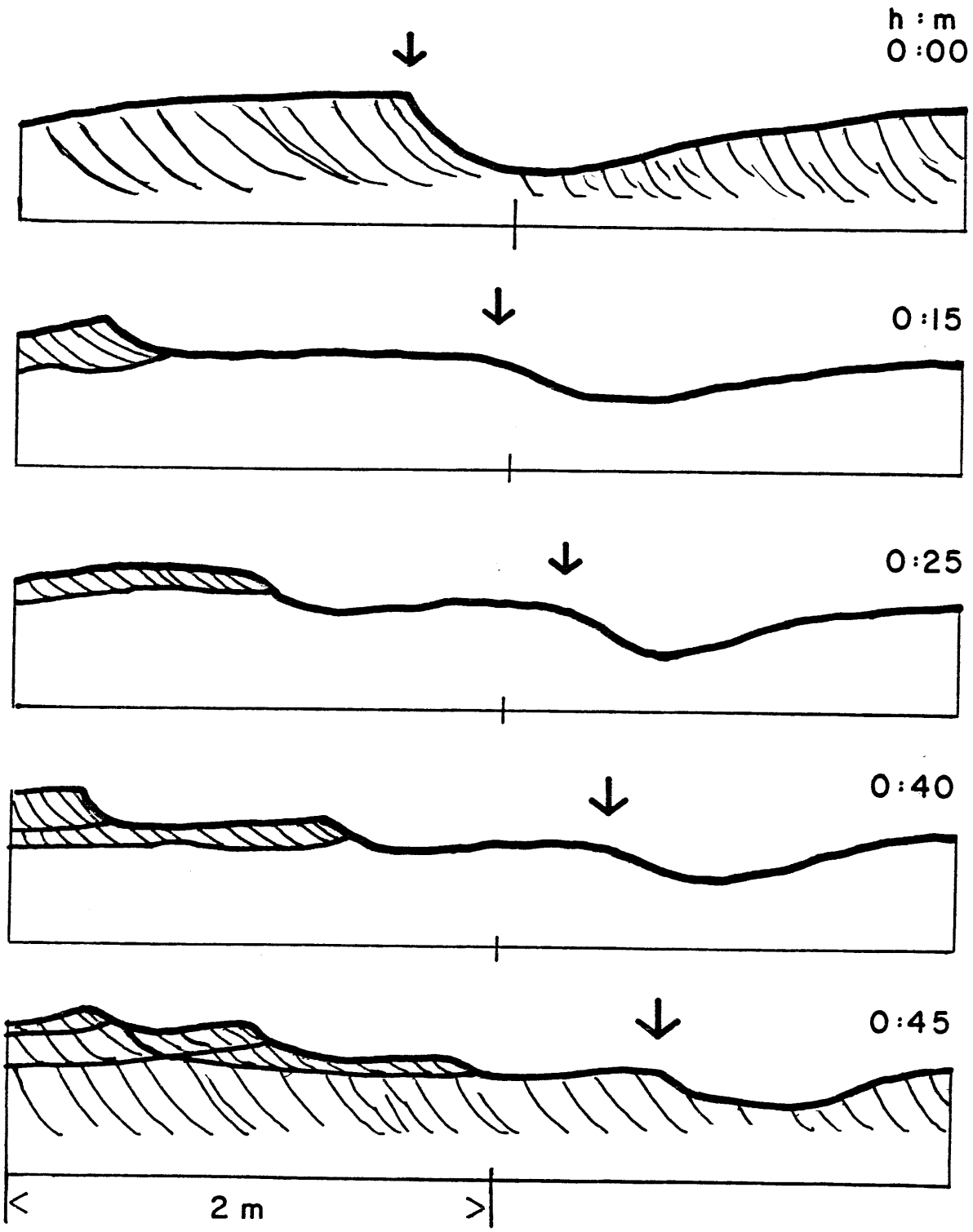

FIGURE 28 -- Migration behavior of two-dimensional dunes (traced from 16 mm films, Run K-11)

2D Dune - Migration Behavior (cont.)

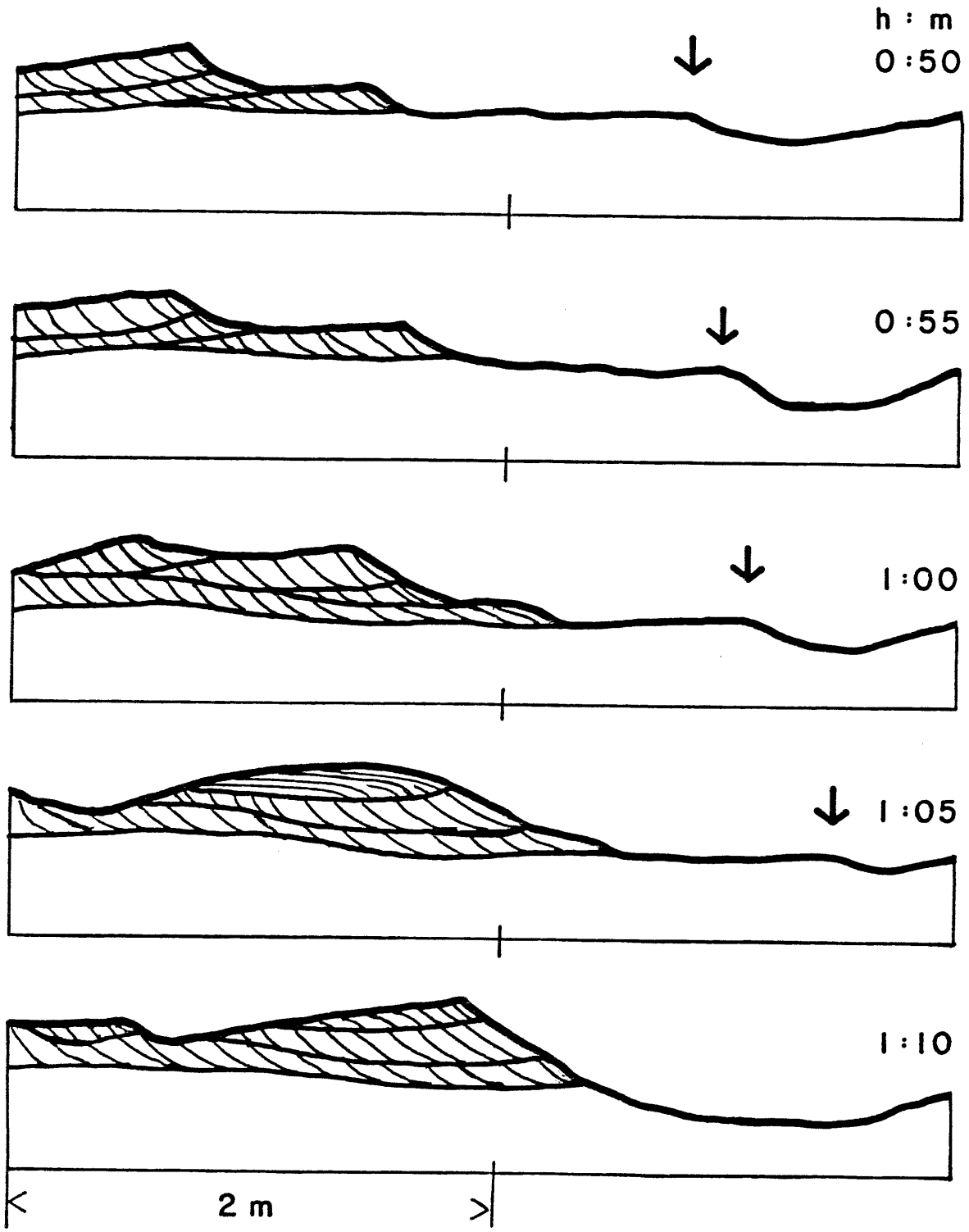

FIGURE 28 -- continued

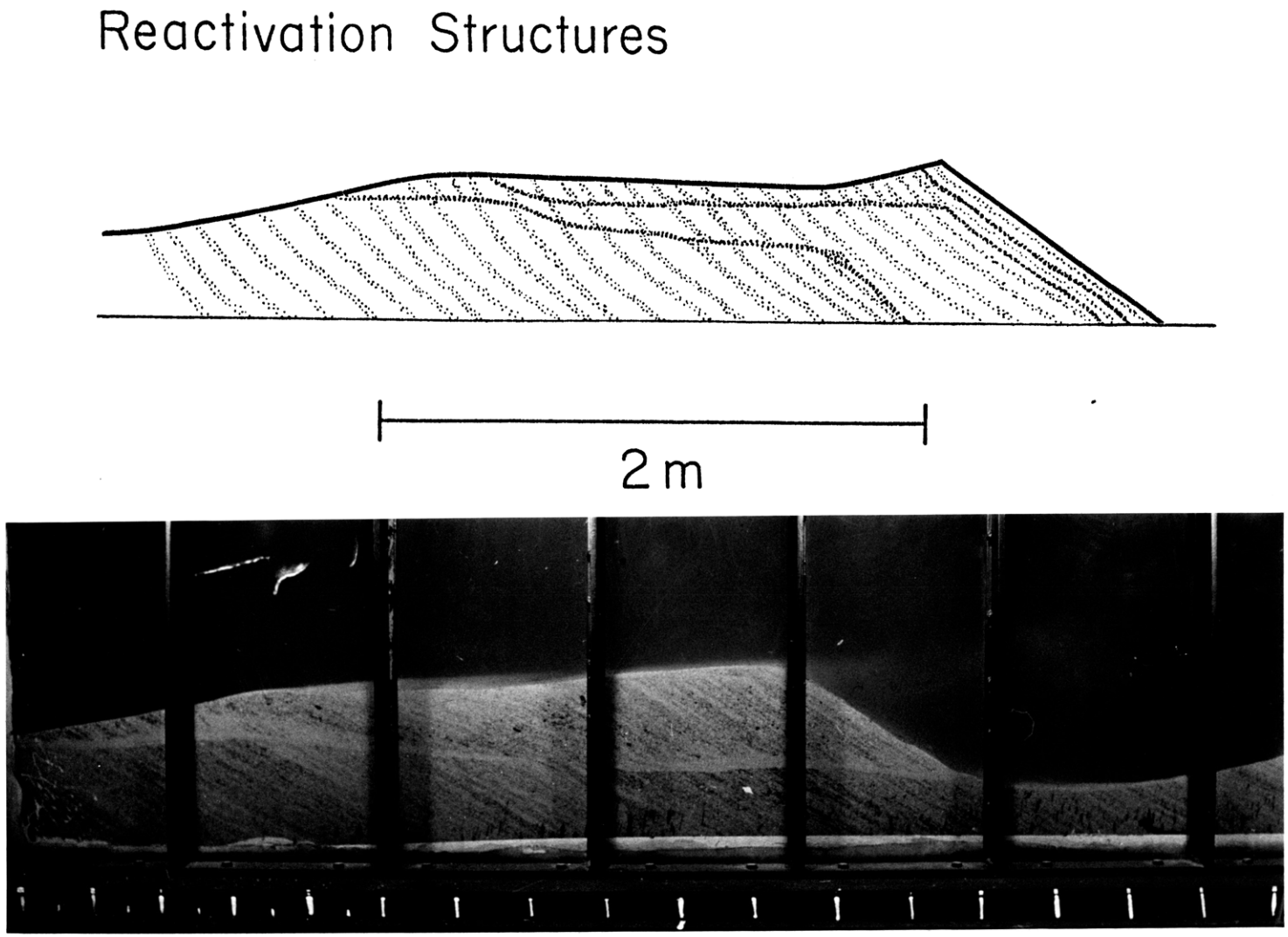

FIGURE 29 -- Reactivation Structures: Two examples found in Three-Dimensional Dunes.

Three-Dimensional Dunes

Sediment transport is much stronger in the range of velocites characterizing 3D dunes. Much sand is thrown into suspension at the crest, in a jet-like flow (Fig. 30). There is a well-defined separation eddy downstream of the crest, often generating currents sufficiently strong to form reverse ripples. The crest shape remains sharp, the brinkpoint and crest coinciding, with well-defined flow separation at that point.

Three-dimensional dunes usually migrate as a single form, with a slipface covering the entire lee side of the dune (analogous to "normal" ripple migration). Superimposed bed forms are relatively rare, but profoundly affect the migration of the major form. A superimposed bed form, as it migrates up the stoss slope of the dune, effectively "strands" the major slipface of the bed form. Most of the sediment transport over the back of the major form comes about in the migration of the superimposed bed forms. Thus, little sediment reaches the major slipface, and its downstream progress is severely retarded. A thin lag deposit consisting mainly of heavy minerals may form over the portion of the major dune downstream of the superimposed form. This serves to preserve the outline of the "stranded" dune when the superimposed form has passed.

The superimposed bed form migrates up the stoss slope, depositing thin (less than 10 cm) trough cross-strata over the stoss-slope "lag" layer. When it reaches the original slipface, the brinkpoint of the superimposed form becomes the brinkpoint

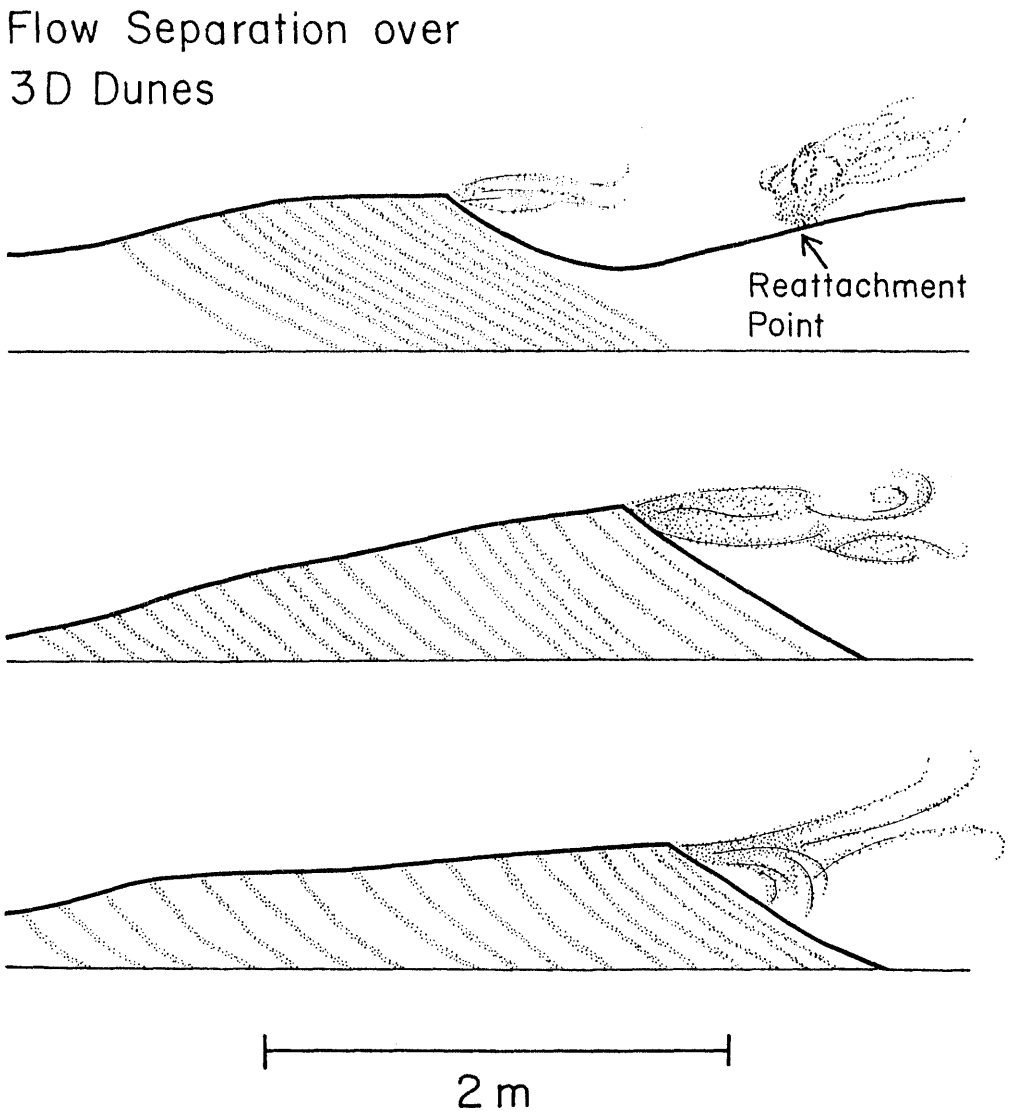

FIGURE 30 -- Flow separation over three-dimensional dunes. (Figure traced from 16 mm films)

for the entire bed form. The entire dune then migrates with a full-height slipface, and the "normal" 3D dune shape.

Higher-Velocity Dunes

The range of velocities characterizing HV dunes is marked by very strong grain motion, with much sand in suspension throughout the entire depth of flow. Strong gusts mark the flow reattachment point on the HV dune, throwing much sand into suspension. Often, not all of the sand settles out of suspension by the time the flow reaches the next HV-dune crest. Thus, sand eroded from the stoss slope of an HV dune is not necessarily deposited on the lee face of that same HV dune.

The stoss slope is smooth for about the upstream third; subdued bed forms are superimposed in the downstream two-thirds. The superimposed bed forms appear like "rollers" (Pratt, 1971): not very asymmetric, with little flow separation apparent. They travel rapidly (5-10 cm/min) up the stoss side, modifying the crest shape and leaving small-scale trough cross-strata.

Generally, HV dunes maintain a constant height as they migrate; the stoss slope may change from flat (almost horizontal) to slightly convex upward with superimposed bed forms.

A direct comparison of the differing modes of bed-form migration is made in Fig. 31. Here, the pathlines of three representative bed-form crests are represented in space and time; the slope of each curve is equivalent to the bed-form migration rate. None of the lines is straight, indicating that bed-form celerity

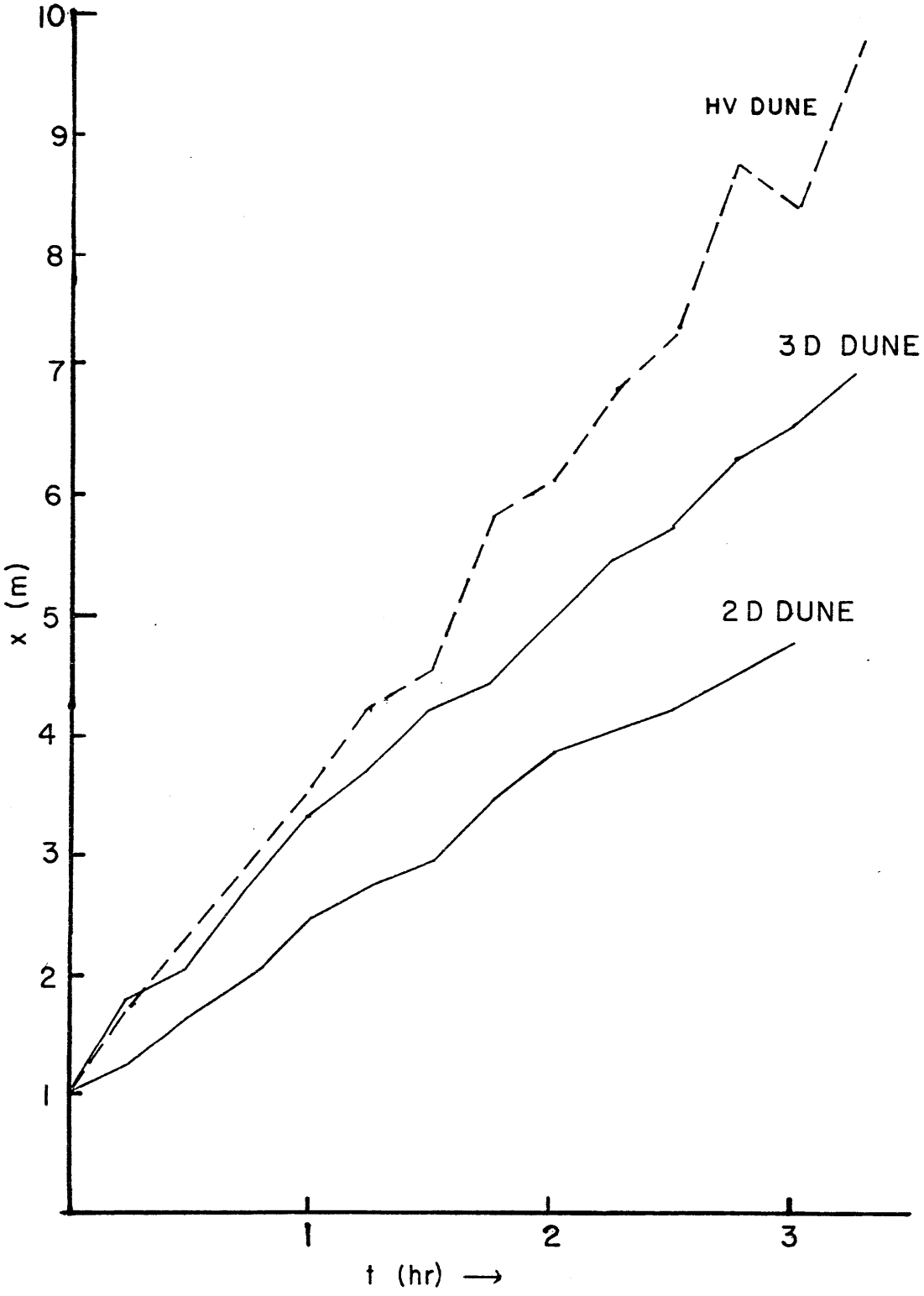

FIGURE 31 -- Pathlines in space-time plot for representative bed forms.

changes as the form migrates. The extent of change differs from the 2D and 3D dune phase to the HV dune phase. 2D dunes and 3D dunes have a fairly constant celerity that changes smoothly as they progress downstream. In contrast, the migration rate of HV dunes changes rather rapidly and erratically; the crest is even seen to move upstream for short periods -- a reflection of the influence of the superimposed bed forms on the shape and position of the crest of the HV dunes.

HYDRAULIC PROPERTIES

The two-phase flow system is controlled by a series of complex feedback mechanisms. A given flow generates a specific bed configuration; the bed configuration in turn exerts a control on the energy loss within the flow, the modified flow modifying the bed forms. The modification of the energy picture is mirrored in the water-surface slope (energy slope), the bottom shear stress, and the bed friction factor.

The development of different bed phases can be characterized by the different trends in the water-surface slope with increasing flow velocity (Pratt, 1971; Costello, 1974). Though hardly conclusive, Fig. 32 suggests that each of the three bed configurations recognized in the experiments has a different rate of increase of energy slope with increasing velocity. A least-squares line was fitted to the data for each separate bed configuration; correlation coefficients ranged from 0.70 to 0.76.

The development of 2D dunes is marked by a lower rate of increase of energy slope than for the development of 3D dunes (Least-squares line slopes: 0.11 versus 0.31). The development of HV dunes is characterized by a leveling off, or perhaps even a slight decrease, in energy slope with increasing flow velocity (least-square line slope = -0.02).

The trends of the energy slope are very similar to those seen by Costello (1974) for sand of similar size. His "bars" (2D dunes) had a lower rate of increase in energy slope; the

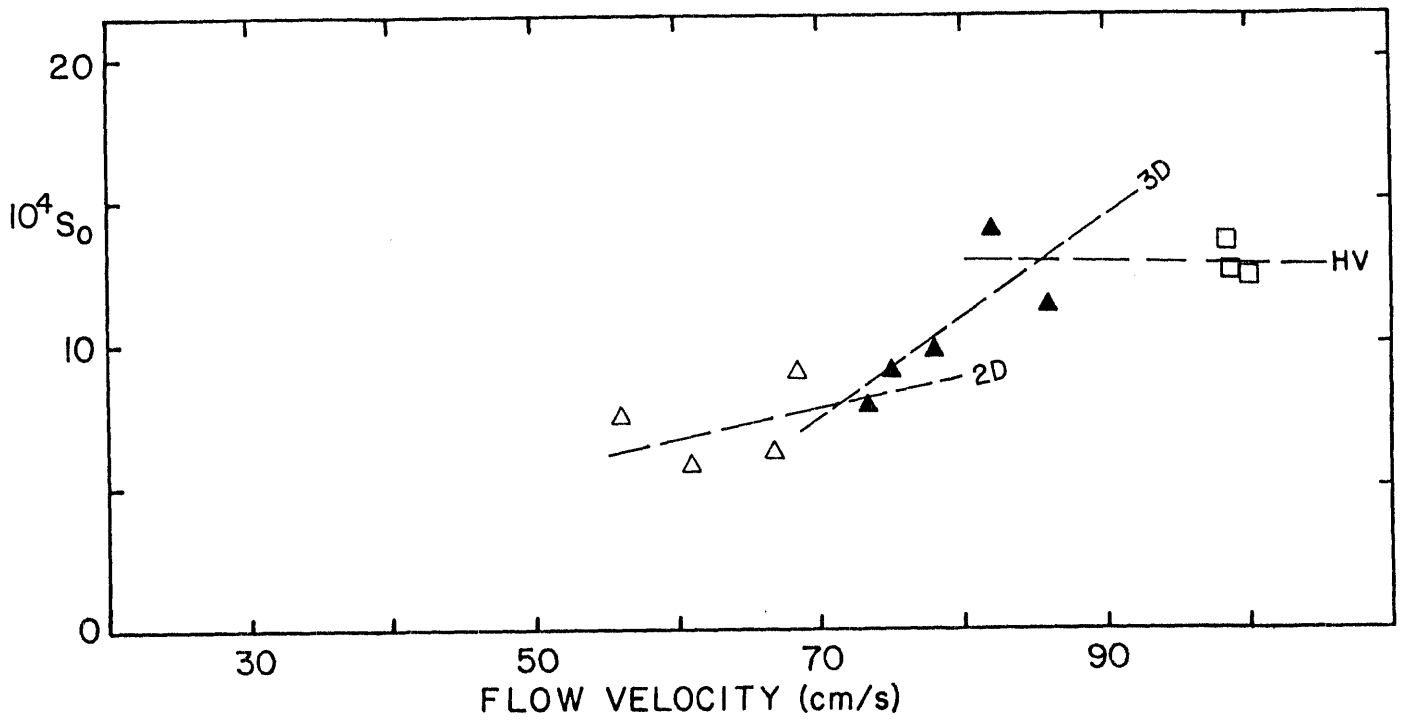

FIGURE 32 -- Energy slope versus flow velocity for the K series. Dashed lines represent best-fit lines for each bed-form type: 2D = 2D dunes; 3D = 3D dunes; HV = higher-velocity dunes.

onset of "dunes" (3D dunes) brought a sharp increase in slope. Higher velocity dunes were not developed in his experiments. Alternatively, the variation of the energy with increasing velocity slope could be characterized as well by a single line, which describes its variation almost as well ($r^2 = 0.48$).

The picture of bottom shear stress is similar to that of energy slope, though more diffuse (Fig. 33). A sharp increase throughout the dune phase is followed by a leveling off in the HV dune field. Scatter in the data precludes subdivision of the dune phase.

The bottom shear stress was calculated from formula $\tau_o = \rho\ g\ R\ S_o$, where ρ = fluid density, g = acceleration of gravity, R = hydraulic radius, S_o = water-surface slope. The effects of the side walls were neglected for two reasons. The roughness elements on the bed (tens of centimeters) were much larger than those on the walls (several millimeters); the bed roughness constituted the major resistance to the flow. The experiments were not primarily concerned with measuring bottom shear stress, and the apparatus did not allow sufficient accuracy in its determination. These calculations were made only to reveal the trend of the variable in this system.

Even more diffuse is the trend of the bed friction factor. Plotted in Fig. 34, f_b decreases with increasing velocity for all bed phases; further, more specific behavior for the individual

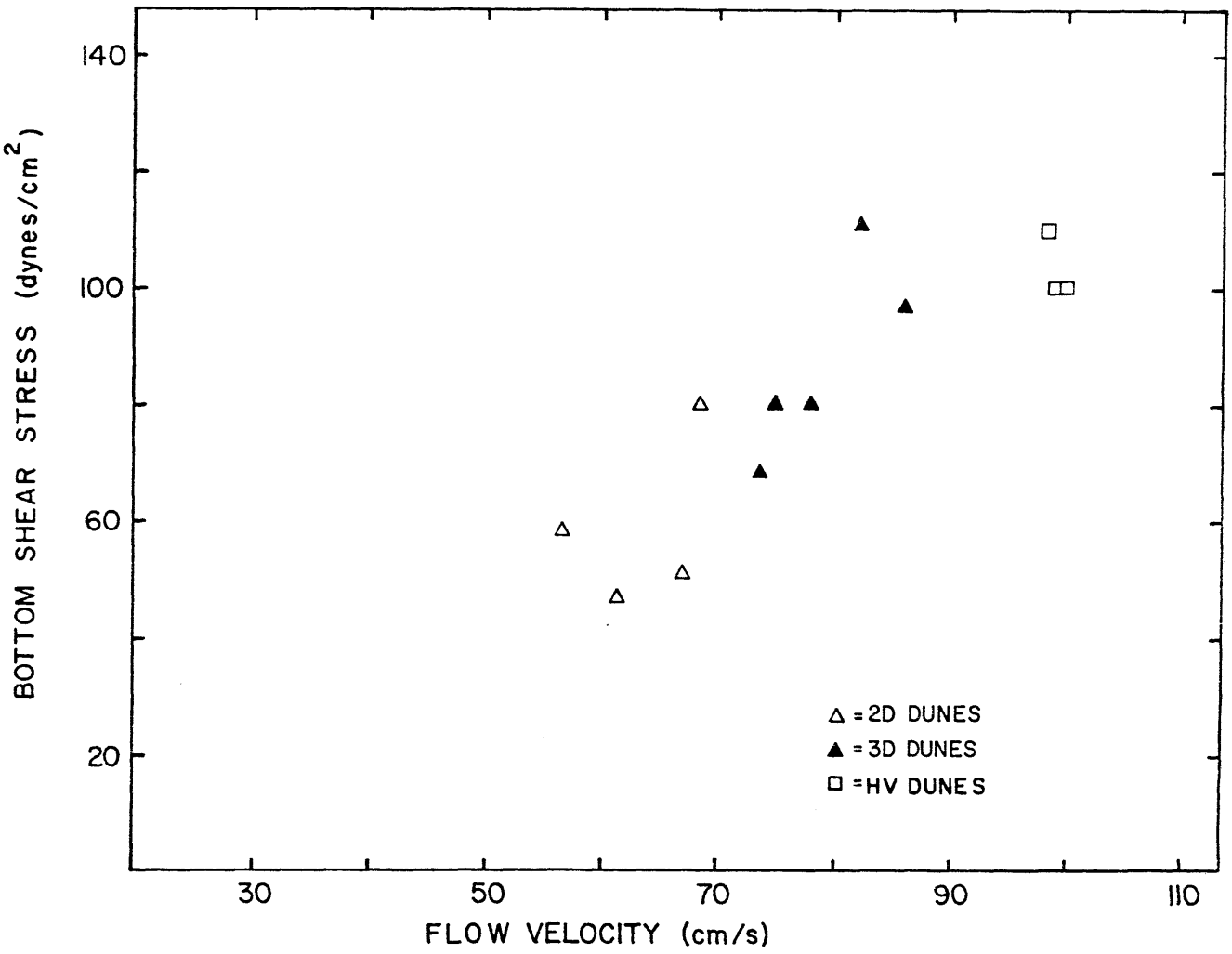

FIGURE 33 -- Bottom shear stress versus flow velocity for the K series.

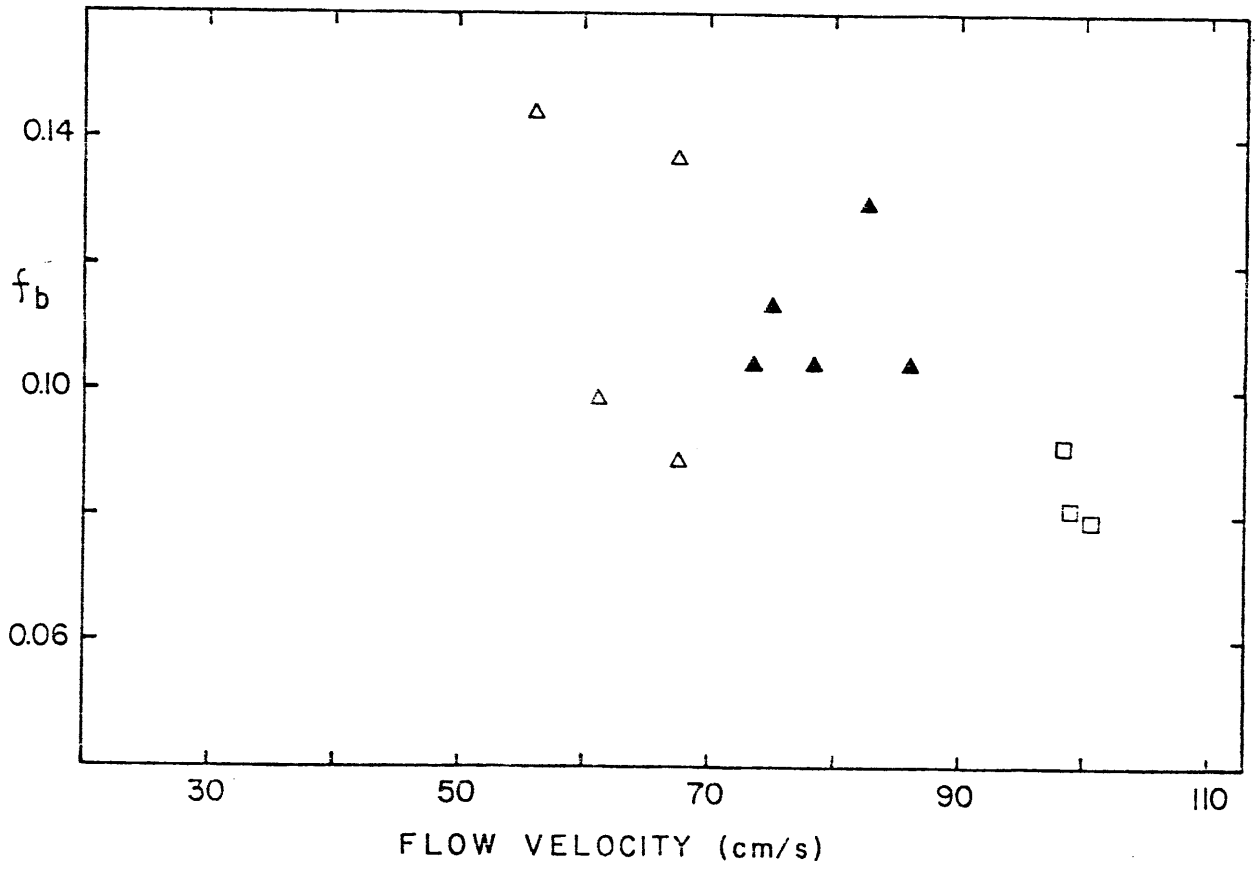

FIGURE 34 -- Darcy-Weisbach friction factor versus flow velocity for the K series.

Open triangles: 2D dunes
Solid triangles: 3D dunes
Squares: HV dunes

configurations is not discernible. In Fig. 35, f_b is plotted against bed-form height. The points lie scattered broadly about the curve for the Darcy-Weisbach friction factor for fully rough turbulent flow. This curve was determined by using bed-form height as the measure of boundary roughness. The data again show a smooth transition between successive bed-form types, f_b increasing with increasing bed-form height.

The response of the bed forms to increasing velocity is depicted in Figs. 36, 37, and 38. Bed-form spacing is a very smooth, linear function of flow velocity; bed-form height increases with velocity in a much less even manner. The spacing-to-height ratio of the bed forms also increases, but very diffusely. The migration rate of the bed forms (Fig. 39) correlates best with flow velocity, increasing along the line:

$$\text{Migration Rate} = (0.11)\ \text{Velocity} - (497.12).$$

The flow over the crests of all bed forms showed definite separation, with a well-defined reverse circulation in the lee in most cases. The flow reattachment point was on the average 5.5 bed-form heights (H) downstream of the brinkpoint. This separation length ranged from 4.5H to 8H, with no significant differences among runs. These values accord well with the experimental observations (Abbott and Kline, 1962; Tani, 1957; Walker, 1961) used by Costello (1974) in his model of the mechanics of dunes and considered by Briggs (1979) in his model of the local mean-velocity field.

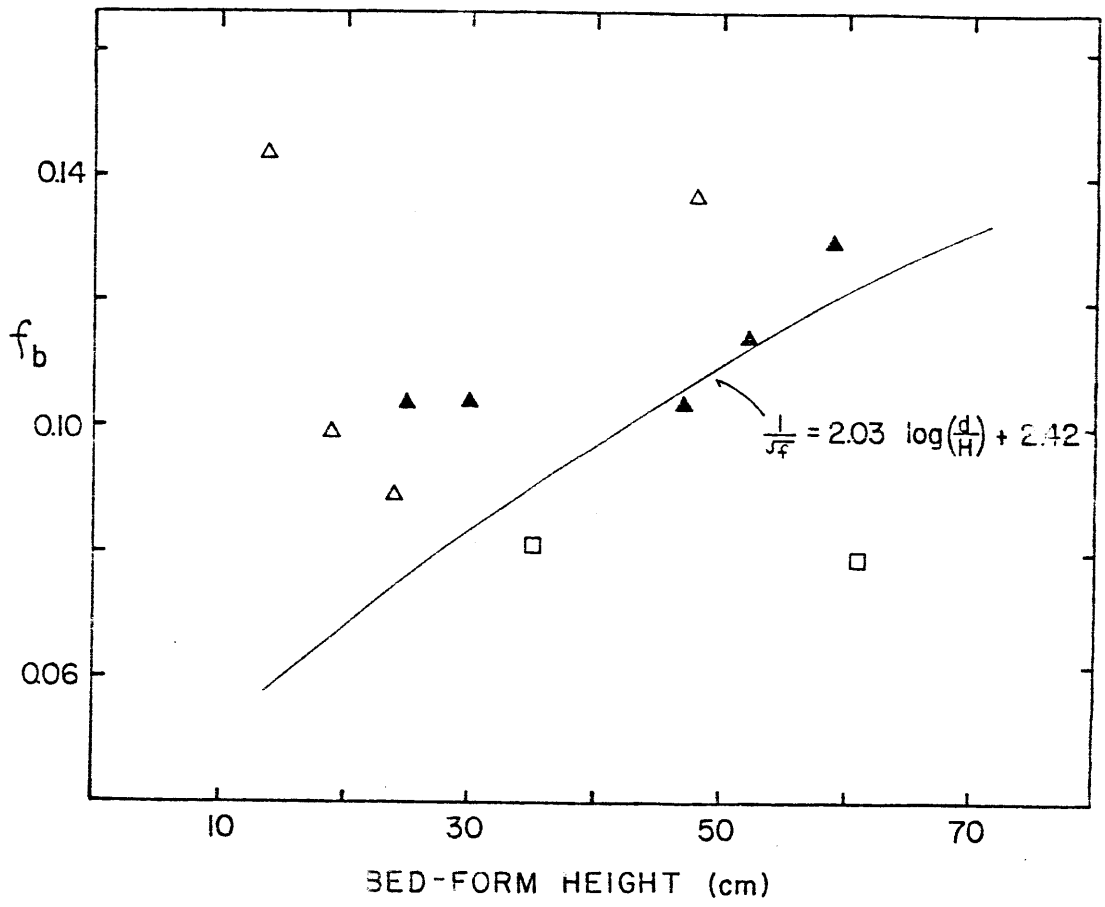

FIGURE 35 -- Darcy-Weisbach friction factor (f_b) versus bed-form height for the K series:

Open triangles: 2D dunes
Solid triangles: 3D dunes
Squares: HV dunes

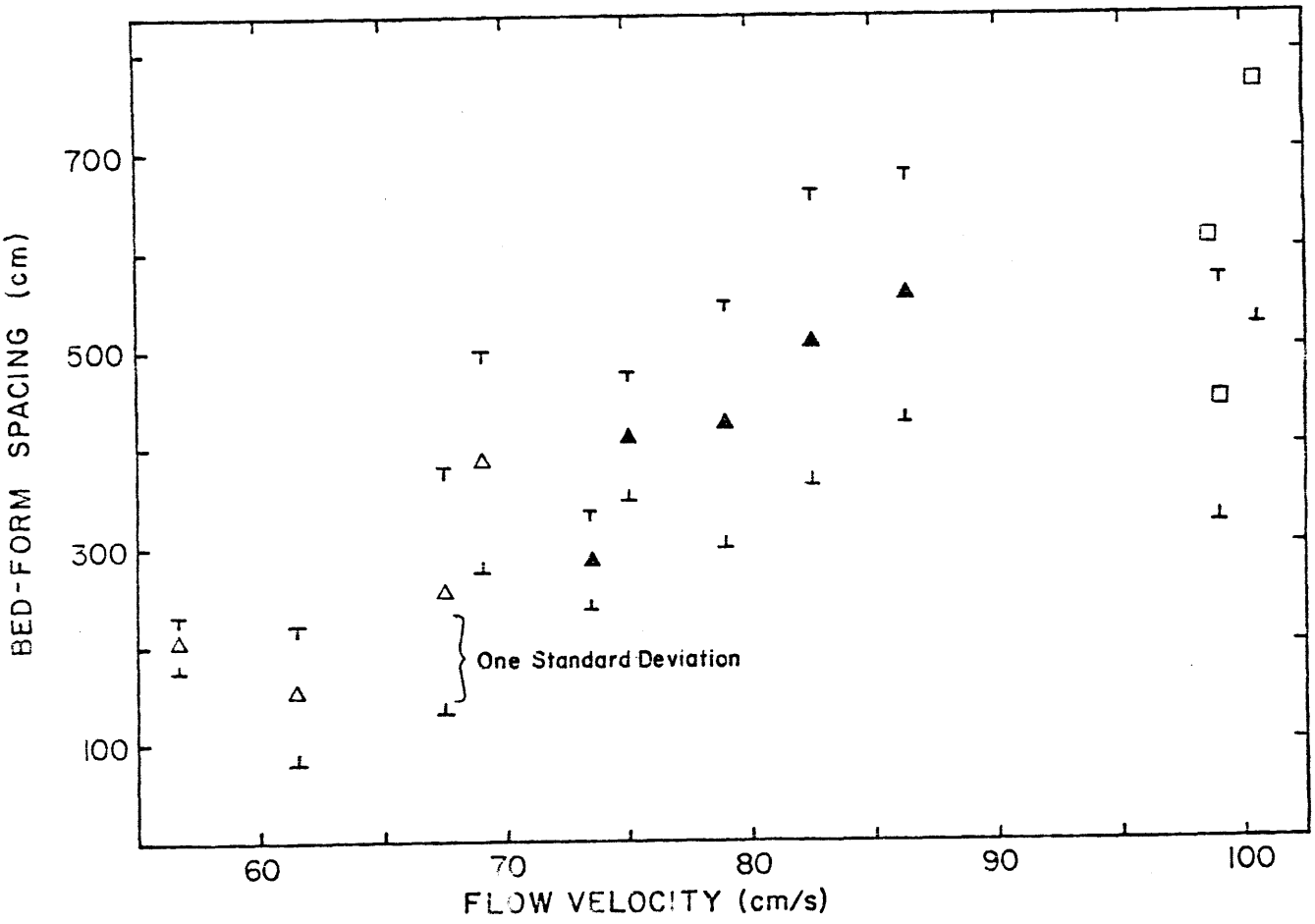

FIGURE 36 -- Bed-form spacing versus flow velocity for the K series.

Open triangles: 2D dunes
Solid triangles: 3D dunes
Squares: HV dunes

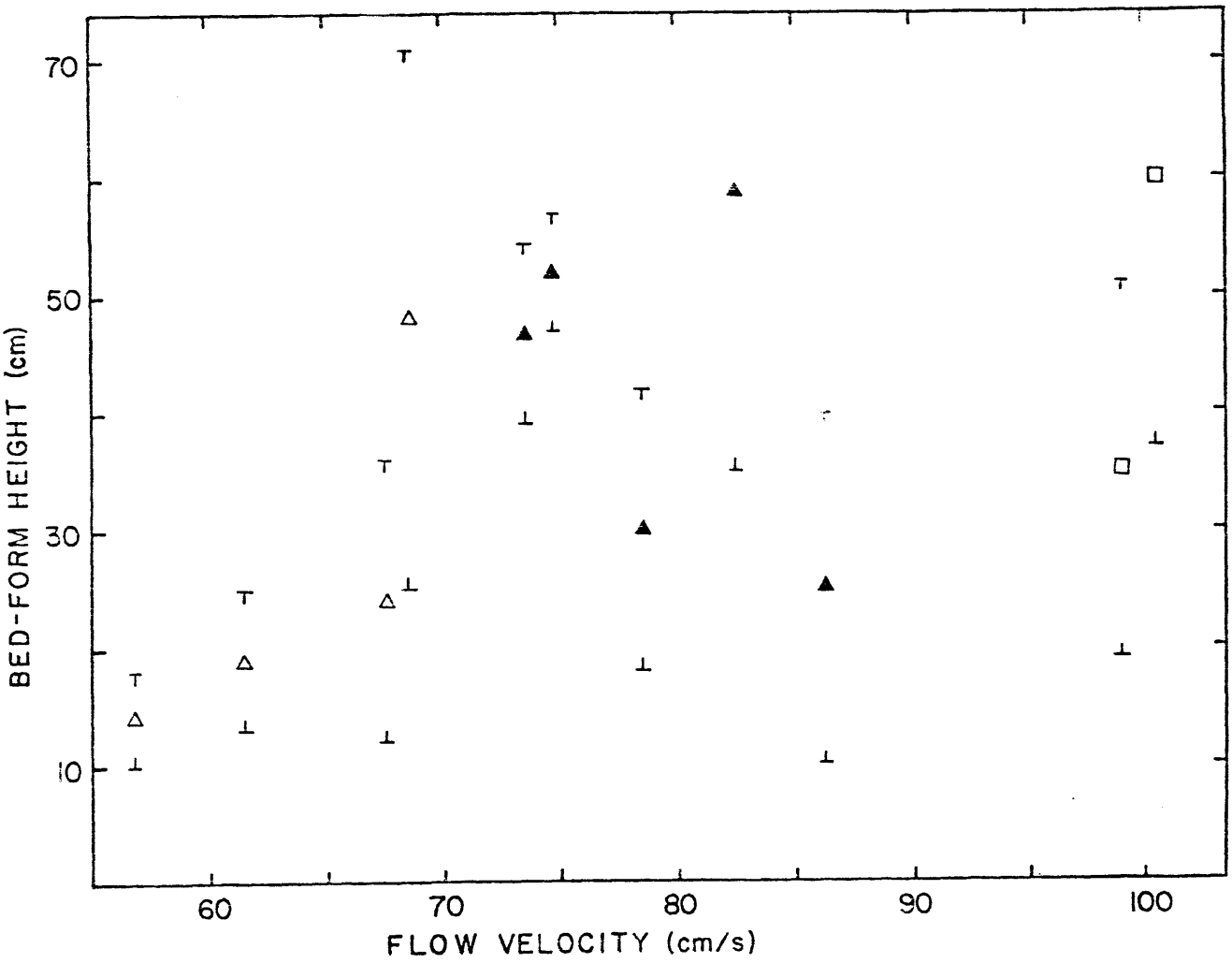

FIGURE 37 -- Bed-form height versus flow velocity for the K series.

Open triangles: 2D dunes
Solid triangles: 3D dunes
Squares: HV dunes

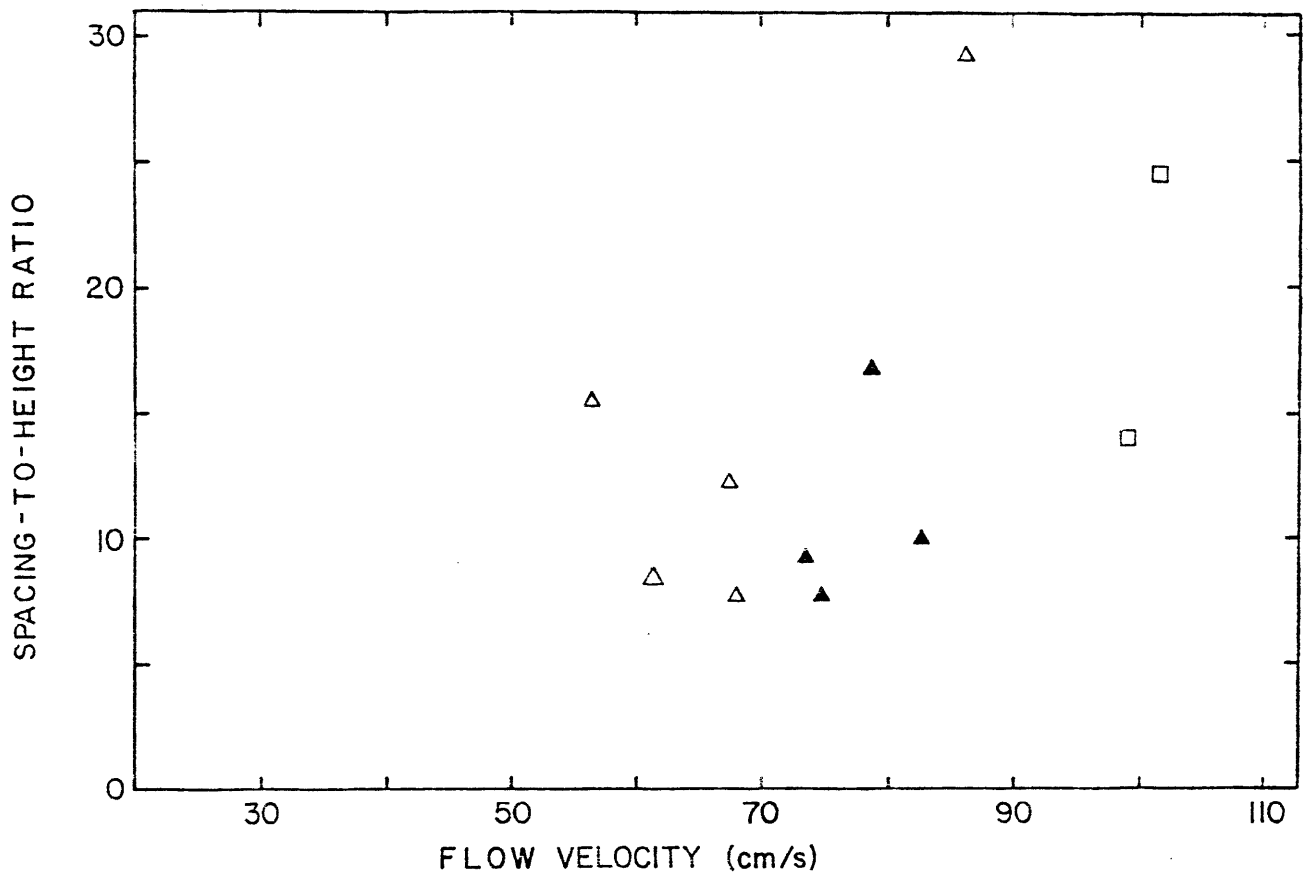

FIGURE 38 -- Bed-form spacing-to-height ratio versus flow velocity for the K series.

Open triangles: 2D dunes
Solid triangles: 3D dunes
Squares: HV dunes

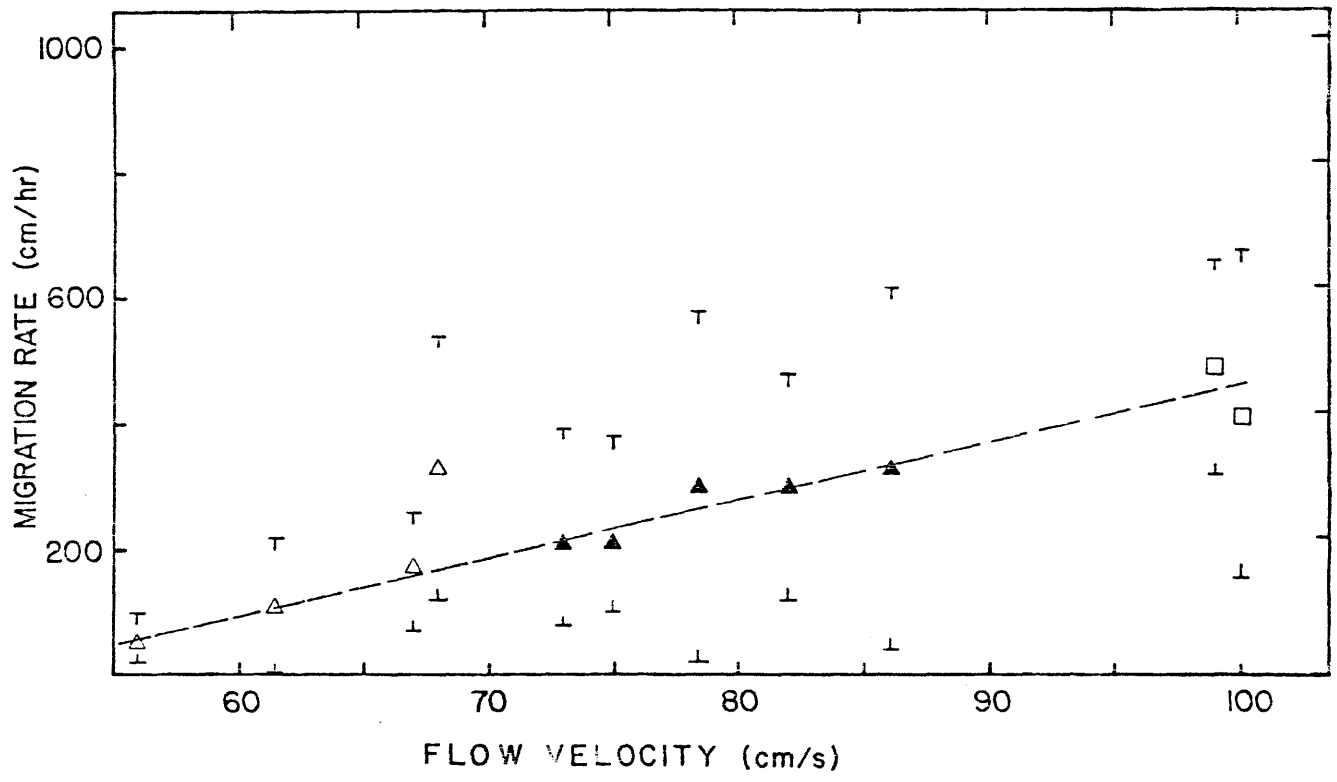

FIGURE 39 -- Bed-form migration rate versus flow velocity for the K series.

Open triangles: 2D dunes
Solid triangles: 3D dunes
Squares: HV dunes

The sum total of the hydrodynamic data, though not conclusive, indicates that the forms called 2D dunes, 3D dunes, and HV dunes are similar dynamically. In the range of velocities achieved, bed-form height, spacing, and migration rate increase monotonically (and almost linearly) with increasing flow velocity. The flow variables (bottom shear stress and friction factor) also demonstrate a smooth progression with increasing velocity. These data then are not inconsistent with the idea that 2D dunes, 3D dunes, and HV dunes are subphases of one type of large-scale bed configuration.

BED-FORM RESPONSE TO CHANGING FLOW CONDITIONS

An important consideration in these experiments was the time required for the bed forms to come into equilibrium with the flow. The sediment transport system may be viewed most simply in terms of process (independent variables) and response (dependent variables) (Allen, 1974). The process is characterized by the rate of energy input to the system, generally expressed by the flow velocity. The response is revealed by the change in morphological attributes of the system, specifically, the geometry of the bed forms.

It is assumed that each given set of flow variables has a unique corresponding bed state composed of statistically similar bed forms (cf. Southard, 1971). The bed forms constituting the bed state have a characteristic geometry, spacing, and height that define that particular bed state. These measures may be any

that represent the distribution of the bed-form parameters: the mean, mode, median, maximum value, or standard deviation. Of course, some measures work better than others; the mean value is generally used, along with some indication of the range of values.

The concept of equilibrium that applies in practice is that of a steady-state equilibrium, which is "a state of an open system wherein properties are invariant when considered with reference to a given time scale, but within its instantaneous condition may oscillate due to the presence of interacting variables" (Chorley and Kennedy, 1971). The flow in the experimental system is regulated to be both uniform and steady; hence a bed state is in equilibrium when the distribution of bed-form parameters does not change with time (i.e., it becomes statistically invariant or stationary). In steady-state equilibrium, the values of individual measures may range widely and rapidly, but their distribution has a characteristic value.

The degree of equilibrium achieved in a flume may be measured in several ways. At equilibrium, the flow is both steady and uniform; that is, the water surface and the average bed surface are parallel. Unfortunately, the problem is in measuring the average bed surface slope -- a very small signal (about 5 cm per 30 m) in the presence of a large amount of noise (5 cm per 0.15 m). More practically, one may observe the bed forms, watching their migration behavior and measuring their spacing and height. As equilibrium is approached, the bed forms will behave

more and more alike, and the values of the bed-form parameters will converge to a mean.

Bed forms in natural systems cannot instantaneously equilibrate with changing flow conditions because their change is due to processes that operate at a finite rate (as discussed in Chapter 2). The inability of the bed forms to keep pace with the changing flow defines a phenomenon known as relaxation (analogous to relaxation in rheology and in magnetism). Chorley and Kennedy (1971, as discussed in Allen, 1974, p. 272-273) single out four main factors that determine relaxation time in sediment transport systems:

> (1) the resistance to change offered by individual morphological components;
> (2) the complexity of the system ...;
> (3) the magnitude and direction of the change in rate of energy supply;
> (4) the energy environment of the change in supply.

The concept of the relaxation time of a bed configuration is valuable because natural flows tend to be unsteady. As discussed in Chapter 2, how fast a bed form can change determines how far out of equilibrium with a particular flow it is. Determination of the relaxation times of specific bed configurations has important consequences. It can indicate the applicability of flume studies to interpretations of natural environments and it can indicate whether data acquired from intertidal environments may be extrapolated to other environments. The relaxation time is also an important component needed in any computational model of bed-form lag time (Allen, 1976a).

In an effort to determine the relaxation times of large-scale bed forms, six flume runs (K-10 through K-12; L-1 through L-3) were made in which data were taken from the time the flow velocity was changed. The bed-form response to the changed flow was measured, and plotted against elapsed time. Three different situations were investigated: the change, with increasing velocity, in the 3D dune field (Fig. 40), and from 3D dunes to HV dunes (Fig. 41); and the change from 3D dunes to 2D dunes with decreasing velocity (Fig. 42). The pertinent data are summarized in Table 8.

TABLE 8

Transition	Runs	Velocity (cm/s)	Bed-Form Height	Bed-Form Length	Time Required
3D -- 3D	K-9 -- 10	78 -- 82	30 -- 59	432 - 517	4.1 hr
3D -- Hv	L-2 -- 3	57 -- 83	25 -- 33	240 - 405	1.3-2.0 hr
3D -- 2D	K-10 - 11	82 -- 67	59 -- 24	517 - 262	2.7 hr

The relaxation times in Table 8 are scaled to 10° C, and were determined both from the graphs presented and from careful scrutiny of the time-lapse films. They are far from definitive figures, but they give a good indication of the time required to attain equilibrium.

The magnitude and direction of the change in rate of energy supply (factor 3 of Chorley and Kennedy, 1971) appears to be the major factor in determining relaxation times. The smallest velocity change (for the transition within the 3D dune phase) took the largest time to relax, even though relatively small adjustments in bed-form size were required. The bed-form parameter

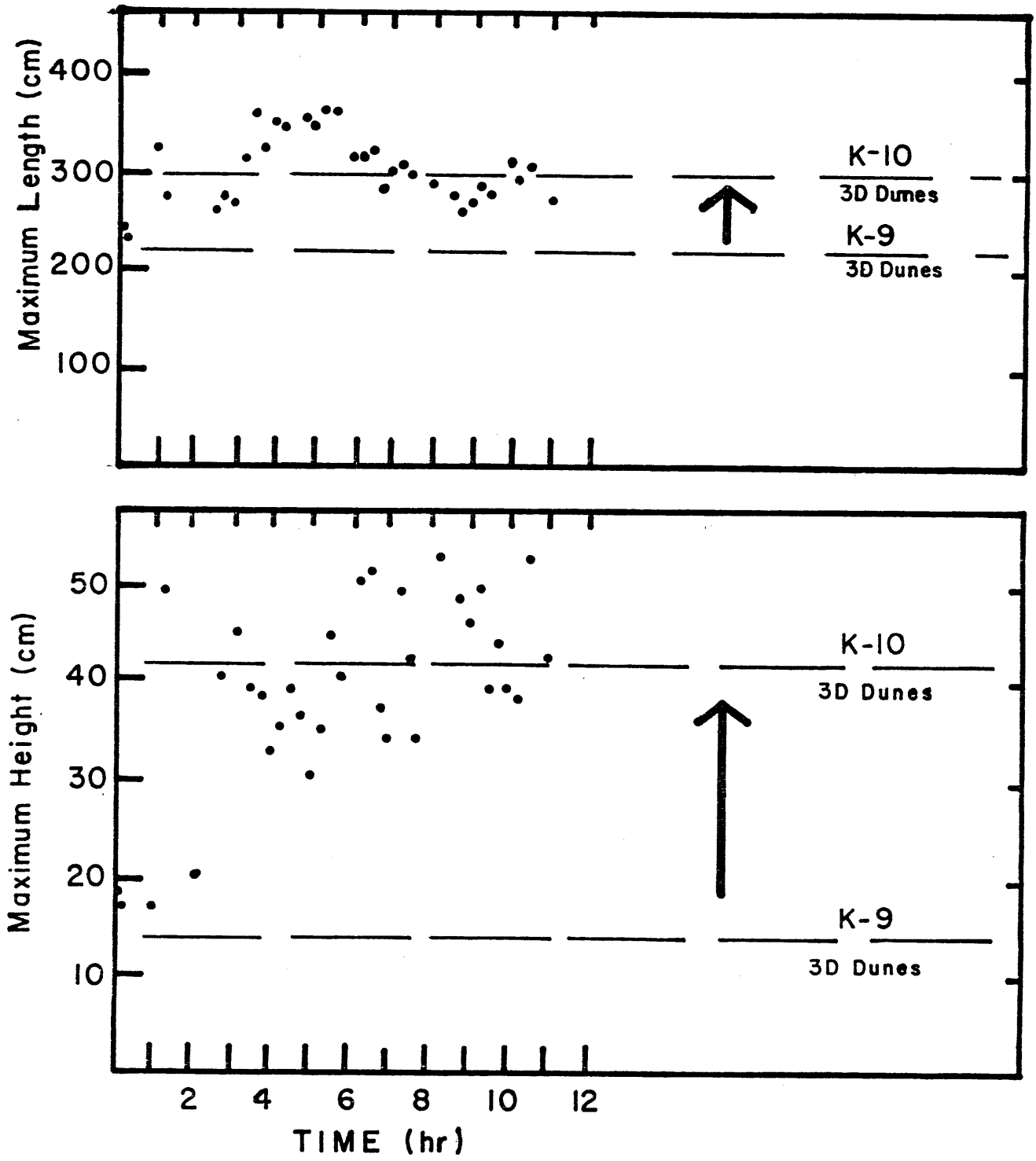

FIGURE 40 -- Bed-form relaxation time for the transition among three-dimensional dunes. Dashed lines represent average equilibrium values.

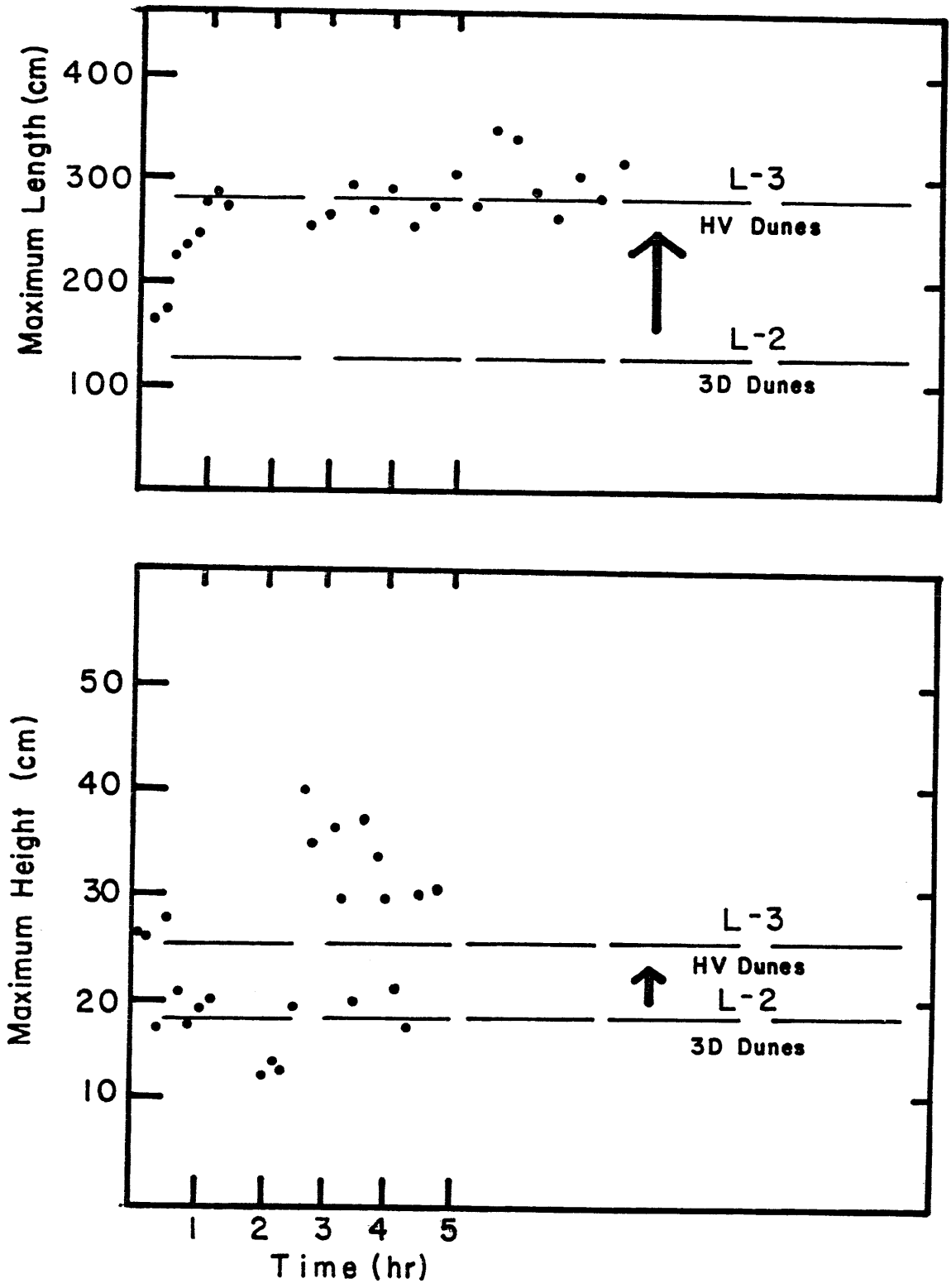

FIGURE 41 -- Bed-form relaxation time for the transition from 3D dunes to HV dunes; dashed lines represent average equilibrium values.

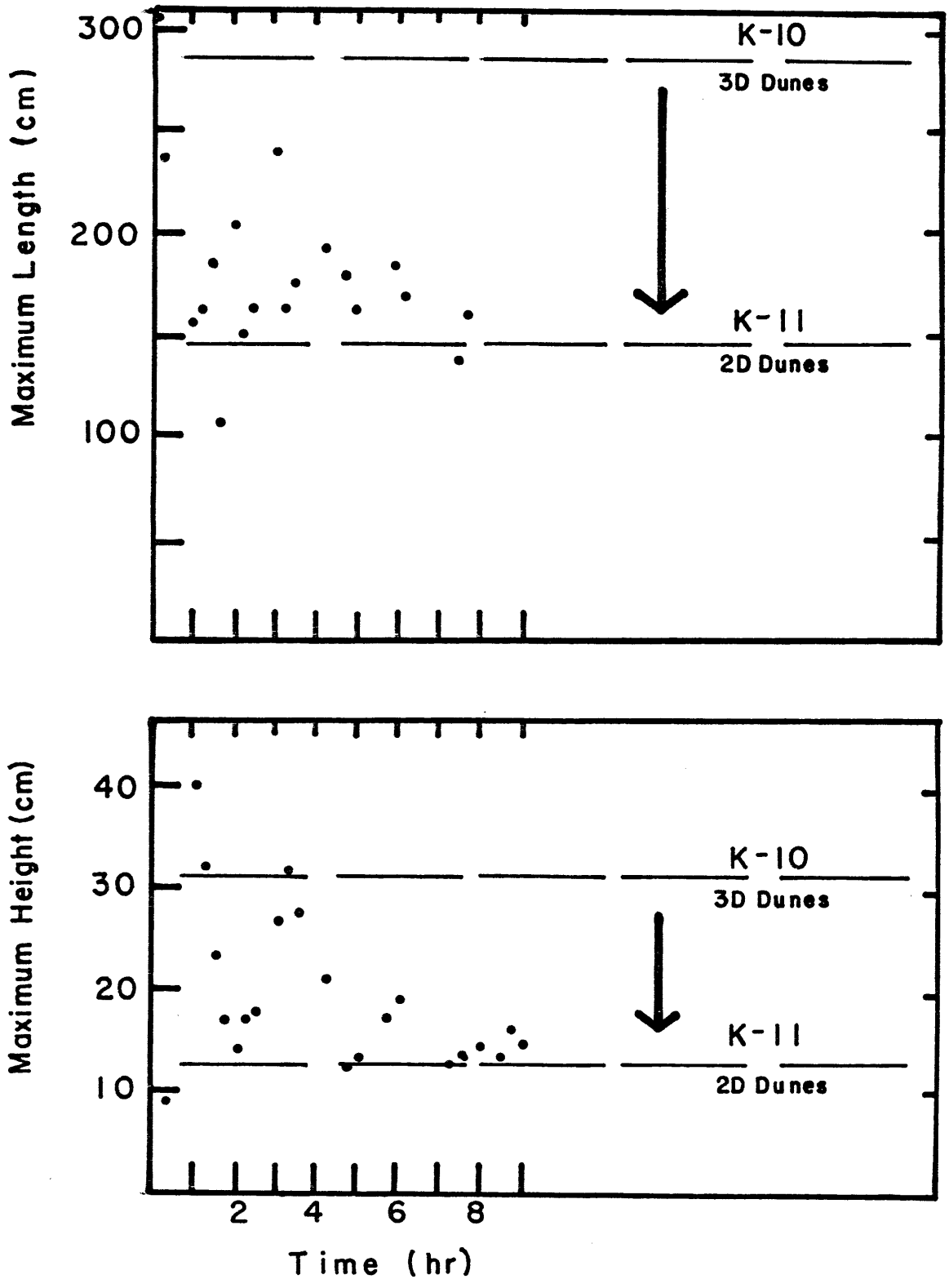

FIGURE 42 -- Bed-form relaxation time for the transition from 3D dunes to 2D dunes; dashed lines represent average equilibrium values.

that must change the most exhibits rapid, asymptotic behavior (Figs. 40b, 41a, and 42b). The companion parameter changes very rapidly (attaining its equilibrium value in about 1 hour) but erratically (Figs. 40a, 41b, and 42a).

The direction of change of flow velocity had an important effect, not reflected in these graphs. It was obvious (from all the runs, not just the last six) that the mode of bed-form response depends on the direction of change. The bed forms represented a "varied population" in which "construction-destruction mechanisms act continuously, causing individual forms to be replaced fairly regularly" (Allen, 1974). Hence, there are two ways in which the morphology of the system can adjust to the changed conditions: individual, existing bed forms may grow or shrink; or new bed forms, better suited to the changed conditions, can appear.

In the present study, the first mechanism dominated when the change was from a lower to a higher flow velocity. Bed-form height and spacing increased steadily, with the individual forms retaining their shapes. When flow velocity was decreased, there was rapid creation of new bed forms on the stoss slopes of the pre-existing forms. These new individuals were 5 to 10 cm high, and intermediate in length between the equilibrium spacings of the previous and present runs. Generally, this "retrograde" change of the bed forms appeared less efficient: the new (equilibrium) forms took longer to become organized. This accords with experiments of Gee (1975) on suddenly varied flow.

Dalrymple et al. (1978) reported a similar bed-form response in the Bay of Fundy. In this environment, most sand waves have 3D dunes superimposed; but in a few instances only ripples or lower-regime plane beds are present on the sand-wave stoss slopes. Their observations suggest that rippled sand waves are a disequilibrium form, because they are always found in decelerating flows. They may be produced by either neap-tide replacement of sand waves with 3D dunes that exist at spring tide, or by bed-form migration into areas of lower current strength and shallower flow depths. During the prograde transition from 2D dunes to sand waves with 3D dunes superimposed, Dalrymple et al. (1987) observed that a gradual increase in bed-form size begins at the same time as the superimposed 3D dunes appear (rippled sand waves do not occur as an intermediate step).

In summary, the data indicate that large-scale bed forms, although containing large volumes of sediment, can respond fairly quickly to changing flow conditions. The relaxation time (in this system) is mainly a function of the magnitude of the change flow velocity. The dominant mechanism of bed-form response is controlled by the direction of change. These findings have important consequences: they may be applied in computational models of dune response (Allen, 1976a); they indicate that the data available from intertidal environments (e.g., Boothroyd and Hubbard, 1975; Dalrymple et al., 1978) may be extrapolated to other environments; they show and that flume data provide a reasonable reference state for field studies.

SUMMARY OF RESULTS

Careful examination of the experimental data leads to the conclusion that a single bed phase or overall type of bed configuration was generated in these experiments. With increasing flow at constant depth there was a smooth progression in the dependent flow variables and the bed-form response to increasing flow velocity. No gap in bed-form properties exists (such as that seen between ripples and dunes), hence all forms are considered to be in the dune stability field.

All bed forms behaved basically as large-scale dunelike features. There are, however, sufficient differences among the bed forms produced to warrant a subdivision of the dune phase. These differences are reflected in the overall bed geometry and bed-form kinematics. This makes the subdivision not only reasonable, but important geologically, because these are the properties that govern the imprint the bed forms make on the geologic record. This classification scheme follows the spirit of that framed by Harms (1969) for ripples. While constituting one overall bed phase, his "low-energy" and "high-energy" ripples could be recognized according to their external morphology and internal structure. By dividing the ripple phase, a more precise estimate of the environment of deposition could be made, hence the importance of this classification to sedimentologists.

CHAPTER 5

SUMMARY OF INVESTIGATION

COMPARISON OF FLUME DATA TO FIELD STUDIES

As discussed in Chapter 1, most field studies have found it worthwhile to divide the large-scale bed configurations into at least two, if not three, types. The distinctions among these forms are based upon the sum total of the field observations, with groups of similar bed forms separated by gaps in spacing and/or height. Careful reexamination of the data (Coleman, 1969; Boothroyd and Hubbard, 1975; Dalrymple et al., 1978) shows that, although there are clusters of data points for each bed-form type, there is considerable overlap in measured parameters. In general, there always exist "transitional" forms, intermediate in size between the bed-form types. Boothroyd and Hubbard (1975, p. 221) described these transitional forms: they occur at the junctures between sand-wave and dune zones and they look like "dwarfed sand waves, with straight crests."

Viewed in the light of the present experimental study, it seems reasonable that these field data represent a continuous progression in bed-form size, similar to that seen in the flume. The differences in environments may select groups from this continuum to be selectively produced and preserved. Again, there are sufficient differences to allow the bed forms to be classified into three types, but dynamically they all behave like large-scale ripples.

The natural-flow equivalents of the three bed-form types recognized in this study are listed in Table 1. These comparisons were made on the basis of the bed-form sequence in each environment (with increasing flow velocity), and of the morphology of the forms (spacing, height, and longitudinal profile). This equivalence established, the detailed data from this study may be applied to the interpretation of bed-form behavior in natural flows.

CONCLUSIONS

This study has accomplished the following:

(1) It has established that the hot-water scale modeling technique is feasible on a large scale. By the use of hot water (50-60° C) in a large flume 1.5 m deep, it has been possible to model flows on the scale of natural flows of sedimentological interest. This increase in scale can be achieved without the usual proportional increase in difficulty and expense. The engineering difficulties are by no means trivial, but they are straightforward; there is nothing wrong with the basic approach.

(2) Using the hot-water scale model, the depth range of flume studies has been tripled (Fig. 12). This study has extended flume observations into the depth range of small rivers and intertidal flows. In doing so, it has helped to bridge the gap extant between studies in flumes and in natural environments.

(3) It has detailed bed-form geometry, kinematics, and dynamics in a depth range in which large-scale bed forms begin to become well differentiated. These differences were only beginning to become noticable in previous flume studies (e.g., Costello, 1974; Boguchwal, 1978). Modeling realistic flow depths has provided an equilibrium reference state for these large-scale bed features which can serve as a basis for interpreting bed forms in more variable and complex natural environments.

(4) It has shown that, in the range of velocities achieved, there are two scales of bed configuration: ripples and dunes. The dune phase may be divided into three subphases: 2D dunes, 3D dunes, and HV dunes. Each subphase is distinguised by its overall bed geometry and bed-form kinematics, but their basic dynamics are the same.

It is interesting to speculate about what bed forms would succeed the HV dunes of this study at higher flow velocities. Flow velocity could be increased substantially before upper-flow-regime conditions prevailed. Perhaps the bed forms would continue to increase smoothly in size with increasing velocity, or they might reach a peak in size (spacing and height), and then decrease in height, approaching the upper-stage plane bed phase. A third option would be a jump in bed-form size to a third order of bed form across a narrow range of velocities. This third order of bed forms would perhaps be the equivalent of sand waves

found in natural flows. Careful consideration of the existing field data leads this writer to consider the seond option as most likely.

(5) It has shown that large-scale bed forms can respond fairly quickly to changing flow conditions. This indicates that studies of the intertidal environment may be extrapolated to other settings and that flume studies provide a valid basis for interpreting bed forms in natural flows.

BIOGRAPHICAL SKETCH

Kevin Michael Bohacs was born in Port Chester, N.Y. on 2 October 1954. The first son of Mary and Julius, he grew up in Greenwich, Connecticut. Here, on the shores of Long Island Sound, Kevin discovered the two main loves of his life: geology and emergency medicine.

His college career was relatively uneventful, other than receiving two commendations for bravery from the Greenwich Fire Department. In the spring of 1976, he was graduated with honors from the University of Connecticut with a Bachelor of Science (summa cum laude, Phi Beta Kappa, and all that). He entered the Massachusetts Institute of Technology in the fall of 1976 to pursue a career in experimental sedimentology.

He is a member of the Society of Sigma Xi, and of the Society of Economic Paleontologists and Mineralogists. When not responding to fires, or working for the Red Cross, Kevin may be found conducting informal investigations into beach and shallow-marine processes.

APPENDIX 1

All data in this appendix are those taken in the original experiments. The original data appear in the Unscaled column.

The s designation appearing after certain data indicates the value of the sample variance, calculated from the original data.

The asymmetry index is the ratio of the trough-to-crest spacing to the crest=to=trough spacing, as indicated in Fig. 17.

RUN K-1

Water Depth	147 cm
Velocity	68.4 cm/s
Temperature	64.8 ^{0}C
Time	12.45 hr
Water Surface Slope	9.25×10^{-4}

Scale Factors: Length Scale 2.10 Velocity Scale 1.45

Bed-Form Measurements

	Unscaled	Scaled
Height	27.61 cm (s=10.94)	58.0 cm (s=23.0)
Spacing	185.75 cm (s=54.85)	390.1 cm (s=115.2)
Migration Rate	0.0381 cm/s	0.0549 cm/s
Spacing-to-Height Ratio	7.61 (s=2.58)	
Asymmetry Index	2.45 (s=1.06)	

* Asymmetry Index = T→C/C→T (after Bucher, 1919)

** Note: All measurements in the upper half of the page are scaled to 10 ^{0}C

RUN K-9

Water Depth	136.8 cm
Velocity	77.8 cm/s
Temperature	58.5 ^{0}C
Time	8.34 hr
Water Surface Slope	9.73 x 10^{-4}

Scale Factors: Length Scale 1.90 Velocity Scale 1.39

Bed-Form Measurements

	Unscaled	Scaled
Height	16.3 cm (s=6.7)	30.9 cm (s=12.7)
Spacing	227.3 cm (s=66.8)	431.9 cm (s= 126)
Migration Rate	2.15 m/hr	2.99 m/hr
Spacing-to-Height Ratio	16.7 (s=10.4)	
Asymmetry Index	3.6	

* Asymmetry Index = T→C/C→T (after Bucher, 1919)

** Note: All measurements in the upper half of the page are scaled to 10 ^{0}C

RUN K-2

Water Depth	145 cm
Velocity	73.4 cm/s
Temperature	65.0 ^{0}C
Time	12.93 hr
Water Surface Slope	7.96×10^{-4}

Scale Factors: Length Scale 2.10 Velocity Scale 1.45

Bed-Form Measurements

	Unscaled	Scaled
Height	22.42 cm (s=3.53)	47.08 (s=7.41)
Spacing	137.97 cm (s=24.14)	289.74 cm (s=50.69)
Migration Rate	1.47 m/hr	2.12 m/hr
Spacing-to-Height Ratio	9.32 (s=1.96)	
Asymmetry Index	N/R	

* Asymmetry Index = T→C/C→T (after Bucher, 1919)

** Note: All measurements in the upper half of the page are scaled to 10 ^{0}C

RUN K-3

Water Depth	143 cm
Velocity	74.9 cm/s
Temperature	66.6 ^{0}C
Time	24.53 hr
Water Surface Slope	9.1 x 10^{-4}

Scale Factors: Length Scale 2.11 Velocity Scale 1.45

Bed-Form Measurements

	Unscaled	Scaled
Height	25.0 cm (s=2.17)	52.7 cm (s=4.58)
Spacing	196.5 cm (s=40.37)	414.7 cm (s=85.2)
Migration Rate	1.45 m/hr	2.1 m/hr
Spacing-to-Height Ratio	7.75 (s=2.03)	
Asymmetry Index	N/R	

* Asymmetry Index = T→C/C→T (after Bucher, 1919)

** Note: All measurements in the upper half of the page are scaled to 10 ^{0}C

RUN K-4

Water Depth	133.6 cm
Velocity	61.5 cm/s
Temperature	61.9 ^{0}C
Time	32.06 hr
Water Surface Slope	5.7 x 10^{-4}

Scale Factors: Length Scale 2.03 Velocity Scale 1.42

Bed-Form Measurements

	Unscaled	Scaled
Height	9.4 cm (s=2.8)	19.1 cm (s=5.7)
Spacing	77.6 cm (s=42.9)	157.5 (s=87.1)
Migration Rate	0.79 m/hr	1.12 m/hr
Spacing-to-Height Ratio	8.5 (s=3.3)	
Asymmetry Index	N/R	

* Asymmetry Index = T→C/C→T' (after Bucher, 1919)

** Note: All measurements in the upper half of the page are scaled to 10 ^{0}C

RUN K-5

Water Depth	120.6 cm
Velocity	56.7 cm/s
Temperature	58.0 ^{0}C
Time	30.56 hr
Water Surface Slope	7.2×10^{-4}

Scale Factors: Length Scale 1.99 Velocity Scale 1.41

Bed-Form Measurements

	Unscaled	Scaled
Height	7.1 cm (s=2.1)	14.1 (s=4.2)
Spacing	104.1 cm (s=20.4)	207.2 cm (s=40.6)
Migration Rate	0.42 m/hr	59.2 m/hr
Spacing-to-Height Ratio	15.5 (s=3.8)	
Asymmetry Index	N/R	

* Asymmetry Index = T→C/C→T (after Bucher, 1919)

** Note: All measurements in the upper half of the page are scaled to 10 ^{0}C

RUN K-7

Water Depth	143.7 cm
Velocity	86.3 cm/s
Temperature	62.3 ^{0}C
Time	66.7 hr
Water Surface Slope	11.24×10^{-4}

Scale Factors: Length Scale 2.01 Velocity Scale 1.42

Bed-Form Measurements

	Unscaled	Scaled
Height	12.5 cm (s=7.6)	25.1 cm (s=15.3)
Spacing	281.4 cm (s=64)	565.6 cm (s=128.6)
Migration Rate	2.36 m/hr	3.35 m/hr
Spacing-to-Height Ratio	29.3	
Asymmetry Index	6.4	

* Asymmetry Index = T→C/C→T (after Bucher, 1919)

** Note: All measurements in the upper half of the page are scaled to 10 ^{0}C

RUN K-8

Water Depth	134.1 cm
Velocity	100.8 cm/s
Temperature	59.9 ^{0}C
Time	14.7 hr
Water Surface Slope	12.21×10^{-4}

Scale Factors: Length Scale 1.96 Velocity Scale 1.40

Bed-Form Measurements

	Unscaled	Scaled
Height	31.5 cm (s=11.8)	61.9 cm (s=23.2)
Spacing	398.5 cm (s=131.2)	783.5 cm (s=258)
Migration Rate	2.97 m/hr	416 m/hr
Spacing-to-Height Ratio	24.5	
Asymmetry Index	4.0	

* Asymmetry Index = T→C/C→T (after Bucher, 1919)

** Note: All measurements in the upper half of the page are scaled to 10 ^{0}C

RUN K-10

Water Depth	129.7 cm
Velocity	82.6 cm/s
Temperature	56.2 ^{0}C
Time	16.4 hr
Water Surface Slope	14.05 x 10^{-4}

Scale Factors: Length Scale 1.88 Velocity Scale 1.37

Bed-Form Measurements

	Unscaled	Scaled
Height	31.5 cm (s=13)	59.2 cm (s=24)
Spacing	275.1 cm (s=87)	517.2 cm (s=163)
Migration Rate	2.19 m/hr	3.00 m/hr
Spacing-to-Height Ratio	10.0 (s=4.2)	
Asymmetry Index	4.1	

* Asymmetry Index = T→C/C→T (after Bucher, 1919)

** Note: All measurements in the upper half of the page are scaled to 10 ^{0}C

RUN K-11

Water Depth	143.3 cm
Velocity	67.6 cm/s
Temperature	55.8 ^{0}C
Time	12.3 hr
Water Surface Slope	6.03 x 10^{-4}

Scale Factors: Length Scale 1.87 Velocity Scale 1.37

Bed-Form Measurements

	Unscaled	Scaled
Height	13.0 cm (s=6.4)	24.4 cm (s=12)
Spacing	139.8 cm (s=70.7)	262.1 cm (s=132)
Migration Rate	1.28 m/hr	1.75 m/hr
Spacing-to-Height Ratio	12.3 (s=7.6)	
Asymmetry Index	4.9	

* Asymmetry Index = T→C/C→T (after Bucher, 1919)

** Note: All measurements in the upper half of the page are scaled to 10 ^{0}C

RUN K-12

Water Depth	130.3 cm
Velocity	99.1 cm/s
Temperature	55.1 ^{0}C
Time	19.14 hr
Water Surface Slope	12,59 x 10^{-4}

Scale Factors: Length Scale 1.87 Velocity Scale 1.37

Bed-Form Measurements

	Unscaled	Scaled
Height	19.0 cm (s=8.9)	35.5 cm (s=16)
Spacing	246.6 cm (s=71.5)	461.1 cm (s=133)
Migration Rate	3.58 m/hr	4.89 m/hr
Spacing-to-Height Ratio	14.0 (s=4.2)	
Asymmetry Index	N/R	

* Asymmetry Index = T→C/C→T (after Bucher, 1919)

** Note: All measurements in the upper half of the page are scaled to 10 ^{0}C

RUN L-1

Water Depth	115.6 cm
Velocity	70.0 cm/s
Temperature	42.0 ^{0}C
Time	42.24 hr
Water Surface Slope	9.53×10^{-4}

Scale Factors: Length Scale 1.75 Velocity Scale 1.32

Bed-Form Measurements

	Unscaled	Scaled
Height	14.0 cm	24.5 cm
Spacing	181.2 cm	317.1 cm
Migration Rate	1.78 m/hr	2.35 m/hr
Spacing-to-Height Ratio	14.8 (s=6.8)	
Asymmetry Index	6.0	

* Asymmetry Index = T→C/C→T (after Bucher, 1919)

** Note: All measurements in the upper half of the page are scaled to 10 ^{0}C

RUN L-2

Water Depth	117.2 cm
Velocity	51.5 cm/s
Temperature	52.2 ^{0}C
Time	9.4 hr
Water Surface Slope	8.69 x 10^{-4}

Scale Factors: Length Scale 1.88 Velocity Scale 1.37

Bed-Form Measurements

	Unscaled	Scaled
Height	13.7 cm (s=5.2)	25.7 cm (s=9.7)
Spacing	127.7 cm (s=36.6)	240.0 cm (s=68)
Migration Rate	2.11 m/hr	2.89 m/hr
Spacing-to-Height Ratio	10.2 (s=3.8)	
Asymmetry Index	3.2	

* Asymmetry Index = T→C/C→T (after Bucher, 1919)

** Note: All measurements in the upper half of the page are scaled to 10 ^{0}C

RUN L-3

Water Depth	109.4 cm
Velocity	83.7 cm/s
Temperature	46.7 ^{0}C
Time	13.05 hr
Water Surface Slope	17.39 x 10^{-4}

Scale Factors: Length Scale 1.82 Velocity Scale 1.35

Bed-Form Measurements

	Unscaled	Scaled
Height	18.3 cm (s=8.2)	33.3 cm (s=14.9)
Spacing	222.8 cm (s=60.6)	405.5 cm (s=110)
Migration Rate	5.51 m/hr	7.44 m/hr
Spacing-to-Height Ratio	14.0 (s=6.4)	
Asymmetry Index	3.0	

* Asymmetry Index = T→C/C→T (after Bucher, 1919)

** Note: All measurements in the upper half of the page are scaled to 10 ^{0}C

APPENDIX 2

Analysis of the drowned-outflow sluice gate

An approximate analysis of the flow pictured in Fig. A2.1 can be made by treating the situation as one of "divided flow" (Henderson, 1966) in which part of the section is occupied by stagnant water and part by moving water. Although the flow will lose some energy between sections 1 and 2, it will lose much more energy in the expanding flow between sections 2 and 3. It is therefore assumed (as an approximation) that $E_1=E_2$; that is, all the loss occurs between sections 2 and 3.

Hence, for the flow between 1 and 2, one may write the equation:

$$\frac{V_1^2}{2g} + d_1 = \frac{V_2^2}{2g} + d \qquad \text{(A2.1)}$$

(V_1, V_2 = velocities at sections 1 and 2; g = acceleration of gravity.)

By definition: $q = V \times (\text{depth})$ (A2.2)

(q = discharge per unit width), hence:

$$\frac{q^2}{2g\ d_1^2} + d_1 = \frac{q^2}{2g\ d_2^2} + d \qquad \text{(A2.3)}$$

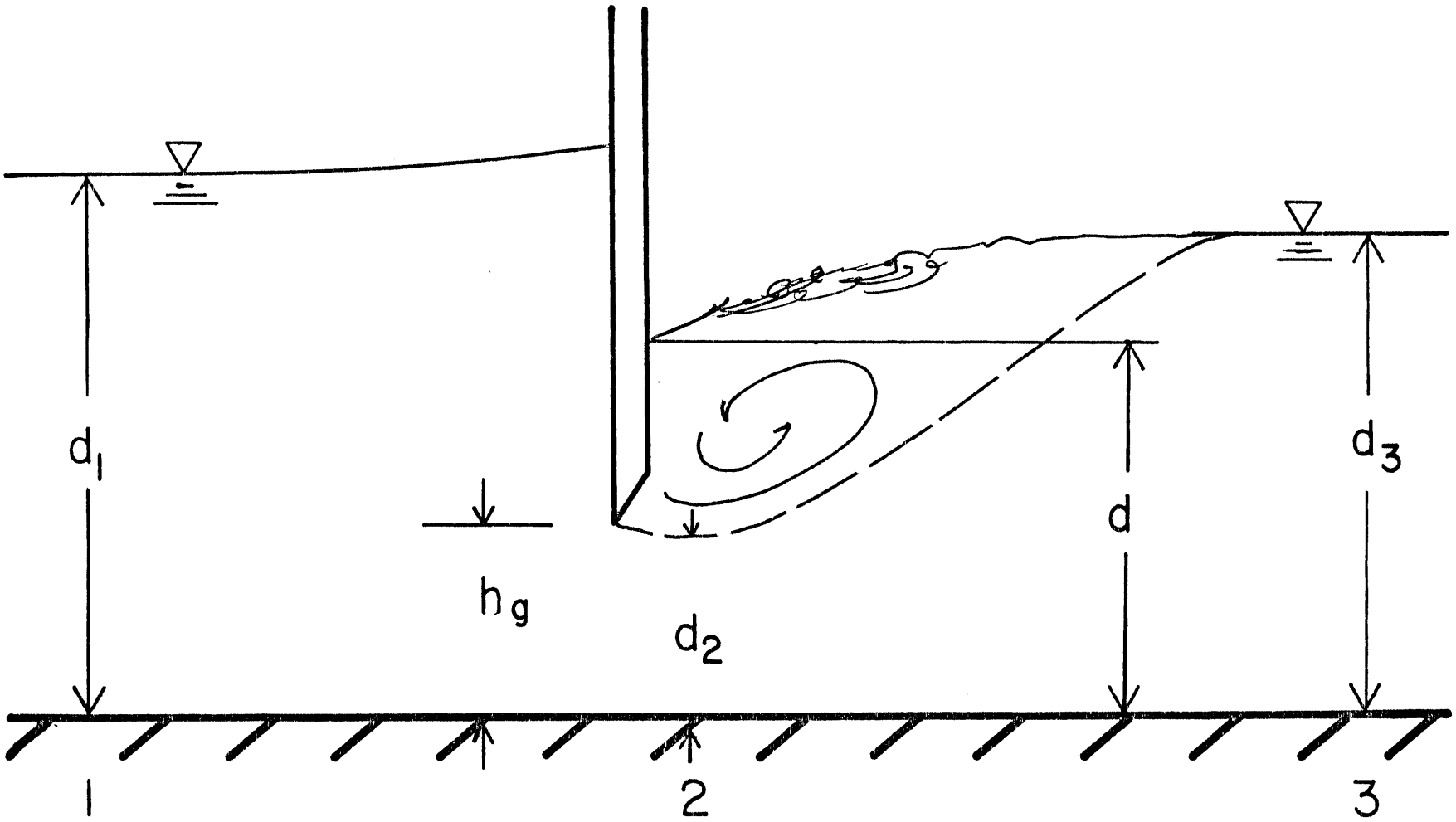

FIGURE A2.1 -- Definition sketch for the approximate analysis of the drowned-outflow sluice gate.

Solving for the discharge per unit width,

$$q^2 = \frac{2g\ (d_1 - d)}{\frac{1}{d_2^2} - \frac{1}{d_1^2}} \qquad \text{(A2.4)}$$

It is taken to be a reasonable approximation that $d_2 = C_c\ h_g$, as in the case of a free-outflow sluice gate. Hence, all the quantities on the right hand side of Eqn. A2.4 are known ($C_c = 0.6$). By definition, q = V x (depth), thus V = q/(depth). Substituting this definition into Eqn. A2.4, one may solve for the velocity at section 1 (the velocity used to characterize the flow in these experiments):

$$V^2 = (d_1 - d)\ \frac{2g}{d_1^2\ (\frac{1}{d_2^2} - \frac{1}{d_1^2})} \qquad \text{(A2.5)}$$

In the present experimental setup, d_2 is constant and d_1 is taken to be constant and equal to 100 cm. Due to the shifting sediment at section 1, this d_1 value is only an approximation; this probably is the reason that Eqn. A2.5 underestimates the discharge. Having measured $(d_1 - d)$, the head loss across the sluice gate, one may calculate the flow velocity corresponding to a given head loss. Table A2.2 contains the velocities calculated from Eqn. A2.5 and the velocities measured in the calibration runs at the same head losses. The calculated values

tend to be consistently lower than the measured velocities, ranging from 6% lower at the lowest velocities to 19% lower at the highest velocities. These discrepancies are to be expected, considering the differences between the simple case analysed and the actual experimental situation. The nature of the approaching flow and the presence of a mobile sand bed are the two major complicating factors. The general agreement between the measured and calculated values (as seen in Fig. 18b), along with the specific calibration made of the sluice gate in the present experiments, indicate that the claimed accuracy of ± 7% is not unreasonable.

TABLE A2.1

Values used in Equation A2.5

g = 980 cm/s

d_1= 100 cm

d_2= C_c h_g = (0.6)(43) = 25.8 cm

TABLE A2.2

Velocities: calculated and measured

(d_1-d) (cm)	V calc. (cm/s)	V meas. (cm/s)	$(V_m - V_c)/ V_m$ x 100 Percent Error
5	26	25	4%
10	37	40	6%
15	45	50	8%
20	52	62	12%
25	59	70	15%
30	64	80	19%

Calculation of the accuracy of the discharge measurements

The general form of the equation for computing discharge by the velocity-area method is:

$$Q = \sum_{i=1}^{m} (v_i b_i d_i)$$

where Q is the total discharge in the cross section, m is the number of segments into which the cross section is divided, and v_i, b_i, and d_i are the mean water velocity, width, and depth in the i^{th} segment.

Herschey (1978) expresses the contributing random uncertainties in making a single determination of discharge by current meter as:

X_b = uncertainty in width measurement

X_d = uncertainty in depth measurement

X_v = uncertainty in the mean velocity in the vertical

X_m = uncertainty due to the limited number of vertical segments

X_Q = overall uncertainty in discharge

(All uncertainties are expressed as percentage standard deviations at the 95 percent confidence level.) The overall uncertainty in discharge is then:

$$X_Q = \pm \frac{\text{sum of the percent errors in the segment discharges}}{\text{sum of segment discharges}}$$

The uncertainty in the mean velocity in the vertical segments arises from the uncertainties due to pulsations in the flow (X_p), the number of points taken in the vertical

(X_e), and the uncertainty in the current meter rating (X_c). The mean-velocity uncertainty may be expressed as the sum of the uncertainties of the components X_p, XG, and X_c. If the segment discharges ($v_i b_i d_i$) are all nearly equal, then:

$$X_Q = \pm[X_m^2 + \frac{1}{m}(X_b^2 + X_d^2 + X_e^2 + X_p^2 + X_c^2)]^{1/2} \quad \text{(A2.6)}$$

In the present case:

$m = 5$

$X_m = 6.5$ (Herschey, 1978, Table 10.15)

$X_b = 0.5$

$X_d = 1.0$

$X_e = 5.0$ (Herschey, 1978, Table 10.17)

$X_p = 3.0$ (Herschey, 1978, Table 10.16)

$X_c = 1.5$ (Manufacturer's data)

Substituting these values into Eqn. A2.6, the overall uncertainty in discharge (at the 95 percent confidence level) is ± 7%.

REFERENCES

Abbott, DE; Kline, SJ; 1962: Experimental investigation of subsonic turbulent flow over single and double backward facing steps. Trans. ASME, J. Basic Engineering, 84, 317-325.

Allen, JRL; 1970: Physical Properties of Sedimentation, Allen and Urwin, London, 248 pp.

Allen, JRL; 1974: Reaction, relaxation, and lag in natural sedimentary systems: general principles, examples, and lessons. Earth-Sci. Rev. 10, 263-342.

Allen, JRL; 1976a: Bed forms and unsteady processes: Some concepts of classification and response illustrated by common one-way types. Earth Surf. Processes 1, 364-374.

Allen, JRL; 1976b: Computational models for dune time-lag: general ideas, difficulties, and early results. Sed. Geol. 15, 1-53.

Allen, JRL; 1978a: Polymodal dune assemblages: an interpretation in terms of dune creation-destruction in periodic flows. Sed. Geol. 20, 17-28.

Allen, JRL; 1978b: Computational models for dune time-lag: Calculations using Stein's rule for dune height. Sed. Geol. 20, 165-216.

Allen, JRL; Collinson, JD; 1974: The superimposition and classification of dunes formed by unidirectional aqueous flows. Sed. Geol. 12, 169-178.

Allen, JRL; Friend, PF; 1976: Changes in intertidal dunes during two spring-neap cycles, Lifeboat Station Bank, Wells-next-the-Sea, Norfolk, England. Sedimentology, 23, 329-346.

Barton, JR; Lin, PN; 1955: Study of sediment transport in alluvial channels. Colorado A & M College, Dept. Civ. Eng. Rep. 55JRB2, March 1955.

Belderson, RH; Stride, AH; 1966: Tidal current fashioning of a basal bed. Marine Geol. 4, 237-257.

Bluck, BJ; 1971: Sedimentation in the meandering River Endrich. Scot. J. Geol. 7, 98-138.

Boggs, A; 1974: Sand wave fields in Taiwan Strait. Geology 2. 251-253.

Boguchwal, LA; 1977: Dynamic scale modeling of bed configurations. Ph.D. Thesis, M.I.T., October, 1977.

Bokuniewicz, HJ; Gordon, RB; Kastens, KA; 1977: Forms and migration in a large estuary, Long Island Sound. Marine Geol. 24, 185-199.

Boothroyd, JC; 1978: Mesotidal inlets and estuaries, in Davis, RA, Jr.; Coastal Sedimentary Environments Springer-Verlag, New York; p. 287-360.

Boothroyd, JC; Hubbard, DK; 1975: Genesis of bedforms in meso-tidal estuaries, in Cronin, LE (ed.) Estuarine Research v. 2, New York, Academic Press.

Bouma, AH; Rappeport, ML; Orlando, RC; Hampton, Mass. 1980: Identification of bedforms in lower Cook Inlet, Alaska. Sed. Geol. 26, 157-178.

Bridge, JS; Jarvis, J; 1976: Flow and sedimentary processes in the meandering river South Esk, Glen Cove, Scotland. Earth Surface Processes 1, 303-336.

Briggs, SR; 1979: A study of Middle Ground Shoal (41°28'N; 70°41'W), sand wave migration, and the local mean-velocity field. Ph.D. Thesis, M.I.T.-Woods Hole Oceanographic Institute Joint Program; 291 pp.

Buckingham, E; 1914: On physically similar systems; illustrations of the use of dimensional equations. Physical Rev. IV, 345-376.

Carey, WC; Keller, MD; 1957: Systematic changes in the beds of alluvial rivers. Proc. ASCE. 83 (Paper 1331), 24 pp.

Cartwright, DE; Stride, AH, 1958: Large sand waves near the edge of the continental shelf. Nature 181, 41.

Chabert, J; Chauvin, JL; 1963: Formation des dunes et des rides dans les modeles fluviaux. Bull. Centre. Rech. Ess. Chatou 4, 31-51.

Chorley, RJ; Kennedy, BA; 1971: Physical Geography. Prentice-Hall, London, 370 pp.

Clifton, HE; Hunter, RE; Phillips, RL; 1971: Depositional structures and processes in the non-barred high-energy nearshore. J. Sed. Petrology 41, 651-670.

Coleman, JM; 1969: Brahmaputra River: Channel Processes and Sedimentation. Sed. Geol. 3, 129-239.

Collinson, JD; 1970: Bedforms of the Tana River, Norway. Geografiska Annaler 52A, 31-56.

Corea, WC; 1981: Synthesis of large-scale cross-stratification from flume studies. Ph.D. Thesis, M.I.T., Cambridge, Mass.

Costello, WR; 1974: Development of bed configurations in coarse sands. M.I.T., Dept. of Earth and Planetary Sciences Report 74-1, October, 1974.

Costello, WR; Southard, JB; 1971: Development of sand bed configurations in coarse sands. AAPG-SEPM Annual Meeting Abstracts 1, 20-21.

Costello, WR; Southard, JB; 1981: Flume experiments on lower-flow-regime bed forms in coarse sand. J. Sed. Petrology (in press).

Daboll, JM; 1969: Holocene sediment of the Parker River Estuary, Massachusetts Contribution No. 3-CRG, Dept. of Geology, Univ. of Massachusetts.

Dalrymple, RW; 1977: Sediment dynamics of Macrotidal sand bars, Bay of Fundy. Ph.D. Thesis, McMaster Univ., Hamilton, Ontario; 630 p.

Dalrymple, RW; Knight, RJ; Lambiase, JJ; 1978: Bedforms and their hydraulic stability relationships in a tidal environment, Bay of Fundy, Canada. Nature 275, 100-104.

D'Anglejean, BF; 1971: Submarine sand dunes in the St. Lawrence Estuary. Can. J. Earth Sci. 8, 1480-1486.

Davies, JL; 1964: A morphogenic approach to world shorelines. Z. Geomorphol. 8, 27-42.

Dingle, RV; 1965: Sand waves in the North Sea mapped by continuous reflection profiling. Marine Geol. 3, 391-400.

Dingler, JR; Boylls, JC; Lowe, RL; 1977: A high-frequency sonar for profiling small-scale subaqueous bedforms. Marine Geol. 24, 279-288.

Dyer, KR; 1971: The distribution and movement of sediment in the Solent, Southern England. Marine Geol. 11, 175-187.

Exner, FM; 1925: Uber die Wechselwirkung Zwischen Wasser und Geshiebe in Flussen. Akad. Wiss. Wien, Sitzungsber., Math. -Natu. Kl., Abt. IIA, 134, 166-204.

Folk, RL; 1974: Petrology of Sedimentary Rocks. Hemphills, Austin, Texas.

Fredsøe, J; 1979: Unsteady flow in straight alluvial channels: modifications of individual dunes. J. Fluid Mech. 91, 497-513.

Fredsøe, J.; 1981: Unsteady flow in straight alluvial channels. Part 2. Transition from dunes to plane bed. J. Fluid Mech. 102, 431-453.

Gee, DM; 1975: Bed form response to nonsteady flows. J. Hyd. Div. ASCE 101, 437-449.

Gilbert, GK; 1914: The transportation of debris by running water. USGS Prof. Paper 86.

Gill, MA; 1971: Height of sand dunes in open channel flows. Proc. ASCE, Hyd. Div. 97, 2067-2074.

Green, CD; 1975: A study of hydraulic and bedforms at the mouth of the Tay Estuary, Scotland in Cronin, LE (ed.) Estuarine Research v. 2, 322-344.

Guy, HP; Simons, DB; Richardson, EV; 1966: Summary of alluvial channel data from flume data, 1956-1961. USGS Prof. Paper 462-I.

Harms, JC; 1969: Hydraulic significance of some sand ripples. GSA Bull. 80, 363-396.

Harms, JC; Southard, JB; Spearing, DR; Walker, RG; 1975: Depositional environments as interpreted from primary sedimentary structures and stratification sequences. SEPM Short Course No. 2, Dallas, Texas.

Hartwell, AD; 1970: Hydrography and Holocene sedimentation of the Merrimack River Estuary, Massachusetts. Contribution No. 5-CRG, Dept. of Geology, Univ. of Massachusetts.

Harvey, JG; 1966: Large sand waves in the Irish Sea. Marine Geol. 4, 49-55.

Hayes, MO; 1975: Morphology of sand accumulations in estuaries in Cronin, LE, (ed.) Estuarine Research v. 2, Academic Press, New York, p. 3-22.

Henderson, FM; 1966: Open Channel Flow. McMillan, New York, 522 p.

Herschey, RW; 1978: Hydrometry: Principles and Practices. J. Wiley, New York, 511 pp.

Hine, AC; 1975: Bed form distribution and migration patterns on tidal deltas in the Chatham Harbor Estuary, Cape Cod, Mass. in Cronin, LE (ed.) Estuarine Research v. 2, New York, Academic Press.

Houboult, JJH; 1968: Recent sediments in the southern bight of the North Sea. Geologie en Mijnbouw 47, 245-273.

Jackson, RG, III; 1975a: Velocity-bedform-texture patterns of meander bends in the lower Wabash River of Illinois and Indiana. GSA Bull. 86, 1511-1522.

Jackson, RG, III; 1975b: Hierarchical attributes and a unifying model of bed forms composed of cohesionless material and produced by shearing flow. GSA Bull. 86, 1523-1533.

Jackson, RG, III; 1976a: Sedimentological and fluid-dynamic implications of the turbulent bursting phenomenon in geophysical flows. J. Fluid Mech. 77, 531-560.

Jackson, RG, III; 1976b: Large-scale ripples of the lower Wabash River. Sedimentology 23, 593-623.

James, ND; Stanley, DJP; 1968: Sable Island Bank off Nova Scotia: Sediment dispersal and recent history. AAPG Bull. 52, 2208-2230.

Johnson, JW; 1942: The importance of considering side-wall friction in bed-load investigations. J. Hyd. Div. ASCE 12, 329-331.

Jones, NC; Kain, JM; Stride, AH; 1965: The movement of sand waves on Warts Bank, Isle of Man. Marine Geol. 3, 329-336.

Karcz, I; 1972: Sedimentary structures formed by flash floods in Israel. Sed. Geol. 7, 161-182.

Keller, GH; Richardson, AF; 1967: Sediments of the Malacca Straight, Southeast Asia. J. Sed. Petrology 37, 102-127.

Klein, G.DeV; 1970: Depositional and dispersal dynamics of intertidal sand bars. J. Sed. Pet. 40, 1095-1127.

Klein, G.DeV; Whaley; ML; 1972: Hydraulic parameters controlling bed-form migration on an intertidal sand body. GSA Bull. 83, 3465-3470.

Kline, SJ; Reynolds, WC; Schraub, FA; Rundstadler, PW; 1967: The structure of turbulent boundary layers. J. Fluid Mech. 30, 741-773.

Kneber, HJ; Folger, DW; 1976: Large sand waves on the Atlantic outer continental shelf around Wilmington Canyon, off eastern U.S. Marine Geol. 22, M7-M15.

Knight, RJ; 1971: Cobequid Bay sedimentology project: a progress report. Maritime Sed. 8, 45-60.

Knight, RJ; 1977: Sediments, bedforms, and hydraulics in a macrotidal environment, Cobequid (Bay of Fundy), Nova Scotia. Ph.D. Thesis, McMaster Univ., Hamilton, 693 pp.

Kumar, N; Sanders, JE; 1974: Inlet sequence: a vertical succession of sedimentary structures and textures created by the lateral migration of tidal inlets. Sedimentology 21, 491-532.

Langhorne, DN; 1973: A sand wave field in the Outer Thames Estuary, Great Britain. Marine Geol. 14, 129-144.

Langhorne, DN; 1981: A study of the dynamics of a marine sand wave. Sedimentology (in press).

Loring, DH; Nota, DJG; Chesterman, W; Wong, HK; 1970: Magdalena Shelf, southern Gulf of St. Lawrence. Marine Geol. 8, 337-354.

Ludwick, JC; 1972: Migration of tidal sand waves in Chesapeake Bay entrance, in Swift, DJP; Duane, R; Pickey, OH; (ed.) Shelf Sediment Transport, 377-410.

McCabe, PJ; Jones, CM; 1977: The formation of reactivation surfaces within superimposed deltas and bed forms. J. Sed. Petrology 24, 707-715.

McCave, IN; 1971: Sand waves in the North Sea off the coast of Holland Mar. Geol. 10, 199-225.

Middleton, GV; Southard, JB; 1977: Mechanics of Sediment Movement. SEPM Short Course No. 3, Binghamton, N.Y.

Neill, CR; 1969: Bed forms in the lower Red Deer River, Alberta. J. Hydrology 7, 58-85.

Nordin, CF, Jr; 1976: Flume studies with fine and coarse sands. USGS Open File Report 76-762, Denver, Colorado.

Offen, GR; Kline, SJ; 1975: A proposed model of the bursting process in turbulent boundary layers. J. Fluid Mech. 70, 209-228.

Pratt, CJ; 1971: An experimental investigation into the flow of water and movement of bed material in alluvial channels. Ph.D. Thesis, Univ. of Southampton, England.

Pratt, CJ; 1973: Bagnold approach and bed-form development. J. Hyd. Div., ASCE 99, 121-137.

Pratt, CJ; Smith, KVH; 1972: Ripple and dune phases in a narrowly graded sand. J. Hyd. Div., ASCE 98 (HY5), 859-874.

Pretorious, ES; Blench, T; 1951: Final report on special observations of bed movement at Ladner Reach during 1950 Freshet. Nat. Res. Council of Canada Report, 12 pp.

Raudkivi, AJ; 1967: Loose Boundary Hydraulics; Pergamon Press, London, England.

Reineck, HE; 1963: Sedimengefuge im Bereich der sudlichen Nordsee. Abh. Senckenb. Naturforsch. Ges. No. 505, 138 pp.

Richards, KJ; 1980: The formation of ripples and dunes on an erodible bed. J. Fluid Mech. 99, 597-618.

Rubin, DM; McCulloch, DS; 1980: Single and superimposed bed forms: a synthesis of San Francisco Bay and flume observations. Sed. Geol. 26, 207-221.

Simons, DB; Richardson, EV; 1962: Resistance to flow in alluvial channels. Trans. ASCE 127, 927-954.

Simons, DB; Richardson, EV; 1963: Forms of bed roughness in alluvial channels. Trans. ASCE 128, 284-302.

Simons, DB; Richardson, EV; 1966: Resistance to flow in alluvial channels. USGS Prof. Paper 462-J.

Singh, IB; Kumar, S; 1974: Mega-and Giant ripples in the Ganga, Yamuna, and Son Rivers, Uttar Prades, India. Sed. Geol. 12, 53-66.

Smith, ND; 1971: Transverse bars and braiding in the lower Platte River, Nebraska. GSA Bull. 82, 3407-3420.

So, CL; Pierce, JW; Sieger, FR; 1974: Sand waves in the Gulf of San Matais, Argentina. Geografiska Annaler A56, 227-235.

Southard, JB; 1971: Representation of bed configurations in depth-velocity-size diagrams. J. Sed. Petrology 41, 903-915.

Southard, JB; 1975: Bed configurations.in Harms, JC; Southard, JB; Spearing, DR; Walker, RG; Depositional Environments as interpreted from primary sedimentary structures and stratification sequences. SEPM Short Course No. 2, Dallas, Texas.

Southard, JB; Boguchwal, LA; 1973: Flume experiments on the transition from ripples to lower flat bed with increasing grain size. J. Sed. Petrology 43, 1114-1121.

Sternberg, RW; 1971: Measurements of incipient motion of sediment particles in the marine environment. Marine Geol. 10, 113-119.

Stride, AH; 1963: Current swept sea floors near the southern half of the British Isles. Quart. J. Geol. Soc. London 119, 175-199.

Stride, AH; 1970: Shape and size trends for sand waves in a depositional zone of the North Sea. Geol. Mag. 107, 469-477.

Tani, I; 1957: Experimental investigation of flow separation over a step. Intl. Union of Theoretical and Applied Mech., Proc. Boundary Layer Research Symposium, Freiburg, Germany, 377-386.

Terwindt, JHJ; 1970: Observations on submerged sand ripples with heights ranging from 30-200 cm occurring in tidal channels of southwest Netherlands. Geol. en Mijnbouw 49 489-501.

VanVeen, J; 1935: Sand waves in the North Sea. Int. Hydrog. Rev. 12, 21-29.

Vanoni, VA; 1974: Factors determining bedforms in alluvial channels. J. Hyd. Div., ASCE, 98 (HY8) 1427-1445.

Vanoni, VA; Brooks, NH; 1957: Laboratory studies of the roughness and suspended load of alluvial streams. Report E-68, Calif. Inst. of Technology Sedimentation Lab.

Visher, GS; Howard, JD; 1974: Dynamic relationship between hydraulics and sedimentation in the Altahara Estuary. J. Sed. Petrology 44, 502-521.

Walker, GR; 1961: A study of the two-dimensional flow of turbulent fluid past a step. M. Eng. Thesis, U. of Auckland, Auckland, New Zealand.

Werner, F; Newton, RS; 1975: The pattern of large-scale bedforms in the Langeland Belt (Baltic Sea). Marine Geol. 19, 29-59.

Williams, GP; 1970: Flume width and depth effects on sediment-transport experiments. USGS Prof. Papter 562-H, 37 pp.

Yalin, MS; 1964: Geometrical properties of sand waves. Proc. ASCE 90 (HY5), 105-119.

Yalin, MS; 1972: Mechanics of Sediment Transport. Pergamon, London.

Znamenskaya, NS, 1963: Eksperimenta l'noye issledouanie gryadovogo dvizheniya nansov: Gosudarstvennyi Gidrologich-Eskii Institut (Leningrad), Trudy, No. 108, 89-114.